PILOT SCALE PRODUCTION, CHARACTERIZATION, AND OPTIMIZATION OF EPOXIDIZED VEGETABLE OIL-BASED RESINS

A Dissertation
Submitted to the Graduate Faculty
of the
North Dakota State University
of Agriculture and Applied Science

By

Ewumbua Menyoli Monono

In Partial Fulfillment of the Requirements
for the Degree of
DOCTOR OF PHILOSOPHY

Major Department:
Agricultural and Biosystems Engineering

May 2015

Fargo, North Dakota

North Dakota State University
Graduate School

Title

Pilot Scale Production, Characterization, and Optimization of Epoxidized Vegetable Oil-Based Resin

By

Ewumbua Menyoli Monono

The Supervisory Committee certifies that this ***disquisition*** complies with North Dakota State University's regulations and meets the accepted standards for the degree of

DOCTOR OF PHILOSOPHY

SUPERVISORY COMMITTEE:

Dr. Dennis Wiesenborn
Chair

Dr. Scott Pryor

Dr. Dean Webster

Dr. Chad Ulven

Approved:

07/01/2015
Date

Dr. Sreekala Bajwa
Department Chair

ABSTRACT

Novel epoxidized sucrose soyate (ESS) resins perform much better than other vegetable oil-based resins; thus, they are of current interest for commercial scale production and for a wide range of applications in coatings and polymeric materials. However, no work has been published that successfully scaled-up the reaction above a 1 kg batch size. To achieve this goal, canola oil was first epoxidized at a 300 g scale to study the epoxidation rate and thermal profile at different hydrogen peroxide (H_2O_2) addition rates, bath temperatures, and reaction times. At least 83% conversion of double bonds to oxirane was achieved by 2.5 h, and the reaction temperature was 8-15 ^oC higher than the water bath temperature within the first 30-40 min of epoxidation. A 38 L stainless steel kettle was modified as a reactor to produce 10 kg of ESS. Twenty 7-10 kg batches of ESS were produced with an overall 87.5% resin yield and > 98% conversion after batch three. The conversion and resin quality were consistent across the batches due to the modifications on the reaction that improved mixing and reaction temperature control within 55-65 ^oC. The total production time was reduced from 8 to 4 days due to the fabrication of a 40 L separatory funnel for both washing and filtration. A math model was developed to optimize the epoxidation process. This was done by using the Box-Behnken design to model the conversion at various acetic acid, H_2O_2, and Amberlite ratios and at various reaction temperatures and times. The model had an adjusted R^2 of 97.6% and predicted R^2 of 96.8%. The model showed that reagent amounts and time can be reduced by 18% without compromising the desired conversion value and quality.

ACKNOWLEDGMENTS

I would like to thank a number of people who helped me to successfully carry out this research. Firstly, thanks to my advisor Dr. Dennis Wiesenborn for the opportunity he gave me to work in biobased resin and his guidance during the course of my research work. Thanks to my committee members, Dr. Scott Pryor, Dr. Dean Webster, and Dr. Chad Ulven, for their help and corrections during my dissertation proposal and defense.

I will acknowledge Dr. Darrin Haagenson, and Mr. James Bahr for their assistance in understanding procedures and equipment in the Pilot Plant and Research Park. Special thanks to Dr. Judith Espinoza-Perez whose work lead to some initial grants and laid an excellent foundation for my work. Thanks to Dr. Thomas J. Nelson for sharing with me his experiences in epoxidizing sucrose at a 1 kg scale.

I would also like to thank the undergraduate students; Seka Ajavon, Salim Balwazir, Brittney Riebel, Connor Kelley, and Petar Miljkovic who helped me during the epoxidation process and analysis of the resin. Thanks to Megan Even for writing consultations.

Great thanks to my wife, Mrs. Esther Monono for her support and encouragements. Thanks also to my family in Fargo like Mr. & Mrs. Emmanuel Nojang, Dr. & Mrs. Diomo Motuba, Mr. Mbella John, Dr. William Nganje, and many friends for making me feel at home while carrying out my research.

Thanks also my colleagues in the graduate room for the ideals we share in all the classes we did together and the humorous environment in the office.

I want to finally acknowledge financial support from the North Dakota Industrial Commission, North Dakota Soybean Council, Northern Canola Growers Association, and the North Dakota Agricultural Experiment Station.

DEDICATION

To my kids, Etina and Janelle Monono

TABLE OF CONTENTS

LIST OF TABLES

LIST OF FIGURES

LIST OF EQUATIONS

LIST OF APPENDIX TABLES

LIST OF APPENDIX FIGURES

GENERAL INTRODUCTION

The environmental concerns and availability associated with petroleum resources have propelled scientists to develop sustainable and renewable alternatives to petroleum based products (Eissen and Metzger, 2002). Renewable raw materials that have been widely used in chemical industries are vegetable oils, sugar, starch, and cellulose. Vegetable oils and low molecular weight carbohydrates have shown great potential as alternatives to petroleum-based resins, and the interest in using them to produce bio-based resin continues to increase (Cai et al., 2008; Lichtenthaler and Peters, 2004). They are used in various biobased applications due to their very important functionality, cost, availability, low toxicity, and biodegradability (Tan and Chow, 2010).

Vegetable oil is one of the most abundant biobased feedstocks (Tan and Chow, 2010). A molecule of vegetable oil, known as triglyceride, has three fatty acid chains attached to a glycerol chain. There are variable forms of fatty acid within and among different triglyceride molecules. Some of the fatty acid chains have unsaturated bonds that can be chemically modified to epoxy bonds through the process of epoxidation. The purpose of epoxidation is to incorporate oxygen atoms into the double bonds of vegetable oils. The oxygen atom is contained in a three membered ring or cyclic ether known as an epoxy or oxirane group. The epoxidized form of vegetable oil has been successfully used as a biobased epoxy in coatings, polymers, and material science because the epoxy groups are highly reactive. Due to its high reactivity, other new functional groups like alcohols (polyols), esters, alkanolamines, and carbonyls can also be produced. These new resins are used as plasticizers and stabilizers for polymers, lubricants, and resins in composite materials (Guo et al., 2000; Pan and Webster, 2012).

Successful results have been reported when epoxidized vegetable oil (EVO) was used as a plasticizer and stabilizer in polyvinyl chloride (PVC) and as a high-temperature lubricant (Adhvaryu and Erhan, 2002). However, in composite materials and other thermosets in which high thermal and mechanical properties are needed, EVO-based materials are deficient in toughness and strength compared to petroleum-based materials (Espinoza-Pérez et al., 2011; Tan and Chow, 2010). When the glycerol core in vegetable oil was replaced with a sucrose core forming sucrose ester of fatty acid (SEFA), the resulting products had greatly improved thermal properties and mechanical strength (Pan et al., 2011a; Pan and Webster, 2012). The thermosets and coatings exhibited 3-4 times higher modulus, hardness, and ductility than thermosets from EVO with a glycerol core. The higher strength observed in epoxidized SEFA has increased the demand for applications testing and commercialization. Production of epoxidized SEFA beyond the lab bench (300 g) scale is needed to meet this growing demand. Even though epoxidized soybean oil is produced industrially (Cahoon, 2003), the insight needed to scale up epoxidation, such as a 10 kg scale, was not yet reported in the peer-reviewed literature. Therefore, the results from this dissertation should provide important insight in scaling up the epoxidation process from a lab scale (300 g) to a 10 kg pilot scale and higher scale.

The epoxidation process occurs through commonly used schemes shown in Fig. 1. These schemes include *in-situ* peracetic acid formation and then double bond epoxidation. The peracetic acid formation is usually controlled by the dropwise addition of hydrogen peroxide (H_2O_2) into the reaction mixture because the epoxidation reaction is very exothermic, which poses a challenge during scale-up. Producing greater batch sizes of epoxidized SEFA requires larger equipment to synthesize and refine the increased quantities of reactants. The increase in

reactants results in an excessively high reactor temperature depending on the H_2O_2 addition rate and reaction time (Gerlach and Geller, 2004). Controlling reaction temperature in a scaled-up reactor is critical to maximize oxirane formation and minimize reaction time. Most epoxidation studies have assumed that the reactor temperature was similar to the water bath temperature or the temperature of the heating unit and only monitored the water bath temperature (Tan and Chow, 2010). The one study that monitored the actual reactor temperature used it as a means to control H_2O_2 addition rate, but did not show the temperature-time profile (Pan et al., 2011b). Therefore, characterizing the process conditions at different H_2O_2 addition rates, water bath temperatures, and times at a bench-scale is very important in providing better insight into the reaction temperature behavior at these conditions before developing a scaled-up reactor.

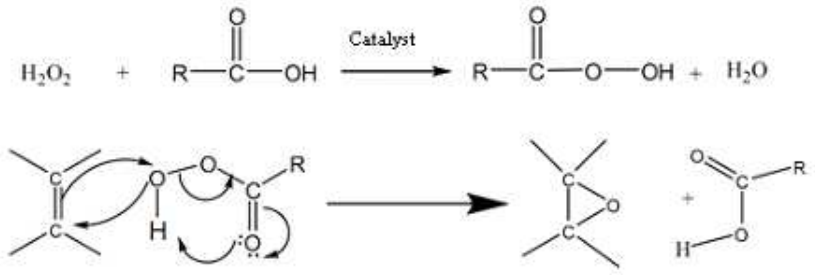

Fig. 1: Epoxidation reaction (Gamage et al., 2009)

Refining the synthesized crude resin represents a significant portion of the total production time and cost. The production time could significantly increase during scale up if adequate refining units are not available to handle the larger volume of synthesized resin. The refining process involves steps to eliminate unreacted H_2O_2, the catalyst, acetic acid, water, and solvent from the crude resin. The refining steps and equipment used to produce epoxidized vegetable oil are frequently not fully described in most epoxidation studies. In studies in which the refining process is described, there are some differences in the refining steps and the quantity

of purifying reagents used (Espinoza-Pérez et al., 2009; Pan et al., 2011b). Therefore, it is important to clearly determine the design and operation of refining units that will reduce the production time.

The success observed in the applications of epoxidized SEFA in coatings and composite materials has stimulated interest to produce the resin beyond pilot scale. Industrial scale production requires the optimization of the epoxidation process conditions which in turn will minimize reagents used without compromising oxirane formation. A model is needed that can predict acceptable conversion of double bonds to oxirane at different scenarios of the amounts of H_2O_2, acetic acid, and catalyst, and reaction temperatures and times. A robust model will be a valuable tool to determine different optimal scenarios to epoxidize SEFA and vegetable oil at an industrial scale.

LITERATURE REVIEW

Vegetable oil

Renewable oils come from two major sources; animal and plant (mostly oil seed crops). In the twenty-first century, vegetable oils are becoming increasingly dominant over animal fats and oils as it contributes approximately 85% of the total oil used compare to 80% in the last decade (Gunstone, 2011). Vegetable oils are triglycerides of various fatty acids (FA). They are termed fatty esters of glycerol (triglycerides) because they contain a glycerol chain attached to three different fatty acids chains as seen in Fig. 2. The types of FA attached to the glycerol vary within the same or different source of oil.

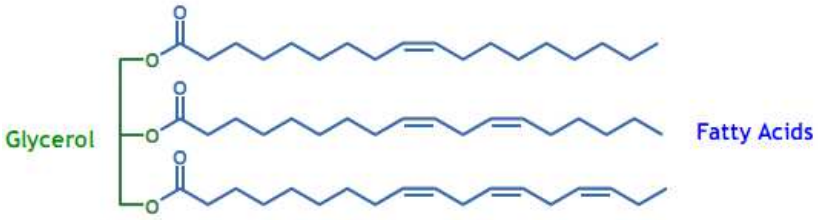

Fig. 2: Chemical structure of a representative triglyceride molecule.

The FA portion is approximately 90% of the total oil weight while 10% of the weight is the glycerine portion (Guo and Petrovic, 2005). By 2010, the four major vegetable oils in the world which contribute approximately 84% of the total vegetable oils and 70% of the total fat and oils were palm, soybean, canola, and sunflower oils (Gunstone, 2011). These major vegetable oils are composed primarily of five FAs; palmitic, stearic, linoleic, oleic, and linolenic. The stereochemistry of the double bonds, their degree of unsaturation, and the length of these FA chains are the most important factors affecting the physical and chemical properties of oils. The

mean proportion of FA compositions for these major vegetable oils and their iodine values are shown in Table 1 while the structures of these common fatty acids are shown in Fig. 3.

Table 1: Proportion of the main fatty acids (C-atoms:double bonds) found in the four major vegetable oils (Gunstone, 2011).

FA type	Palmitic (16:0)	Stearic (18:0)	Oleic (18:1)	Linoleic (18:2)	Linolenic (18:3)	*Iodine value range*
Canola oil	4.0	1.8	60.9	21.0	8.8	*100-115*
Palm oil	44.3	4.3	39.3	10.0	<0.5	*50-60*
Soybean oil	10.6	4.0	23.3	53.7	7.6	*123-139*
Sunflower oil*	5.0	3.9	65.0	25.0	<1	*125-140*

* Mid-oleic oil variety

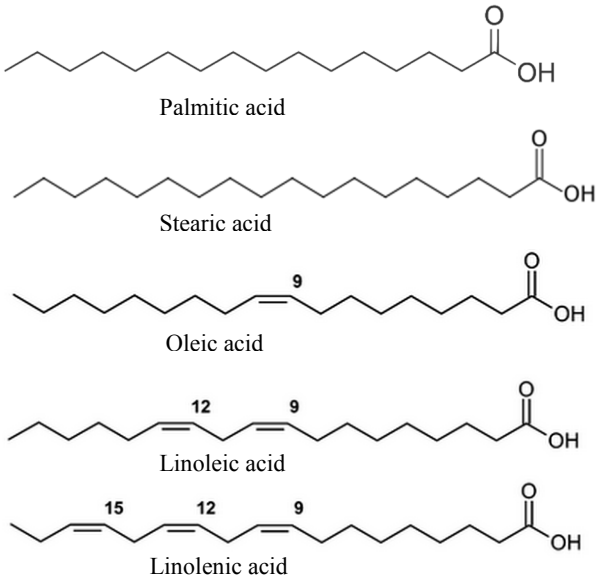

Fig. 3: Chemical structure of the five major fatty acids found in vegetable oil.

In food industries, a balance between high saturated and high unsaturated fatty acids vegetable oil is important. High consumption of oils with high saturated FAs has been linked to many health problems like high cholesterol and heart diseases. On the other hand, oils with high unsaturated FAs are relatively unstable to oxidative deterioration, hence low shelf life. To improve the shelf life of oils with high degree of unsaturation, hydrogen is added to unsaturated

bond through a chemical process known as hydrogenation. This process reduces the amount of double bonds and improves the shelf life, but the hydrogenation process increases the amount of saturated fat that has also been linked to cardiovascular disease (Korver and Katan, 2006). Vegetable oil with high oleic FA proportion is usually the balance between high saturated and unsaturated fatty acids. Oilseed crop breeding programs have modified the FA composition to achieve high oleic acid content. For example sunflower oleic acid content has increased over the years to up to 70-80 % from its traditional low oleic acid content of 20% (Grompone, 2011), Therefore, the food and health concerns, oxidative stability, and the need for high quality biobased resin will always dictate the future composition of fatty acids in various vegetable oils.

Vegetable oils which are rich in unsaturated fatty acids (high degree of double bonds) are important in the production of biobased resin. The degree of unsaturation in the oil is measured by the iodine values (amount of iodine in grams absorbed by unsaturated double bonds in 100 g of oil under specific conditions). The higher the iodine value, the higher the number of unsaturated carbon double bonds. Therefore, palm oil which has approximately 50% of saturated FA is not suitable for biobased resin production compared to the other three in Table 1. By 2010, the amount of vegetable oil produced from canola, soybean, and sunflower oils relative to the total vegetable oils were 15.5%, 27.1%, and 9.0%, respectively (Gunstone, 2011). Most studies on using vegetable oils for biobased resins production have been done with soybean, canola, and lastly sunflower in decreasing order. Even though some studies have shown that some sunflower resins are a better stabilizer in polyvinyl chloride than soybean resin (Benaniba et al., 2001; Bouchareb and Benaniba, 2008), its low production and variable oleic content has limited its

expansion compared to soybean oil and canola (Grompone, 2011). Therefore, this dissertation will concentrate on soybean and canola oils.

Soybean oil production and demand

Due to its favorable agronomic characteristics, valuable oil, and high-quality protein, soybean is the dominant oilseed produced in the world (Wang, 2011). In the past three year, the US is the second highest producer of soybean oil in the world with about 9.2 million metric tons per year, which is approximately 20% of the world's soybean oil production (USDA, 2015). However, the US is the highest producer of soybean oilseed with an average of 103 million metric tons (~ 20% world production) per year in the past three years (USDA-ERS, 2015). China is highest producer of soybean oil but fourth producer of soybean oilseed in the world because they import most of the oilseed used for soybean oil production from the US, Brazil (second oilseed producer) and Argentina (third oilseed producer) (USDA, 2015). The US and world's soybean oil production has been increasing by approximately 1-2% and 4-5% annually, respectively over the past decade due to increased crop production and improved seed varieties, fertilizers and pest control, and management practices. For example in the US, total soybean farm hectares were reduced from 3.0 million in 2002 to 2.6 million in 2007, but total production in 2007 was slightly the same at approximately 7.1 million tons due to improved cultural practices (USDA-ERS, 2012).

Soybean is composed of protein – 40%, oil – 22%, carbohydrate – 25%, fiber – 7%, ash – 5%, and hull – 8% (Crum et al., 1992). It is the second most cultivated crop in the US after corn and it is usually planted in crop rotation with corn. Therefore, soybean is mostly produced around the Corn Belt regions with Iowa, Illinois, Minnesota, Indiana, and Nebraska the leading

soybean producing states while North Dakota was ranked 11th by the end of 2010 (USDA-NASS, 2013). Soybean oil, therefore; accounts for 90% of total edible oil consumed in the US due to its availability and low cost (Wang, 2011).

Average price for soybean oil in the US increased from $0.75 per kg between 2008-2010 to $1.1 per kg between 2011-2013 but fell to $0.85 per kg in 2014 (USDA, 2015). The price for soybean oil is still cheaper than other vegetable oils produced in the US. The price for soybean oil has been increased over the last decade due to the demand and uses in edible and non-edible purposes. By 2012, the use of soybean oil in non-edible purposes like biodiesel, lubricant, paints, and resin were approximately 30% of the total soybean oil supplied (USDA-ERS, 2013). Production of soybean oil has always been driven by the need for the high protein meal for the poultry, cattle, and swine industries. The lower meat production in 2008, coupled with the increase in canola meals and distiller grains did not make the production of soybean to increase in the US as compared to competing countries like China and Argentina (Wang, 2011). However, the increasing demand for soybean oil in other countries, soy biodiesel demands, other soy-based products will cause the US production of soybean oil to increase by 6% by 2019 (USDA-ERS, 2015). Production and demand in other countries might also cause global soybean oil production to increase more than 6% (Wang, 2011).

Canola oil production and demand

Canola is a modified rapeseed in which erucic acid and glucosinolate contents have been reduced to less than 2% and 30 μM/g of oil, respectively (Gunstone, 2004). Canola in some literature and in many parts of the world including Europe is still known as rapeseed. High erucic acid has been linked to heart disease in animals, while high glucosinolate was detrimental to

livestock growth and adversely affects seed processing (Przybylski, 2011). In the late 1950's, plant breeding programs were initiated in Canada in which low level erucic acid and glucosinolate traits were backcrossed with other adapted cultivars. Hence by the mid 1970's more than 95% of rapeseed produced in Northern America was canola varieties (Gunstone, 2004).

Canola grain is composed of oil – 44%, protein – 26%, carbohydrate – 8%, fiber – 14%, ash – 5%, and hull – 15% (Crum et al., 1992). It is the third largest vegetable oil crop in the world after soybean and palm oil with an annual average oil production of 26.1 million metric tons per year between in 2012 - 2014. The major world producers of canola oil are China, Canada, and India with approximately 6.3, 3.0, and 2.3 million metric tons per year between 2012-2015, respectively (USDA, 2015). The US production of canola oil stood at 0.51 million metric tons in 2012 with North Dakota producing 90% of the US canola oil (USDA-ERS, 2012). Table 2 shows US canola oil supply and prices from 2005 to 2014.

Table 2: US Canola oil supply and price (USDA, 2015)

Year	Production	Imports	Total	Price
	million metric tons			$/kg
2005/06	0.42	0.73	1.15	0.68
2006/07	0.42	0.71	1.14	0.89
2007/08	0.46	1.02	1.48	1.44
2008/09	0.50	1.05	1.55	0.87
2009/10	0.49	1.07	1.56	0.94
2010/11	0.52	1.42	1.95	1.29
2011/12	0.51	1.50	2.01	1.26
2012/13	0.58	1.25	1.83	1.24
2013/14	0.72	1.54	2.26	0.96

In the early 2000s, there has been an increased interest in the US in using canola oil for industrial applications like biodiesel, lubricants, hydraulic fluids, and penetrating oils to fuel, soap, and resin production, but its industrial use is still very low compared to soybean oil

(USDA-ERS, 2015). This is because there has been an increasing demand for canola oil in the food industries which has made the prices for canola oil to be 30% higher than soybean oil in the late 2000s. The high demand for canola oil for edible purpose is due to its low saturated fats and high oleic contents as seen in Table 1, making it preferable for food consumption because of the health and shelf life advantages.

There is high industrial use of canola oil in Europe compared to the US because canola is the primary oil crop grown (Gunstone, 2004). The increase in demand for biodiesel in Europe and vegetable oil in China and India within the last decade has made canola oil world trade to double (USDA-ERS, 2012). This growing demand for canola oil for both food and industrial consumption will cause production of canola oil to increase in the future, which might make prices for canola oil to be competitive with that of soybean oil.

Sucrose ester of fatty acids

Sucrose ester of fatty acids (SEFA) is a combination of sucrose and vegetable oil fatty acids where sucrose replaces glycerol in the center core chain. Sucrose ester of unsaturated fatty acid was first reported in coatings in the early 1960s (Walsh et al., 1961). Their study showed that the sucrose ester had a uniform fatty acid distribution, low viscosity, rapid air-drying time, and good coatings properties.

Sucrose is a low molecular weight disaccharide and a renewable product of eight hydroxyl groups (three primary and five secondary) as seen in Fig. 4 and can be used in many different ways in place of petroleum products (Lichtenthaler and Peters, 2004). The sucrose ester of fatty acids is formed if the OH groups are substituted with fatty acid from vegetable oil as seen in Fig. 5. A SEFA molecule has more fatty acid networks than the original triglyceride,

which therefore increases the functionality of any resin that is produced from SEFA (Pan and Webster, 2011).

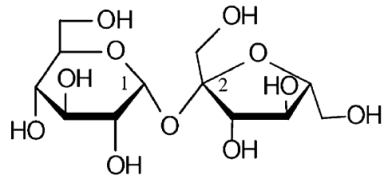

Fig. 4: A structure sucrose molecule (β-D-fructofuranosyl α-D-glucopyranoside) (Walsh et al., 1961).

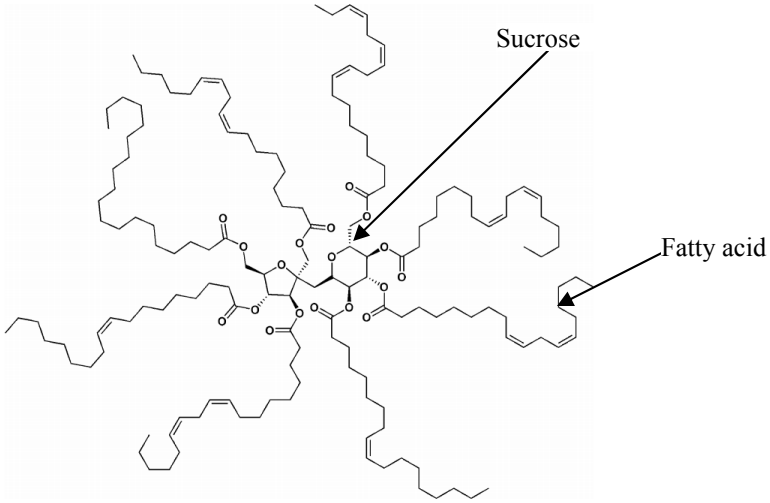

Fig. 5: A representation of a fully substituted sucrose ester of fatty acid from soybean oil (Pan et al., 2011b).

Even though SEFA was used in coatings in the early 1960s, commercial production was not possible because achieving a high degree of substitution (DS) of the fatty acid for the hydroxyl groups in sucrose has always been challenging. The DS of a given form of SEFA is defined as the average number of substituted hydroxyl groups by fatty acids per sucrose molecule. The maximum DS that could be achieved in the 1960s was 7 out of the 8 hydroxyl groups (Pan et al., 2011a). In the last decade, Procter and Gamble (P&G) successfully developed

a process to commercially produce such esters with the brand name SEFOSE that has a high DS of at least 7.7 (a mixture of sucrose hexa, hepta, and octaester, with a minimum of 70% by weight of octaester) (Corrigan, 2003). If the source of the fatty acid is from soybean oil, it is commonly known as sucrose soyate (SS). Therefore in this study, the term SS will be used when referring to SEFOSE made from soybean oil. P&G Chemicals and Cook Composites and Polymers jointly received the Presidential Green Chemistry Award from the U.S. Environmental Protection Agency (EPA) in 2009 on Sefose-based alkyd resin technology; that technology enabled the formulation of paints and coatings with less than half the emission of volatile organic compounds of traditional solvent-borne alkyd coatings (P&G, 2009).

Epoxidized vegetable oil (EVO)

Epoxidation process

Epoxidation is a process of forming an epoxide functional group by reacting peracetic or peroxy acid with aromatic and/or alkene double bonds. Epoxide, also known as oxirane, is cyclic ether of three member ring with one oxygen atom and two carbon atoms. Swern and Greenspan were among the first researchers to study the epoxidation of vegetable oil with hydrogen peroxide in the presence of acetic acid and a catalyst (Gall and Greenspan, 1955; Luong et al., 1967; Swern et al., 1945). Most epoxidation processes today still follow this synthesis route used by these researchers more than half a century ago, even though process conditions and reagent ratios have changed to optimize oxirane yield.

The epoxidation process requires an oxygen source that will be incorporated into the double bonds. There are 2 common sources of oxygen that have been reported in literature: (i) epoxidation with organic and inorganic peroxides like H_2O_2 with a metal catalyst (Luong et al.,

1967); and (ii) epoxidation with diatomic oxygen catalyzed by some transition metals (Guenter et al., 2003). Even though oxygen is the cheapest and most environmentally friendly oxidant, hydrogen peroxide is mostly used as an oxidizing agent because epoxidation of vegetable oil using diatomic oxygen degrades a portion of the oil to smaller volatile compounds like ketones and aldehydes (Goud et al., 2007). The use of oxygen as oxidant in epoxidation is limited to some simple petrochemicals (Sheldon, 1991). The epoxidation process with hydrogen peroxide involves in situ formation of peracid with acetic acid (in some cases; formic acid) in the presence of a catalyst as seen in Fig. 1. The peracetic acid is formed in the aqueous phase, and reacts with a double bond of a fatty acid in the organic phase.

There are 4 major categories of epoxidation process mainly due to the type of catalyst used (Tan and Chow, 2010). These categories are conventional, acidic ion exchange resin (AIER), chemo-enzymatic, metal-catalyzed epoxidation process.

Conventional process: This process is also known as the Prileshajev epoxidation in which peracetic or performic acids were generated from hydrogen peroxide and the corresponding acid in the presence of a mineral acid catalyst like sulfuric or phosphoric acid (Gerbase et al., 2002; Petrović et al., 2002). The mineral acid catalyst in addition to the acetic acid increases the acidity of the reaction which cause faster corrosion of reactor and higher amount of base reagent needed to neutralize and remove the acid from the end product (Gurbanov and Mamedov, 2009). Another disadvantage of a strong mineral catalyst is that it can initiate oxirane cleavage to undesired functional groups like hydroxyl or ether groups (Vlček and Petrović, 2006).

AIER process: the process is similar to the conventional process except for the use of AIER catalyst, such as a simple ionic exchange resin like Amberlite IR 120 H, in place of mineral acid. Being solid and insoluble, the benefits of AIER as a catalyst are improved selectivity, suppressed undesirable side reactions, and ease of separation of catalyst from resin (Sinadinovic-Fiser et al., 2001). Peracetic acid formation occurs within the resin matrix as bead pores are small enough to allow H_2O_2 and acetic acid to penetrate but not fatty acid. Meanwhile, the epoxidation reaction occurs outside the AIER matrix. Particle size of an AIER catalyst influence the rate at which the epoxy bonds are formed because it influences the penetration of H_2O_2 and acetic acid and hence the rate of peracetic formation (Goud et al., 2007).

Some reviews of the different catalysts used during epoxidation of oils showed that only Amberlite IR 120 H has been reported as an AIER catalyst (Abdullah and Salimon, 2010; Patil and Waghmare, 2013). These reviews concentrated their analysis on the use of Amberlite IR 120 H to epoxidize different types of oils, but not on the use of different catalyst concentrations or types. However, Gurbanov and Mamedov (2009) successfully showed that other cation exchangers can be used as they had up to 98% conversion rate when they used a chlorinated cation exchange KU-2×8 as the catalyst. Amberlite IR 120 also has Na^+ ionic from but has not been used in the epoxidation of vegetable oil. Product properties from Sigma Aldrich technical information bulletin indicates that these two ionic forms (H^+ and Na^+) have the same polystyrene matrix, bead size, moisture percent, and total exchange capacity (Aldrich, 2013). However, a comparative study in the epoxidation of vegetable oil has not been conducted between these two forms of Amberlite. Another strong cation resin that has similar properties to Amberlite IR 120

H and has not been reported in epoxidation of oils is Marathon C (Dow chemical company, Ohio).

In the epoxidation of oils, cation exchangers are a more effective catalyst than anion exchangers, because of the use of an acid (acetic or formic) as the oxygen carrier. In a cation exchanger, a negatively charged ion covalently bound to the polystyrene terminals while H+ or Na+ are free or exchangeable cations. Sulfonic acid groups mostly used as the bound ion in a strong cation exchange resins while carboxylic groups are used in weak cation exchangers (Aldrich, 2013). The free, positively charged ions are exchanged with the ions found in acetic or formic acid thereby creating ionic drift. Anion exchange resins have mostly ammonium groups at the terminal of the polystyrene and cannot attract ions from acetic or formic acid.

***Chemo-enzymatic process*:** Lipase catalyst was used in some studies and it exhibited excellent stability and activity during the epoxidation process (Rüsch gen. Klaas and Warwel, 1999; Vlček and Petrović, 2006). Hilker et al. (2001) showed that temperature and H_2O_2 concentration affected the activity of lipase biocatalyst; however, no significant difference was seen in chemo-enzymatic activity below 60 ^oC and H_2O_2 concentration below 60%.

Metal-catalyzed process: A high-valence catalyst like molybdenum, titanium, rhenium, or tungsten is used to improve the efficiency of the epoxidation process (Tan and Chow, 2010). The use of methyltrioxorhenium as a catalyst showed lesser amount of H_2O_2 and reaction time was needed to complete the epoxidation when compared to the conventional process (Cai et al., 2009; Gerbase et al., 2002).

In addition to these different epoxidation processes, differences in process conditions (see next section) have made it difficult to compare results and side reactions may occur during the

epoxidation, resulting in other undesirable products as seen in Fig. 6. It has been reported in some studies that as temperature increases above 65 or 70 ^{o}C and/or at higher acid concentration, the rate of oxirane cleavage increases (Cai et al., 2008; Dinda et al., 2008; Mungroo et al., 2008; Vlček and Petrović, 2006). Also, increasing the reaction above the time in which the maximum double bond conversion has been achieved, increase the probability of oxirane (Goud et al., 2006).

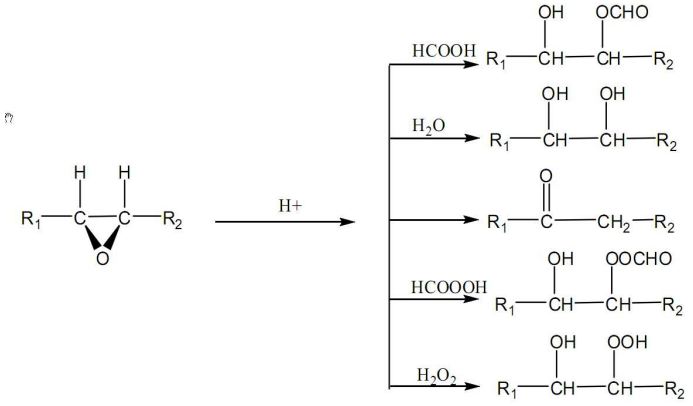

Fig. 6: Possible oxirane cleavage or side reactions leading to polyols, ketone, carboxylic groups (Gamage et al., 2009).

Reactor process conditions

Different epoxidation conditions and methods have been used together with a wide variety of oil from different sources like soybean, linseed, canola, jatropha, rubber, palm, cotton, mahua, and karanja as shown in Table 3. These conditions include different hydrogen peroxide (H_2O_2) rates, molar ratios of reagents, temperature, reaction time, stirring speeds, and catalysts amounts.

Hydrogen peroxide rates: Most epoxidation studies did not report the different H_2O_2 addition rates but rather the durations at which H_2O_2 was added. This duration in Table 3 varied

based on the amount of H_2O_2 or the oil being epoxidized. Therefore, the addition rates were also different in those studies. The addition of H_2O_2 was dropwise over the reported duration.

Table 3: Summary of epoxidation processes and conditions for various types of vegetable oil reported in the scientific literature. The temperature reported was the bath temperature, except where noted otherwise.

Epoxidation process	Vegetable oil	Batch size (g)	Process conditions			Conversion (%)	References
			Temperature (°C)	H_2O_2 addition duration (h)	Reaction time (h)		
Conventional	Soybean	150	45, 55 65, 75	12	12	Nd	(Cai et al., 2008)
	Jatropha	nd	30, 50, 70, 85	0.5	3.5, 4.5, 10	35-88	(Meyer et al., 2008)
	Cottonseed	nd	30, 45, 60, 75	0.5	4	80	(Dinda et al., 2008)
AIR	Canola	22.6	40, 55, 65, 75	0.5	7	50-90.8	(Mungroo et al., 2008)
	Canola	50, 300	50-60	0.5	5	95-98	(Espinoza-Pérez et al., 2009)
	Soybean	100	30, 60, 75	0.5	8	73.1-97.7	(Sinadinovic-Fiser et al., 2001)
	Sucrose ester of fatty acid	170	55-65*	variable	nd	99.4-99.9	(Pan et al., 2011b)
	Rubber, neem, mee	40, 1000	50-60	1, 2.5	5.5, 8	86-91	(Gamage et al., 2009)
Chemo-enzymatic	Soybean	25	50	0.083	24	50-98.9	(Vlček and Petrović, 2006)
	Soybean, sunflower, linseed, rapeseed	7.8	RT	54 µl every 7.5 min	16	88-99	(Rüsch gen. Klaas and Warwel, 1999)
Metal-catalyzed	fatty acid	11.7	30	2	2	31-96	(Cai et al., 2009)
	soybean	30	RT	nd	1-2	16-92	(Gerbase et al., 2002)

RT – room temperature; nd – no data; AIR – acidic ion exchange resin; *Reaction temperature

A study was conducted on the effect of H_2O_2 addition rate on the epoxidation of free linoleic acid (Orellana-Coca et al., 2005). The addition was made in portions in which zero portion was when all H_2O_2 was added at the beginning, five portions was when H_2O_2 was divided into five portions and added at 0, 1, 2, 3, 4 h, and then H_2O_2 was divided into ten portions and added at 0-9 h. The reaction was run for 24 h. These addition rates are different than those in previously reported literature. Moreover, the experiment was conducted for 24 h and it was only at this point that the three addition rates were not significantly different.

***Molar ratio of reagents*:** The amount of acetic acid and H_2O_2 are always reported based on molar ratios relative to the double bonds or unsaturation of the vegetable oil being epoxidized. Different molar ratio of oil unsaturation: acetic acid: H_2O_2 has been explored in many optimization studies (Espinoza-Pérez et al., 2009; Gamage et al., 2009; Goud et al., 2007; Milchert et al., 2010; Mungroo et al., 2008; Vlček and Petrović, 2006). The ratio of 1:0.5:2 was shown to be optimal and has been used in most other epoxidation studies (Saurabh et al., 2011; Tan and Chow, 2010).

***Temperature*:** Temperature is an important factor that influences the rate of a chemical reaction, as shown by the Arrhenius equation. Increasing temperature increases reaction rate of epoxidation and also the reaction rates of side product formation. Many studies have reported that maximum oxirane conversion is attained faster as temperature increases; however, oxirane cleavage easily occurs if the reactions continue at temperatures >65 ^{o}C (Dinda et al., 2008; Goud et al., 2010; Goud et al., 2006; Mungroo et al., 2008; Okieimen et al., 2002). Reaction temperature and time are inversely proportion, therefore, the longer the reaction continues after the maximum oxirane has been attained, the greater the risk of the oxirane cleavage. There must

be a balance between reaction temperature and reaction time. Reviews on the epoxidation process have reported that the optimal temperature is between 55 - 65 ^{o}C at 5-6 h (Saurabh et al., 2011; Tan and Chow, 2010).

***Reaction time*:** Different reaction times have been reported as seen in Table 3. Increasing reaction time above the optimal condition increases cost and risk of oxirane cleavage. As discussed in the previous paragraph on temperature, the reaction time between 5-6 h is optimal between 55 - 65 ^{o}C.

Stirring Speed: The epoxidation mixture is in three phases (organic, aqueous, and solid) and proper mixing is very important for achieving acceptable results. Stirring speed is one process condition that affects oxirane formation, but it is a factor that depends on reactor and stirrer design. Many studies have shown that no significant difference in oxirane content was observed above a stirring speed of 1800 rpm [amount not indicated] (Dinda et al., 2008); 1500 rpm [22.6 and 28.8 g of oil] (Goud et al., 2006; Mungroo et al., 2008); and 400-500 rpm [179 and 300 g of oil] (Espinoza-Pérez et al., 2009; Pan et al., 2011b). The difference in threshold speeds and mixing has been mainly due to the different quantity of oil epoxidized and/or stirrer used (Tan and Chow, 2010). The most important consideration is that mixing should be sufficient to ensure that the reactants mix properly and assist heat transfer, and increasing stirring speed above this minimum does not influence epoxidation (Dinda et al., 2008; Espinoza-Pérez et al., 2009).

***Catalyst type and amount*:** The catalyst types used during epoxidation have been elaborated in the previous section on epoxidation process. Amberlite IR 120 H is commonly been used due to the ease to separate the catalyst from the resin and also the minimal occurrence

of undesirable side reactions (Sinadinovic-Fiser et al., 2001). The amounts of Amberlite commonly been used is calculated based in 20% of oil weight (Espinoza-Pérez et al., 2011; Pan et al., 2011b; Saurabh et al., 2011), but Amberlite at 6 – 35% of weight have been tested in some optimization studies (Espinoza-Pérez et al., 2009; Mungroo et al., 2008).

Refining process

After the epoxidation process, the crude resin is washed with water and sodium carbonate (Na_2CO_3) solution. The water and Na_2CO_3 wash is to remove excess H_2O_2 and acetic acid that is dissolve or suspended in the crude resin. In most literatures on epoxidation, the washing steps and quantity of reagent used have not been fully described. Even when the quantity of reagent was indicated, there has been no justification on how the amounts were derived. There have been some discrepancies on the way this process is carried out and some might not be economical at a larger scale.

Some articles proposed that the crude resin be washed several times with excess warm water until the resin is free of acid (Dinda et al., 2008; Goud et al., 2007; Okieimen et al., 2002). Meanwhile Gamage et al. (2009) purified the crude by washing the resin with accurate amount of sodium hydro carbonate, in which the amount was not indicated. The washing protocol pursued by Cai et al. (2008) was that the crude be washed with warm water (35-45 ^oC) then dilute solution of Na_2CO_3 until the pH is neutral. In the article by Pan et al. (2011b), the crude was first washed with water five times, then a saturated Na_2CO_3 solution to complete the removal of acetic acid. In Espinoza et al. (2009), the resin was first washed three times with saturated Na_2CO_3 solution and then three times with water solution. The volume of Na_2CO_3 solution and water was three times that of the volume of the vegetable oil being epoxidized. Both Pan et al.

(2011b) and Espinoza et al. (2009) had six washing steps which will likely used the same volume of water during the washing steps since saturated Na_2CO_3 solution is prepared with water. However, Pan et al. (2011b) used less Na_2CO_3 because of five initial water wash and only one saturated Na_2CO_3 wash.

After the washing process, the resin is dried with anhydrous magnesium sulfate ($MgSO_4$). The anhydrous $MgSO_4$ has high affinity for water and adsorbs water molecules from the resin. Most articles did not indicate the amount of $MgSO_4$ used but Espinoza et al. (2009) used 20% of the weight of the resin for the quantity of $MgSO_4$. In Pan et al. (2011b), the amount of $MgSO_4$ used was approximately 6-7% of the weight of the resin. There was no calculation done to justify these values. The difference in the quantity of $MgSO_4$ used may have been due to time allowed for the aqueous and organic phases to separate during the last washing step.

The solid hydrated $MgSO_4$ is usually been removed from the resin through a vacuum filtration unit. However, the type of filtration system to be used must be based on the cost, scale, difficulty to filter, and ease of filtration (Rushton et al., 2000). There are different types of solid-liquid filtration system; pressure, vacuum, centrifugal, gravity, depth filters, granular beds, cartridges, precoat, and membranes (Wakeman, 2011). Epoxidized vegetable oil is usually viscous and diluting the resin in a solvent is usually common in easing the filtration process. The higher the solvent used to rapidly complete the filtration unit, the longer the time needed for devolatilization. Therefore, there must be a balance between the amount of solvent used and solvent removal time. The entire refine process time need to be evaluated.

Energy balance during epoxidation process

Thermal energy balance based on the conservation of energy (first law of thermodynamics) is an important element that can best describe the heating and cooling in a jacketed reactor. In a batch reactor, the accumulated or stored energy within the reactor is given by the difference between energy generated by the reaction and the energy exchanged with the surroundings. In the case of a well-insulated jacket reactor, energy loss to the surrounding will be negligible; therefore, energy exchange will be between the reaction mixture and the circulating fluid in the steam jacketed area (Nassar and Mehrotra, 2011). In an exothermic reaction like the epoxidation process, the simple expression of the heat balance using the first law of thermodynamics in a control volume batch reactor will be;

Stored energy = Generated energy – Exchanged energy – energy loss (Caccavale et al., 2011).

The stored energy is the rate of change of internal energy within the reactor and is related to the total mass of the reaction solution and agitator ($m_r + m_a$), to the specific heat capacity of the total solution and agitator ($c_r + c_a$), and to the rate of change of the reactor temperature (T_r) (Caccavale et al., 2011). The heat generated by the chemical reaction is more complex to calculate as it is the product of the specific molar energy change due to reaction (ΔE_r) and the amount of moles converted in the reactor per unit time (RV_r) (Caccavale et al., 2011). The heat exchange is the rate at which heat is being exchanged between the reaction solution and the wall of the reactor. It depends on the overall heat coefficient (U), heat exchange surface area (A), and the temperature difference between the reactor and the heating or cooling fluid ($T_r - T_f$) (Nassar and Mehrotra, 2011). Therefore, equation 1 will be;

$$(m_r c_r + m_a c_a)\frac{dT_r}{dt} = \Delta E_r \dot{M}_r V_r - UA(T_r - T_f) - q_{loss} \quad \text{(Eq. 1)}$$

Since H_2O_2 is added dropwise, the volume and wetted surface area will be changing during the exothermic phase. These parameters need to be estimated over time. The above equation assumes there is no evaporation from the reaction. In case of evaporation, the heat of evaporation ($M_v * \lambda_v$) needs to be subtracted from the exchange energy. The amount of heat generated during the exothermic process can be calculated by adding the stored and exchanged heat energy if the heat transfer coefficient (U) and specific heat capacity of the reaction (c_r) can be estimated.

Chemical and physical properties of epoxidized vegetable oil

The most important physical properties are viscosity and opacity (transparent); meanwhile, the chemical quality of an EVO resin is mostly determined by the oxirane oxygen content or epoxy equivalent weight, the number of unconverted double bond from the iodine value test, the amount of water content in the resin after drying, acid number for any residual acid, and the hydroxyl value due to oxirane cleavage (Parreira et al., 2002). Low iodine value, low hydroxyl value, and low water content are desirable for an epoxidized vegetable oil resin. Low iodine values indicate a higher degree of conversion of the unsaturated atoms in the fatty acid chain. A low hydroxyl value indicates that very few epoxy bond were degraded to hydroxyl group. This value will not be important if polyols are to be made from the EVO. A low water content should be maintained because water causes degradation of the epoxy group.

Acceptable values for some of these chemical qualities for a commercial epoxidized soybean oil are less than 0.05 for an iodine value, oxirane content greater than 6.3%, and water content less than 300 ppm (Parreira et al., 2002). However, oxirane content will vary based of the

oil type or variety and the degree of epoxidation. The degree of epoxidation or conversion yield can be calculated from the iodine value before and after epoxidation.

The detailed description and the methods used to evaluate these properties are presented below;

Iodine value (IV): is a measure of the degree of unsaturation of fats and oils. It is the amount of iodine in grams needed to react with unsaturated double bonds in 100 g of oil under specific conditions. Iodine value can be estimated from the proportion of total fatty acid content by using equations 2 and 3 (AOCS, 1998).

For triglyceride: IV = (% palmitoleic acid x 0.950) + (% oleic acid x 0.860) + (% linoleic acid x 1.732) + (% linolenic acid x 2.616) + (% gadoleic acid x 0.785) + (% erucic acid x 0.732) (Eq. 2)

For free fatty acids: IV = (% palmitoleic acid x 0.998) + (% oleic acid x 0.899) + (% linoleic acid x 1.810) + (% linolenic acid x 2.735) + (% gadoleic acid x 0.818) + (% erucic acid x 0.749) (Eq. 3)

It can also be determined analytically through the most widely used Wijs method (AOCS, 2003).

***Oxirane oxygen (OO) content*:** is found by quantifying the number of epoxy units present in the resin. The maximum or theoretical oxirane oxygen (OO_t) is predicted from iodine value using equation 4.

$$OO_t = \frac{\frac{IV_o}{2A_i}}{100 + \left(\frac{IV_o}{2A_i}\right)A_o} \; x\, A_o \; x\, 100 \qquad \text{(Eq. 4)}$$

where, $A_i = 126.9$ and $A_o = 16.0$ are atomic weights for iodine and oxygen, respectively and IV_o is the initial iodine value of the oil sample.

The value of oxirane is expressed in percent, for example an OO of 6.1% means 6.1 g O_2 in 100 g or resin.

Actual oxirane oxygen (OO_a) of a resin can be determined analytically through titration by using the American Oil Chemist Society (AOCS) Cd 9-57 protocol. A hydrogen bromide solution opens the epoxide ring by bromination and a hydroxyl is formed. The end point of the titration, which is indicated by a color change, is caused by the presence of excess free hydrogen bromide after all the epoxide groups have been consumed. The conversion of unsaturated to epoxy groups in percent can be calculated from the actual OO and maximum possible as seen in equation 5.

$$\text{Conversion (\%)} = \frac{OO_a}{OO_t}\ x\ 100 \qquad \text{(Eq. 5)}$$

Epoxide equivalent weight (EEW): inversely indicates the amount of epoxy or oxirane groups in a resin sample. Unlike oxirane content which is the weight of oxygen atom in a 100 g of resin, the EEW gives the weight in grams of resin containing 1 mole equivalent of epoxide (g/mole). It can be determined by epoxy titration according to ASTM D 1652 protocol or can be readily obtained from the actual OO content using equation 6.

$$\text{EEW} = \frac{1600}{OO_a} \qquad \text{(Eq. 6)}$$

The number 1,600 is derived from the molecular weight of oxygen multiplied by 100 g of resin.

Hydroxyl value: is the amount of reactive hydroxyl groups available for reaction. It is determined using the standard method AOCS Tx 1a-66. It is a wet analytical method and is reported in mg KOH per gram of sample, which is the amount in milligrams of KOH equivalent to the hydroxyl groups found in a gram of sample.

Moisture content: can be determined using a Karl Fischer titration instrument by adding iodine in the presence of sulfur dioxide, methanol, and in excess pyridine (base). The methanol reacts with sulfur dioxide and pyridine to form an intermediate alkylsulfite salt, which is then oxidized by iodine to an alkylsulfate salt. This oxidation reaction consumes water contained in the oil sample and the end point is potentiometrically monitored. The result is expressed as a percentage which indicates the mass of water in 100 g of the oil sample.

Viscosity: is defined as the internal resistance of a fluid to flow and is highly dependent on temperature. The viscosity of an EVO is definitely higher than its corresponding vegetable oil due to the added oxirane functionality. This oxirane group increases the polarity of the triglyceride chain, which then increases the intermolecular forces between molecules. Viscosity will therefore vary with the source of vegetable oil used and the degree of epoxidation. One study showed that the viscosity of synthetic epoxy resin (petroleum-based) was 209±2.8 mPa·s, epoxidized soybean oil was 169±0.1 mPa·s, and epoxidized canola oil was 129±2.0 mPa·s (Espinoza-Perez, 2009). This viscosity data were obtained at 40 ^{o}C with a cone-and-plate viscometer at shear rate of 5,994 s^{-1}. The data showed that the synthetic epoxy resin was more viscous than the vegetable based resin due to its higher content of epoxy groups per gram of resin.

Viscosity of an epoxy resin is an important parameter in handling, mixing, and processing. This has made industries to set acceptable limits. For example, in a composite industry, a viscosity above 500 mPa·s can cause voids, problems with fiber wetting, and may require longer injection time (La Scala and Wool, 2005). Higher viscosity may also be difficult to handle during the production of polyols, polyurethanes, adhesives, and other resins. Solvent is

usually used to reduce the viscosity at the required level but excessive use of solvent is also environmentally hazardous. Therefore, there must be a balance in the resin chemistry between the viscosity and amount of solvent to be used.

***Acid number (AN)*:** is the acid concentration in a solution. Its value is obtained by measuring the mass of potassium hydroxide (KOH) base in mg which is required to neutralize the acid in one gram of a sample. The AN measures both weak and strong acids in a sample and can be used to measure residual acid in a resin. The AN can then be used in equation 7 to determine the acid equivalent (e_a) of a given amount of resin sample.

$$e_a = \frac{AN\ x\ Wt\ of\ resin\ x\ percent\ solid}{56{,}100} \qquad \text{(Eq. 7)}$$

There are two commonly used ASTM standard test methods; ASTM D-664 and ASTM D-974 for determining the AN. Mahajan et al. (2006) recommended the use of D-974 method to the D-664 in determining AN because it showed better repeatability and reproducibility. However, Wang et al (2008) reported that D-664 is accurate for deeply colored samples and blends, but they were unable to compare same trial with the D-974 method.

Uses of epoxidized vegetable oil

The high reactivity of epoxy groups makes EVO important intermediates for many different applications such as polyols for coatings and polyurethane foams (La Scala and Wool, 2005) and casting resins and adhesives (Guo et al., 2006). Epoxidized soybean oil is currently the only epoxidized vegetable oil being produced commercially. It is mostly being used as a plasticizer and plastic stabilizer in the PVC industry as it is a good substitute for phthalates which has many health concerns (Fenollar et al., 2009). The triglyceride backbone chain in EVO produces a flexible, semi-flexible or rigid elastomeric network structure when subjected to

anhydride curing, amine curing or UV curing (Tan and Chow, 2010). Also, ESO has been shown to be excellent in high temperature lubrication due to its oxidative and frictional behavior (Adhvaryu and Erhan, 2002; Lathi and Mattiasson, 2007). This is because the -O- cross linking between the EVO and the metal surface helps reduce friction between the moving parts.

The EVOs used in composite materials have been shown to have lower thermal and mechanical properties in their final product compared to synthetic resin (Guenter et al., 2003). This is due to lower oxirane functionality in EVO compared to synthetic resin. The common practice is therefore to blend EVO resins with synthetic resin with an appropriate curing agent (Tan and Chow, 2010). Some studies have been conducted to improve the properties of the composite materials in such epoxy blends and also to increase the proportion of EVO to 35-50% in the epoxy blends (Espinoza-Pérez et al., 2011; Fenollar et al., 2009).

The low modulus and thermal strength observed from EVO-based thermosets propelled the interest to develop a better biobased epoxy resin network. Epoxidation of SS has led to the development of novel and highly-functional classes of resins pioneered at North Dakota State University and used as thermosets in coatings (Kovash et al., 2014; Nelson et al., 2013; Yan and Webster, 2014), and composite materials (Hosseini et al., 2013). The thermosets and materials from epoxidized sucrose soyate (ESS) have been shown to substantially improve hardness, storage modulus, and glass transition temperature compared to previous epoxidized vegetable oil-based resins (Hosseini et al., 2013; Yan and Webster, 2014). The high epoxy functionality of ESS led to a rapid gelation and higher cross link density similar to the synthetic epoxy resin (Pan et al., 2012). The good thermal and mechanical properties observed with ESS has attracted interest from many companies for application testing.

Reaction Scale-up of EVO

Scale-up in the mind of an engineer or chemist involves the expansion of an existing process or the development of a new process. Scale-up involves a change from lab scale to pilot scale or from pilot scale to a commercial scale. The question in scale-up is "how do we replicate a result to a pilot or industrial scale design from a standard lab methodology?" The question is critical because when moving from one scale to another, unexpected physical or chemical problems are usually encountered (Bisio, 1985).

The challenges in scaling-up a process are to achieve effective heat and mass transfer rates and materials handling in larger units. Good mixing has been identified as one of the ways to solve heat and mass transfer concerns (Donati and Paludetto, 1997). The small-size lab reactor has a relatively higher surface-to-volume ratio; hence, there is an adequate rate of heat transfer by conduction and radiation through the walls and surfaces of the lab reactor, even with minimum mixing. The adequate rate of heat transfer helps maintain the reaction temperature at the desired level at a small but the rate of heat transfer must be improved as the scale increases (Bisio, 1985).

Scaling up the epoxidation process requires the use of larger amount of reactants, therefore controlling the heat and mass transfer is critical in maximizing oxirane conversion and reducing reaction time and cost. Most epoxidation experiments were carried out at a lab-bench scale of 25 – 300 g, except Gamage et al.(2009), who scaled-up epoxidation of rubber oil, neem and mee fruit oil from 40 g to 1 kg batches. The scale-up process increased the H_2O_2 addition time from 1 h to 2.5 h as temperature was controlled at 60 ^oC. Gerlach and Geller (2004) showed that the needed reaction time significantly increased to allow complete epoxidation; the

scale used by those researchers ranged from 0.5 g to 100 g resin batches. However, when mixing rate was improved (700 – 800 rpm), the reaction time was reduced from 20 h to 12 h.

The epoxidation reaction is highly exothermic and computed to be 243 kJ mol^{-1} for each double bond (Salzano et al., 2012). As the moles of double bonds increases as the reactant volume increases, the amount of heat release or build up in the reactor will also increase. Irrespective of the scale, the reaction temperature and process duration need to be within the optimal conditions in order to have consistent properties during scale-up and between batches.

Process economy and materials cost

Optimizing the scale-up procedure should not only involve technical aspects but also the economic aspects of the process. In a lab scale, time and money are not always the major factors during processes but in a commercial scale they are always the key to continue any industrial process. To follow a direct route from lab to commercial scales requires lots of information that are usually unavailable and sometime changes in the processes during scale-up due to economics or technical feasibility might not be elaborated (Bisio, 1985). Pilot scale production is therefore an important intermediate step which provides the necessary information for industrial scale production.

The amount of reactants for the epoxidation process was calculated based on the molar ratio of acetic acid: H_2O_2: double bond of 0.5:2: 1 and catalyst (Amberlite) was approximately 20% of vegetable oil weight (Espinoza-Pérez et al., 2009; Pan et al., 2011b). Table 4 is the sample calculation of the amount of reactants needed for 1 kg batch of SS. Table 5 then shows the cost of the epoxidation reagents based on the amounts calculated in Table 4. Labor and capital cost were not included which will be a significant additional production cost.

Table 4: Calculations showing the quantity of reagent needed to epoxidized 1 kg batch of sucrose soyate.

Chemical	MW (g mol^{-1})	Grams	Moles Calculations
Sucrose Soyate	2,423	1,000	$\frac{1000\ g}{2423\frac{g}{mol}} * \frac{12\ eq\ double\ bond}{1\ mol}$ = 4.95 moles of d.b.
Acetic acid	60.05	149.0	$\frac{149.0 g}{60.05\frac{g}{mol}} = 2.48$ moles [0.5x moles of SS]
Amberlite	N/A	200	N/A (20% wt. of SS) $1000\ g\ sucrose\ soyate * 20\% = 200 g\ amberlite$
Hydrogen peroxide (50% wt. solution)	34.015	673.5	$673.5 g\ solution * 50\% * \frac{1\ mol}{34.015 g} = 9.90\ moles$ [2x moles of SS]

Table 5: Cost of reagents to epoxidized and purify 1 kg of sucrose soyate

Material	Qty (kg or L)	Unit Cost $	Total cost $
Sucrose soyate	1	5.4/kg	5.4
Amberlite IR 120H	0.2	0.90/kg	0.18
Hydrogen Peroxide	0.6735	0.81/kg	0.55
Acetic Acid **(L)**	0.149	1.57/L	0.23
Sodium Carbonate	0.025	4.95/kg	0.12
Magnesium Sulfate	0.065	0.40/kg	0.03
Hexane **(L)**	0.35	0.32/L	0.11
Total			**6.62**

The unit costs for the reagents were based on prices found online (ICIS Chemicals, 2006-2008); meanwhile, the price for SS was obtained from P&G's price quote for a drum (P&G, 2014). Prices may fluctuate over time but will not deviate far from the values obtained in Table 5. The cost of SS is the most significant expense at 82% of the total cost, but the unit cost may be greatly reduced if non-food grade SS can be produced commercially. After SS, H_2O_2 is clearly a very important cost. H_2O_2 is the oxidizer during epoxidation; therefore, it is one of the reagents that is consumed during epoxidation. Its cost may be reduced through the systematic optimization of epoxidation. The other reagents that are consumed in the production of epoxidized vegetable oil include Na_2CO_3, and $MgSO_4$. These two reagents represent relatively

low costs in Table 5; however, further reduction of these costs is still warranted through more efficient washing and drying steps. Amberlite, acetic acid, and hexane are consumed but aid during synthesis and refining of resin. The cost of these reagents may be substantially reduced if adequate and inexpensive recycling processes are established.

PROBLEM STATEMENT AND OBJECTIVES

Problem Statement

In the last decade, researchers at NDSU have been exploring biobased resin structures that will be competitive with petroleum-based resin in the coating and material science industries. The mechanical and thermal strength of thermosets and coatings made from epoxidized sucrose soyate (ESS) were 3-4 times higher than those from epoxidized vegetable oil (EVO) (Pan and Webster, 2012). This prompted the interest in ESS from many companies for many applications testing. Scaling up lab scale production is needed to meet the current demand for the resin. However, there are many challenges in scaling up EVO from the lab scale to a pilot or industrial scale. Scaling up the epoxidation process requires the proper design and fabrication of a reactor and refining units that would contain a larger amount of reactants, and be able to control heat and mass transfer. The reactor and refining units need to achieve resin properties similar to the lab scale and to reduce reaction time and cost.

The epoxidation process is exothermic (ΔH = -243 kJ mol^{-1} for each double bond) which increases the reaction temperature (Salzano et al., 2012). Reaction temperature increases the rate of oxirane formation, but some studies have reported that temperatures above 65 ^{o}C can cause significant oxirane cleavage (Adhvaryu and Erhan, 2002; Dinda et al., 2008; Goud et al., 2006). It is therefore important to maintain the reaction temperature within the optimal range in order to have consistent resin properties from batch to batch and irrespective of the batch size. At a scale < 150 g, which was the scale in most epoxidation studies, the temperature difference between the reaction mixture and the heating unit may not be significant; therefore, at a small scale it is easy to maintain reactor temperature close to the heating unit temperature during the exothermic

activities. However, as the scale increases, the heat flux from the reaction mixture through the wall of the reactor may become insufficient. This could significantly increase the reactor temperature to a level well above the optimal epoxidation level. Therefore, before the design and fabrication of a reactor for scale-up, it is worthwhile to determine the behavior of the reaction temperature at different H_2O_2 addition rates, heating temperature, and reaction times at a bench-scale.

The process conditions to produce an epoxy functional group from an unsaturated fatty acid chain are similar for all vegetable oils. The fatty acid in sucrose soyate is from soybean oil but fatty acids from canola oil can also be used to produce sucrose esters of fatty acids. This is because soybean and canola oil represent 40% of the total vegetable oil produced in world and >70% in the US. Also, soybean and canola oil have a moderate degree of unsaturation which is important for different biobased resin applications.

At a lab scale, time and money are not always the major factors during processes but at an industrial scale, they are always the key to a viable process. To make the process of ESS synthesis more efficient at an industrial scale, it is important to optimize the epoxidation process conditions and reagents used. The optimization study will therefore provide valuable information and data for an industrial scale production of epoxidized vegetable oil-based resin.

Objectives

The overall objective of the research is to scale up and optimize the production of ESS while maintaining or reducing batch time and achieving high conversion and low degradation. The specific objectives below are grouped into three papers:

Objective 1: Characterize the epoxidation process conditions of canola oil at 300 g laboratory scale for reactor scale-up and the reactor temperature profile at different H_2O_2 additions rates, water bath temperature, and reaction time.

Objective 2: Develop and characterize the performance of a reactor and refining units that would produce 10 kg of epoxidized sucrose soyate (ESS) with a process timeframe and resin quality similar to the 300 g laboratory scale.

***Objective 3*:** Optimize the reagent amounts and process conditions of epoxidized sucrose soyate for industrial scale production, and develop a model that can predict the conversion of double bonds to oxirane at different process scenarios.

PAPER 1: CHARACTERIZING THE EPOXIDATION PROCESS CONDITIONS OF CANOLA OIL FOR REACTOR SCALE-UP[1]

Abstract

Novel epoxidized vegetable oils are of current interest for a variety of applications in coatings and polymeric materials. Samples are needed at quantities beyond gram scale to test such applications. However, scale-up of this very exothermic reaction requires an increased understanding of actual reaction temperature (T_r), which may be much higher than the water bath temperature (T_b). Canola oil (300 g) was epoxidized at three H_2O_2 addition rates (4.6, 2.3, and 1.2 g min^{-1} mol^{-1} unsaturation); at three T_b (55, 65, and 75 ^oC); and at three reaction times (2.5, 4, and 5.5 h). The addition rates were obtained by adding 180 g of H_2O_2 over 0.5, 1, and 2 h. Maximum ΔT ($T_r - T_b$) was attained within 30-40 min of reaction time; thereafter, reactor temperatures gradually declined even though H_2O_2 addition continued. The maximum ΔT (8.7 - 15.8 ^oC) increased as the T_b and H_2O_2 addition rate increased; but, no clear trend was observed in the time maximum ΔT values were attained. The ΔT vs time profile was a useful indicator of the extent of epoxidation and can be used as a criteria to stop epoxidation reaction. The greatest source of variation in oxirane content was from T_b and reaction time. Therefore, T_r must be maintained within the optimal range during the high exothermic periods, if high resin quality and minimal process time is to be achieved during scale-up.

---

[1] This paper was published in February 2015 as Monono, E. M, Haagenson, D. M., and Wiesenborn, D. P. 2015. Characterizing the Epoxidation Process Conditions of Canola Oil for Reactor Scale-up. *Industrial Crops and Products 67 (2015) 364-372*. Ewumbua Monono had primary responsibility for collecting and analyzing laboratory data. Ewumbua Monono was the primary developer of the conclusions that are advanced here. Ewumbua Monono also drafted and revised all versions of this paper. Darrin Haagensen and Dennis Wiesenborn served as proofreader and checked the statistical analysis conducted by Ewumbua Monono.

Introduction

Vegetable oil is one of the most abundant biobased feedstocks and has fatty acid chains with unsaturated double bonds that can be used to produce a wide variety of valuable products (Saurabh et al., 2011). In an effort to address the rising cost and increasing demand for petroleum-based epoxy resin, and transition to sustainable alternatives, epoxidized vegetable oil (EVO) has been successfully used in coatings, polymers, and material science (Tan and Chow, 2010). The epoxy groups are highly reactive and can be directly crosslinked or converted to other valuable functional groups like hydroxyl (polyols), hydroxyl ester, polyurethane, and carbonyl groups, which are used as plasticizers and stabilizers for polymers, lubricants, and resins in composite materials (Guo et al., 2000; Pan and Webster, 2012). The potential modifications to EVO also include substitutions for its glycerol backbone, which can greatly improve the thermal and mechanical strength of composite materials and coatings made from EVO (Pan and Webster, 2012). However, knowledge and equipment are needed to produce novel EVOs and their derivatives in sufficient quantities (much more than gram scale) for product application trials.

There are four major categories of epoxidation processes (Table 3): conventional sulfuric acid, acidic ion exchange resin (AIR), chemo-enzymatic, and metal-catalyzed epoxidation, based on the type of catalyst used (Tan and Chow, 2010). Each of these processes has its advantages, but the AIR process has been the most often reported in the epoxidation of vegetable oil, because of ease of catalyst separation and refining, and the low number of side reactions (Sinadinovic-Fiser et al., 2001). Table 3 also shows that the AIR process gives the best conversion for varied oil type, batch size, and process conditions. In order to have consistent resin properties from batch to batch, the process conditions needed to produce epoxy bonds must be the same

irrespective of the batch size and oil type. The epoxidation reaction with peracetic acid formed in the presence of a catalyst is shown in Fig. 1.

The reaction is very exothermic, which poses a challenge to scale-up. Producing greater batch size requires increasing the reactor size and quantities of reactants but this could result in an excessively high reactor temperature, depending on the H_2O_2 addition rate and reaction time. Controlling reaction temperature (T_r) in a scaled-up reactor is critical to maximize oxirane conversion and minimize reaction time. Most studies in Table 3 assumed that the reactor temperature was the water bath temperature (T_b) or temperature of heating unit. Meanwhile, the one study that monitored the actual reactor temperature used it as a means to control H_2O_2 addition rate, and did not show the temperature-time profile (Pan and Webster, 2012). At a scale < 150 g, which was the scale in most of these studies, the difference between T_r and T_b may not be significant; therefore, it is easier to maintain reactor temperature closer to T_b during the exothermic activities. However, as the scale increases, the heat flux from the reaction mixture through the wall of the reactor may become insufficient. This could significantly increase T_r to a level well above the optimal epoxidation level. Therefore, it is worthwhile to determine temperature behavior at different H_2O_2 addition rates and T_b at bench-scale.

Hydrogen peroxide addition duration, which is inversely proportional to H_2O_2 addition rates (R), has not been commonly discussed in epoxidation reports. H_2O_2 was almost always added into the reaction mixture at a fixed addition rate and duration (Table 3) irrespective of the T_r. In one instance, addition rate was variable based on T_r control within 55 – 65 ^oC (Pan et al., 2011b). Typical H_2O_2 addition rates and durations might be problematic in scale up, because the chemical bonds release more heat relative to the ability of the reactor to dissipate it. In the case

of varying H_2O_2 addition rates as a function of the T_r, it has been observed that total reaction time increases during scale up because of prolonged cooling time (Gerlach and Geller, 2004). Therefore, reaction scale-up requires a better understanding of the T_r as affected by different combinations of H_2O_2 addition rates and T_b, and at a given reaction time. The characterization of T_r at the different process conditions, such as those in Table 3, has not been reported.

Other process conditions that could affect oxirane formation, but which are not included in Table 3, are stirring speed and molar ratio of oil unsaturation: acetic acid: H_2O_2. In terms of stirring speed, different optimum stirring rates have been reported; however, the difference in threshold speed was mainly due to the different quantity of oil epoxidized and/or stirrer used (Tan and Chow, 2010). The most important consideration is that stirring should be sufficient to ensure that the reactants mix properly and assist heat transfer, and increasing stirring speed above this minimum does not influence epoxidation (Dinda et al., 2008; Espinoza-Pérez et al., 2009). The molar ratio of oil unsaturation: acetic acid: H_2O_2 has been explored in some studies. The ratio of 1:0.5:2 was shown to be optimal (Espinoza-Pérez et al., 2009; Goud et al., 2007), and has been used in most epoxidation studies where the ratio was not the subject of interest. Therefore, stirring speed and molar ratio were not varied in our study.

The overall goal is to scale up production while maintaining or reducing batch time and achieving high conversion and low degradation. The objective was to evaluate the effect of different H_2O_2 addition rates T_b, and reaction time on oxirane formation and to characterize the temperature-time profile at these different process conditions. These conditions and results will be used as a benchmark for further reactor scale-up.

Materials and Methods

Materials

Commercial edible-grade canola oil was acquired locally. The ion exchange resin catalyst, Amberlite IR120, was purchased from Acros Organics (Morris Plains, NJ). Aqueous H_2O_2 (50 %), pyridine, 33% hydrogen bromide in acetic acid, and potassium hydroxide (KOH) were purchased from Sigma Aldrich (St. Louis, MO). Glacial acetic acid, acetic anhydride, butyl alcohol, anhydrous sodium carbonate, and hydrogen potassium phthalate were purchased from EDM Chemicals (Gibbstown, NJ). Anhydrous magnesium sulfate was acquired from Mallinckrodt Baker, Inc. (Phillipsburg, NJ).

Epoxidation process

Epoxidation reactions were carried out in duplicate in a 1 L three-necked round bottom flask equipped with a mechanical stirrer (Arrow Engineering Co., Inc., Hillside, N.J.). A glass shaft with a semi-circular Teflon stirrer blade (long-groove keyhole) of 75 mm diameter was attached to the stirrer and operated at 500 rpm. The flask was placed in a thermostated Precision water bath (model 50, Winchester, VA) immersed entirely up to the base of the neck. The equipment and the molar ratio of oil unsaturation: acetic acid: H_2O_2 of 1:0.5:2 was the same as that reported in Espinoza-Pérez et al., (2009); but, this study evaluated different T_b and H_2O_2 addition rates, and the internal reactor temperature was measured.

Canola oil (300 g) with a molar unsaturation of 0.44 moles per 100 g of oil (calculated based on fatty acid composition), 37.5 mL of acetic acid, and 55 g of ion exchange resin (IR) Amberlite IR120 were first added to the flask. Flask contents were stirred while they were close to equilibrium with T_b. A pump (FMI lab pump-model QV, Syosset, NY) added 180 g of

aqueous solution of H_2O_2 (50%) at a constant addition rate over 0.5 h [4.6 g min^{-1} mol^{-1} unsaturation ($R_{4.6}$)], 1 h [2.3 g min^{-1} mol^{-1} unsaturation ($R_{2.3}$)], and 2 h [1.2 g min^{-1} mol^{-1} unsaturation ($R_{1.2}$)]. The total reaction time was 5.5 h including H_2O_2 addition time. Approximately 25 mL of the flask contents were collected at 2.5 h and 4 h to determine the percent oxirane formation at those intermediate times. The flask contents were collected using a 25 mL pipette and while the contents were being stirred.

Temperature data were sensed every 15 s using two type T thermocouples (Omega, Stamford, CT) and the average logged once per min using a CR10 datalogger (Campbell Scientific, North Logan, Utah). Each thermocouple probe was housed in a stainless steel sheath of 150 mm length and 3.2 mm diameter, and had a 300 mm retractable cable than can expand to 1.2 m. The probe tip was placed approximately 1 cm above the stirring blade adjacent to the stirrer shaft. T_b was monitored by a resistance temperature detector (RTD) within the water bath.

After the reaction, the IR was filtered off using cheesecloth, and the filtrates from the 2.5, 4, and 5.5 h samples were allowed to stand in a separatory funnel for 30 min. The lower aqueous layer was then discarded. The organic layer (crude resin) was first washed twice with two volumes (50 mL for intermediate samples and 600 mL for final samples) of water at 40°C and then with 50 mL or 600 mL of saturated sodium carbonate solution at 40°C to neutralize and remove acetic acid. The resin was deemed completely neutralized when effervescence stopped and resin pH was above 7 as determined by pH indicator strip. The saturated sodium carbonate solution was prepared by mixing 40 g of anhydrous sodium carbonate in 100 mL of water. The resin was finally washed twice with 50 mL or 600 mL of water to remove all excess sodium carbonate solution and the neutralized acetic acid. The organic layer was dried overnight with

anhydrous magnesium sulfate. The amount of magnesium sulfate used was 20 percent of the weight of the undried resin. The hydrated magnesium sulfate was removed by filtration under vacuum with Whatman No. 4 filter paper.

Resin characteristics and yield

Actual oxirane oxygen (OO_e) contents of the resins were determined in duplicate using the American Oil Chemist Society (AOCS) method Cd 9-57. The maximum theoretical oxirane oxygen content (OO_t) was estimated at 6.6 % based on the fatty acid profile for this canola oil (Espinoza-Pérez et al., 2009). Therefore, the conversion of unsaturated to epoxy groups was calculated using equation 5.

Hydroxyl value was determined using the standard method AOCS Tx 1a-66 as one measure of degradation of oxirane groups. The results are reported in mg KOH per equivalent of the hydroxyl group in 1 g of sample.

The resin recovery yield was calculated using equation 8. The weight of the epoxy resin included refined resin from samples that were drawn at 2.5 h and 4 h.

$$\text{Recovery yield (\%)} = \frac{Weight(g) of\ epoxy\ resin}{Weight\ (g) of\ canola\ oil}\ x\ 100 \qquad \text{(Eq. 8)}$$

The viscosity was measured in duplicate at 40 ^{o}C using a HAAKE Viscotester model VT 550 (Paramus, NJ) with a cone and plate sensor PK 0.5^{o}. The resin was confirmed to be shear-thinning with a Flow Behavior Index of 0.6, as previously shown for epoxidized canola oil by Espinoza- Pérez et al. (2009). For the purpose of routine viscosity measurements, data were collected at 775.6 rpm at a shear rate of 162.1 s^{-1}.

FTIR spectra were collected from epoxy resins using a Nicolet 6700 FTIR Spectrometer (ThermoFisher Scientific, Madison, WI) operating with 32 scans and a resolution of 4 cm^{-1}. The

spectrometer was equipped with a deuterated triglycine sulfate (DTGS) detector and spectra were collected with the Smart ARK multiple reflection ATR accessories (ThermoFisher Scientific, Madison, WI) equipped with a 45º ZnSe crystal. Peak identities were determined with OMNIC Software version 7.0 (ThermoFisher Scientific, Madison, WI). Peaks of interest were between 3,015 – 3,005 cm^{-1} (C-H stretching of oxirane group) and between 830 – 820 cm^{-1} (C-O-C stretching of oxirane group).

Experimental setup

A 3^3 factorial design was developed with three factors: H_2O_2 addition rate (R), T_b, and reaction time each at three levels. The same two flasks were used simultaneously throughout the study and were considered as replicates. Three different H_2O_2 addition rates ($R_{4.6}$, $R_{2.3}$, and $R_{1.2}$), reaction times (2.5 h, 4 h, and 5.5 h), and water T_b (55, 65, and 75 ºC) were selected. The addition rates of $R_{4.6}$, $R_{2.3}$, and $R_{1.2}$ were 180 g of H_2O_2 added over 0.5, 1, and 2 h, respectively, considering the molar unsaturation of 1.32 moles in 300 g of canola oil. The experimental units were two flasks with canola oil being epoxidized at a given T_b, addition rate, and sample collected at a given reaction time. Therefore, there were 27 experimental units with 2 replicates each for analysis of variance (ANOVA). The response variable for the ANOVA was the oxirane oxygen content or conversion of carbon double bonds to oxirane.

Statistical analysis

Two-way ANOVA was performed using SAS 9.3 (Cary, NC) at 0.05 significance level. The ANOVA analyzed the influence of H_2O_2 addition rates, reaction time, T_b, and their interaction on conversion of carbon double bonds to oxirane. Means comparison for the different

treatments was done using Tukey's test. The SAS program was also used to calculate correlation coefficients.

Results and Discussion

Temperature-time profile of an epoxidation reactor

Temperature is an important factor that influences the rate of a chemical reaction, as shown by the Arrhenius equation. Increasing temperature increases reaction rate of epoxidation and also the reaction rates of side product formation. Therefore, there must be a balance between maximizing oxirane formation and minimizing side reactions when selecting optimal temperature. Selecting and maintaining a constant temperature is important, but it is not easy because epoxidation is exothermic; thus, the reactor temperature rose sharply above T_b during initial H_2O_2 addition (Fig. 7). Reaction temperature at different T_b and addition rates were monitored over time between duplicate flasks. Variability in T_r for both flasks at any given time was mostly less than 1.0 ^oC; however, a difference of up to 1.4 ^oC was observed for some cases. Generally, the highest temperature differences between the two flasks were observed at the maximum temperatures.

The temperature-time profiles in Fig. 7 are similar irrespective of the addition rate; however, the T_r profiles are higher and steeper at the fastest addition rate (Fig. 7a) compared to the slower addition rates in Figs. 7b and 7c. The T_r reached 90 ^oC at the fastest addition rate (Fig. 7a) at T_b of 75 ^oC, but the maximum T_r fell with decreasing addition rate. Time zero in Fig. 7 corresponds to the beginning of H_2O_2 addition. T_b was measured by an inbuilt RTD, which verified that the set point T_b values of 55 ^oC, 65 ^oC, and 75 ^oC were maintained throughout each reaction.

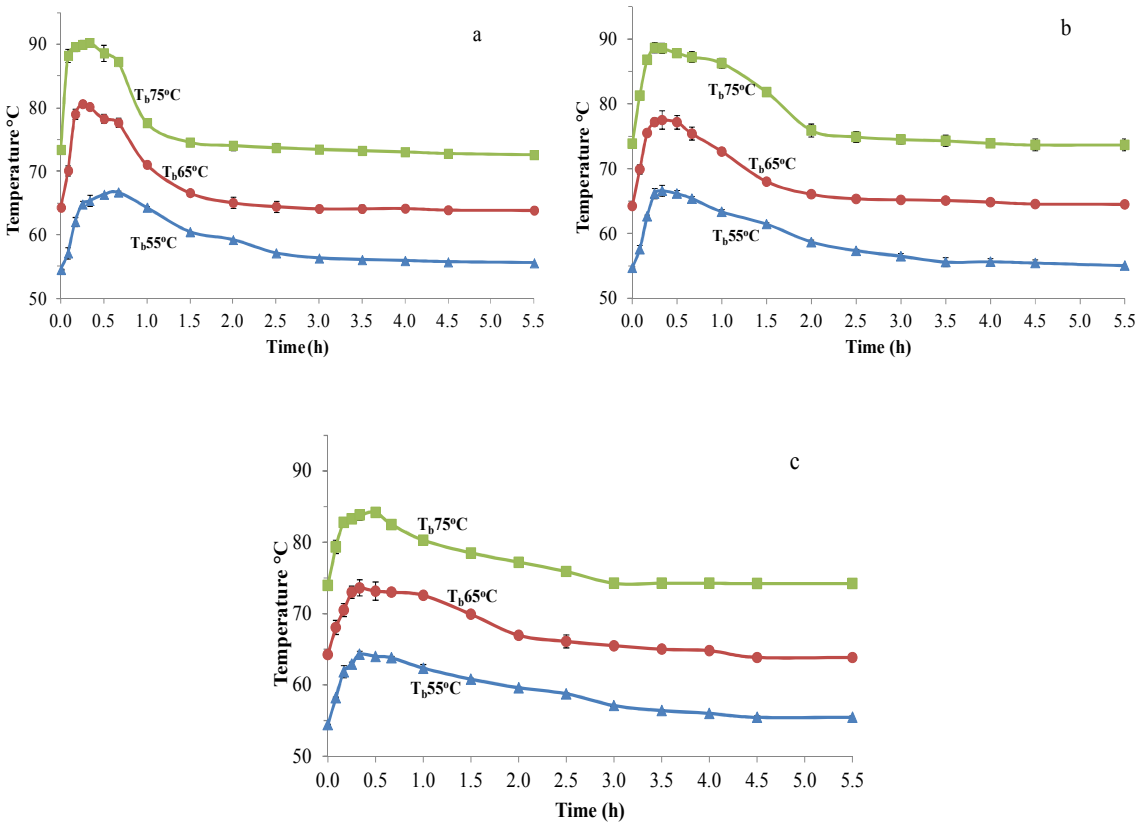

Fig. 7: Temperature-time profiles for three H_2O_2 addition rates (a) 4.6 g min^{-1} mol^{-1} unsaturation; (b) 2.3 g min^{-1} mol^{-1} unsaturation; and (c) 1.2 g min^{-1} mol^{-1} unsaturation at three water bath temperatures (55, 65, and 75 °C). Error bars indicate standard deviation (n=2).

Many studies (Table 3) have reported the effect of T_b on oxirane formation, but have not documented the actual internal reactor temperature-time profile. These studies typically assumed the T_r to be the same as the T_b. Fig. 7 shows that such an assumption is not accurate; T_r was much greater than T_b for a significant amount of time (~1 h) as shown in the ΔT-time profile in Fig. 8. For a given addition rate, even though there were slight differences in the maximum ΔT attained at the different T_b, the ΔT profiles at the different T_b values were strikingly similar, especially at the lowest addition rate (Fig. 7c). The reaction ΔT values were calculated relative to the reactor temperature at time zero rather than T_b because the reactor temperatures at time zero

were slightly lower (0.5 – 1.0 ^{o}C) than T_b. This could be due to the different locations of the water bath and reactor temperature sensors or the higher accuracy and repeatability of the RTD in the water bath than the type T thermocouple in the reactor. Before the end of H_2O_2 addition at $R_{2.3}$ and $R_{1.2}$ (addition duration of 1.0 h and 2.0 h, respectively), the T_r started dropping gradually after the maximum ΔT was attained in just 18 – 30 min (Figs. 3b and 3c). The drop in ΔT was more gradual when the reaction was conducted at the lowest addition rate (Fig. 8c). At T_b 65 ^{o}C and 75 ^{o}C, the T_r was approximately 1-1.5 ^{o}C less than the T_b for the final 1 – 2 h (Fig. 8). This essentially indicated the end of epoxidation, and thus the T_r returned to time zero temperature.

The maximum height (ΔT_{max}) represents the point at which the heat generation rate equals the heat removal rate. Meanwhile, the steepest slope before ΔT_{max} indicates the highest reaction rate throughout the reaction. The ΔT_{max} were attained within the first 30 min of reaction time, but ΔT_{max} and peak times varied with addition rates and T_b as shown in Table 6. Apart from the highest addition rate ($R_{4.6}$) at T_b = 55 ^{o}C, the value for the ΔT_{max} fell as the addition rate was reduced. It was expected that the peak time should increase as the addition rate decreased, but peak time showed no clear trend.

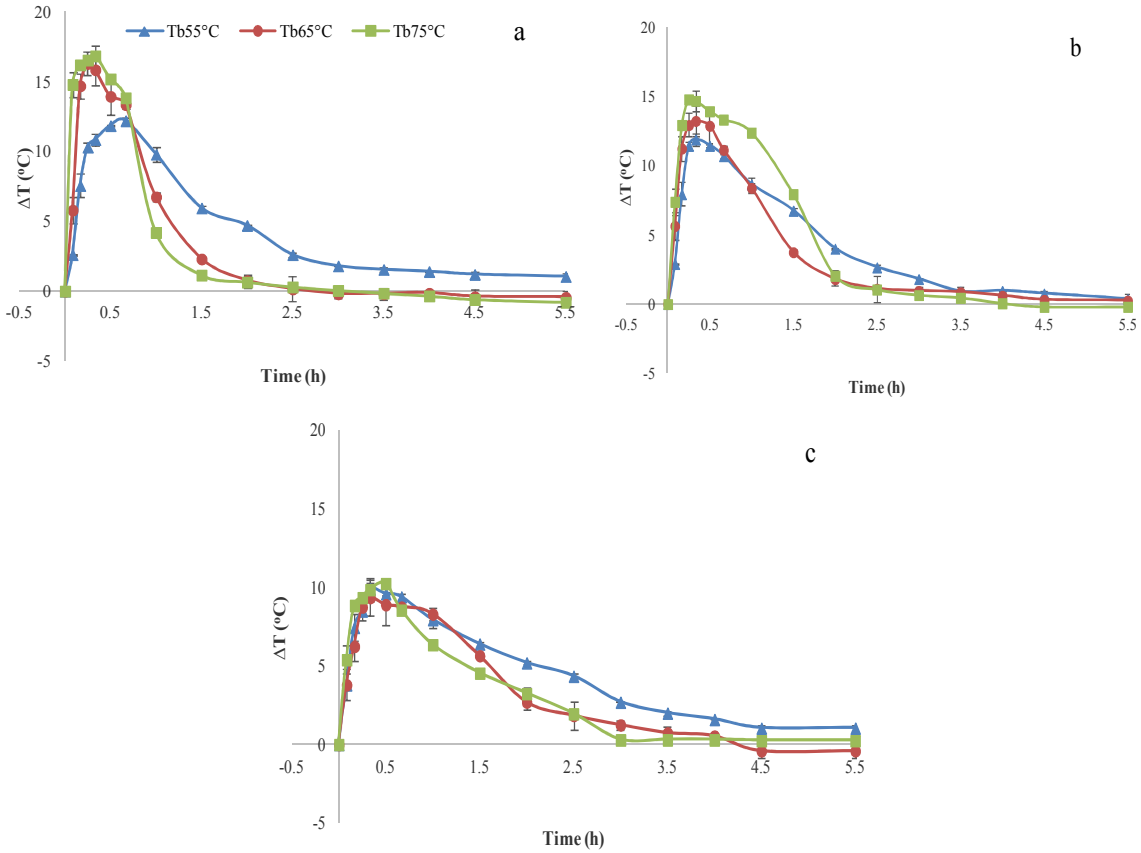

Fig. 8: Delta temperature (ΔT)-time profile for three H_2O_2 addition rates (a) 4.6 g min^{-1} mol^{-1} unsaturation; (b) 2.3 g min^{-1} mol^{-1} unsaturation; and (c) 1.2 g min^{-1} mol^{-1} unsaturation at three water bath temperatures (55, 65, and 75 °C). Error bars indicate standard deviation (n=2).

This inconsistency may be due to the volume and the temperature (~ 15-20 °C) of H_2O_2 added at the different rates. That is, at the highest addition rate ($R_{4.6}$), 180 g of H_2O_2 at 15-20 °C was added over 30 min; meanwhile at the lowest addition rate ($R_{1.2}$), this same volume of H_2O_2 was added over 2.0 h. The average ΔT over the first 2.5 h of reaction time is probably a better indicator of the extent of epoxidation than ΔT_{max}. The lowest average ΔT observed with the lowest addition rate corresponds to the smallest area under the temperature-time profile in Fig. 7c. Reducing the addition rate from $R_{2.3}$ to $R_{1.2}$ reduced the average ΔT by 15% to 30%. If high

epoxidation can be achieved with low average ΔT, then reduction in addition rate during high exothermic peroid could be one important strategy in controlling temperature when scaling up.

Table 6: Maximum ΔT (ΔT_{max}) and time for the different combination of H_2O_2 addition rate (R) [g/min/mole] and bath temperature (T_b) [^oC].

Process condition	ΔT_{max} (^oC)	Peak time (min)	ΔT at 2.5 h (^oC)	ΔT_{avg} (^oC) (1st 2.5 h)
$R_{4.6}$_T_b55	12.2±0.2	40.0±2.8	2.6±0.2	7.1±4.2
$R_{4.6}$_T_b65	16.3±0.2	15.0±1.4	0.2±0.1	8.2±6.8
$R_{4.6}$_T_b75	16.9±0.4	18.5±0.7	0.3±0.4	9.1±7.5
$R_{2.3}$_T_b55	11.9±0.9	20.0±0.7	2.7±0.2	7.1±4.2
$R_{2.3}$_T_b65	13.4±1.1	18.0±0.0	1.1±0.2	7.5±5.2
$R_{2.3}$_T_b75	14.8±1.2	17.0±1.4	1.1±0.8	9.1±5.8
$R_{1.2}$_T_b55	9.9±1.4	24.5±2.1	4.4±0.1	6.6±3.0
$R_{1.2}$_T_b65	9.4±0.5	24.0±0.7	1.8±0.9	5.8±3.3
$R_{1.2}$_T_b75	9.9±0.7	30.0±2.1	2.0±0.1	6.2±3.5

At the onset of H_2O_2 addition, there are two reactions that occur: first, the formation of peracetic acid through the reaction of H_2O_2 and acetic acid, and second, the formation of the oxirane bond through the reaction of peracetic acid with fatty acid double bonds as shown in Fig. 1. Both reactions are exothermic. The estimated energy release during epoxidation is 243 kJ mol^{-1}, where approximately 230 kJ mol^{-1} is from the reaction of double bonds with peracetic acid (Salzano et al., 2012) and 13.7 kJ mol^{-1} is for peracetic acid formation (Dul'neva and Moskvin, 2005). Thus the energy released from the reaction of double bonds with peracetic acid is approximately 15 times more than that from the reaction of peracetic formation. The sharp increase in the reaction temperature-time profile within the first 30 to 40 min of H_2O_2 addition is mainly due to the high rate of the epoxidation reaction relative to the heat transfer rate through the wall of the glass reactor. The rate of energy release is directly proportional to the rate of epoxidation reaction. The T_r starts dropping even as H_2O_2 addition continued for the addition

rates $R_{2.3}$ and $R_{1.2}$ (above 1 h H_2O_2 addition duration). This is because the rate of heat transfer from the reaction mixture to the water bath increases as the temperature gradient increases, and also the rate of heat produced decreases as the concentration of double bonds reduces.

Effect of H_2O_2 addition rate, temperature and reaction time on oxirane content

The effects of H_2O_2 addition rate, T_b, and reaction time on oxirane content were investigated by looking at trends in oxirane values and the extent of epoxidation, and then by conducting a statistical analysis. The oxirane and conversion values in Table 7 were means of 4 replicates; that is, 2 replicates during epoxidation and 2 replicates each during oxirane titration. The standard deviation of the oxirane values were generally less than 0.1% (coefficient of variability < 3%), though some exceptions were observed. The letters for the mean comparison was not done randomly across Table 7, but by comparing the means horizontally at each reaction time (2.5 h, 4 h, and 5.5 h) and vertically at each T_b.

The results at reaction time 2.5 h show that oxirane content and the extent to which double bonds were converted to epoxy groups increased with increasing T_b and addition rates. At the highest addition rate ($R_{4.6}$) and T_b (75 ^oC), the oxirane content was already > 95% of the maximum achievable oxirane content. Even at the lowest addition rate ($R_{1.2}$), conversions of 90% and 93% at T_b of 65 ^oC and 75 ^oC, respectively, were observed. This very high completion of epoxidation within 2.5 h were consistent with the maximum areas for plots of ΔT versus time in Fig. 8 observed during this period, as well as the very low ΔT values at 2.5 h (Table 6). Even at the lowest T_b (55 ^oC) and addition rate ($R_{1.2}$), epoxidation was 83% complete at 2.5 h of reaction time.

Table 7: Effect of H_2O_2 addition rate (R) and bath temperature (T_b) on oxirane content (%) [upper values] and conversion of carbon double bonds to epoxy groups (%) [lower values] at different reaction time. Bold values indicate maximum values within each column.

Time	$R_{4.6}$ (g/min/mole)			$R_{2.3}$ (g/min/mole)			$R_{1.2}$ (g/min/mole)		
	T_b=55 °C	T_b=65 °C	T_b=75 °C	T_b=55 °C	T_b=65 °C	T_b=75 °C	T_b=55 °C	T_b=65 °C	T_b=75 °C
2.5 h	5.92±.09 89.7^{c}	6.14±.03 93.1^{dm}	**6.31±.03** **95.7^{e}**	5.76±.09 87.3^{b}	6.18±.05 93.7^{dp}	**6.22±.1** **94.2^{d}**	5.51±.02 83.6^{a}	5.95±.09 90.2^{c}	6.16±.07 93.3^{d}
4 h	6.04±.02 91.6^{g}	6.12±.06 92.7^{ghm}	6.17±.09 93.5^{hn}	6.13±.08 92.9^{gho}	6.19±.05 93.8^{hp}	6.13±.07 92.8^{gh}	5.88±.10 89.1^{f}	6.14±.15 93.0^{gh}	**6.39±.12** **96.8^{i}**
Final (5.5 h)	**6.37±.11** **96.5^{k}**	**6.33±.08** **95.9^{kl}**	6.14±.01 93.0^{jn}	**6.19±.19** **93.3^{jo}**	**6.24±.04** **94.5^{jl}**	6.16±.07 93.3^{j}	**6.18±.05** **93.7^{j}**	**6.32±.06** **95.8^{kl}**	6.12±.05 92.8^{j}

Note: Maximum oxirane content of 6.6 % was used. Same letters vertically and horizontally indicate that the values are not significantly different.

Sampling was not done before 2.5 h, because the relative amounts of reactants would be altered if samples were collected before all H_2O_2 was added. Therefore, the first sample (2.5 h) was taken after completion of H_2O_2 addition; the time between the end of H_2O_2 addition and the first sampling varied among the different H_2O_2 addition rates (2 h for $R_{1.2}$, 1 h for $R_{2.3}$, and 0.5 h for $R_{4.6}$). Due to this difference in sample time and end of addition rate, the conversion percent was significantly higher for the same T_b as the addition rate increases. Similar high conversions of > 75% in 3 h at 60 °C were reported by Gamage et al. (2009); meanwhile, 30% – 40% conversion in 1 h of reaction time was reported when epoxidation was conducted between 55 °C and 75 °C (Goud et al., 2006; Mungroo et al., 2011; Vlček and Petrović, 2006). Continuing the reaction beyond 2.5 h was necessary to observe if a higher oxirane content could be achieved. High oxirane content is desired for a better-crosslinked network in composite materials, polymer, and coatings. This better network will in turn improve mechanical and thermal properties of the

products. However, if the resin is used as a plasticizer, extending the reaction time might not be cost effective.

As the reaction continued to 4 h, the oxirane contents increased nearly 0.4%, and were significantly different for samples that were produced at T_b of 55 ^oC and the two low addition rates ($R_{1.2}$ and $R_{2.3}$) when compared to 2.5 h sampling. Even at high T_b of 75 ^oC at this lowest addition rate, an increase (~0.2%) in oxirane content was observed and it was significantly different from values at 2.5 h sampling. At the highest ($R_{4.6}$) and moderate ($R_{2.3}$) addition rates, oxirane content actually fell significantly at T_b of 75 ^oC and 65 ^oC ($R_{4.6}$ only). Meanwhile at T_b of 55 ^oC, the increase in oxirane content was 0.14-0.3%. After 2.5 h, the reaction was nearly complete (Fig. 7) and T_r essentially returned to T_b for samples at 65 ^oC and 75 ^oC. But samples at T_b 55 ^oC still experienced slight exothermic activities after 2.5 h. The maximum achievable oxirane content of 6.39% was attained at $R_{1.2}$ and T_b 75 ^oC.

The oxirane contents after 5.5 h of reaction and at T_b 55 ^oC significantly increased (> 0.30%) compared to the 4 h samples except $R_{2.3}$. The oxirane content of 6.18% at 55 ^oC and $R_{2.3}$ indicates that epoxidation is continuing where some slight exothermic reaction (ΔT = 0.5 ^oC at 5.5 h) could be seen in Fig. 8. Extending the reaction time beyond 5.5 h at this lowest T_b and addition rate could have increased the oxirane content. At T_b 65 ^oC, there was an increase of 0.05 – 0.2% in oxirane content compared to the 4 h reaction time. Some oxirane values at T_b 55 ^oC and 65 ^oC at 5.5 h significantly increased from the oxirane content observed at 4 h. This increase justifies extending the reaction time to 5.5 h at these temperatures. At T_b 75 ^oC, the oxirane content reduced as the reaction time continued beyond 4 h. Oxirane cleavage likely occurs when

the reaction continues at this high temperature, which is similar to results reported by Mungroo et al. (2008); Dinda et al. (2008); and Okieimen et al. (2002).

Fig. 9 visually shows without any statistical analysis how oxirane content changes by varying T_b and addition rates. In Fig. 9a where oxirane content for different addition rate were averaged at the same T_b, it was observed that the difference in oxirane content at 4 h was getting closer. This is because more oxirane was formed at lower T_b while at 75 ^oC, the oxirane content seems to be the same with the 2.5 h sampling. When oxirane contents at different T_b were averaged at the same addition rate, the oxirane contents were approximately the same (Fig. 9b) at 4 h for the different addition rates. Looking at Fig. 9 during 4 h reaction time, a difference in oxirane content was clearly visible in Fig. 9a compared to Fig. 9b.

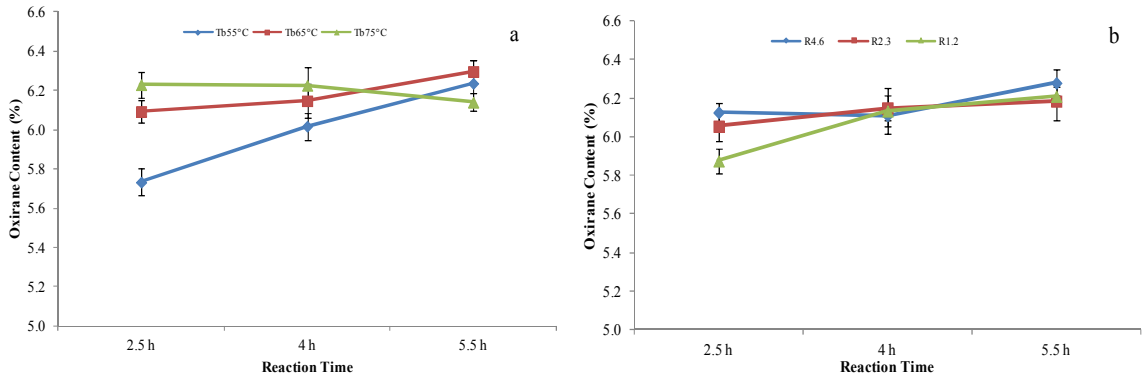

Fig. 9: Effect of (a) bath temperature, T_b; and (b) addition rate, R on oxirane content. Error bars show standard deviation (n=4).

To statistically test the effect of T_b, addition rate, and reaction time on oxirane content, an ANOVA test was conducted (Table 8). Oxirane formation was significantly impacted by all of these factors and their interactions with p-value < 0.0001. However, T_b had a greater influence on oxirane content than addition rate, as indicated by the F-value, which was approximately seven times higher than that for addition rate. Most of the variability in oxirane content was

based on T_b (21.3%), reaction time (18.1%) and interaction between T_b and reaction time (25.7%). Variability due to addition rate was only 4.2% and even its interaction with other factors were less than 7%. Some studies have shown that the change in H_2O_2 concentration (30% or 50%) used influences the oxirane content (Espinoza-Pérez et al., 2009; Goud et al., 2007; Mungroo et al., 2011; Santacesaria et al., 2011); but in our study, it is observed that the effect is not as great as that experience from varying T_b and time to stop the reaction.

Table 8: ANOVA on the effect of bath temperature (T_b), H_2O_2 addition rate (R), and reaction time (t) on oxirane content. Values in parenthesis represent percent variation attributable to source of variation.

Factors	DF	Type I SS	MS	F-value	*p*-value
T_b	2	207 (21.3%)	103.78	67.26	< 0.0001
T	2	176.56 (18.1%)	88.28	57.22	< 0.0001
R	2	40.58 (4.2%)	20.29	13.15	< 0.0001
T_b x t	4	250.76 (25.7%)	62.69	40.63	< 0.0001
T_b x R	4	61.15 (6.3%)	15.29	9.91	< 0.0001
R x t	4	67.11 (6.9%)	16.78	10.87	< 0.0001
R x T_b x t	8	46.07 (4.7%)	5.76	3.73	0.0009
Error	81	124.98 (12.8%)	1.54		
Total	107	974.78			

The ANOVA analysis supports the trend observed from Fig. 9 that T_b had a greater influence on oxirane content than addition rate. Therefore, knowing the T_r, which is usually higher during the peak epoxidation, is important to better control the reaction. The interaction between T_b and addition rate, T_b and reaction time, and addition rate and reaction time were also statistically significant ($p < 0.0001$). The significant interactions between these factors indicate that oxirane content differences between one factor is not consistent across the other factor.

Oxirane content change over time (p-value < 0.0001) and the F-value was slightly lower than that for T_b. It is normal to expect oxirane content to change over time as more oxirane is

either being formed or destroyed when the reaction continues. Also, varying the T_b and addition rate influences the oxirane content at different reaction time. The desire is to have the maximum possible oxirane content at the shortest possible time under the most controllable temperature and addition rate. The highest mean oxirane values of 6.32 – 6.39%, which represents 95.8 – 96.8% conversion of double bonds to epoxy groups, was observed in four treatment combinations. These values were not significantly different (p-values < 0.05), as determined by Tukey's test. The treatment combinations with the highest oxirane values at 5.5 h reaction time were at T_b 55 ^oC and 65 ^oC, and at the highest and lowest addition rates. Irrespective of the addition rate, the highest oxirane content for each treatment at T_b 55 ^oC and 65 ^oC was achieved at 5.5 h (bold values in Table 7). However, at T_b 75 ^oC, the highest oxirane content were achieved at 2.5 h for addition rates $R_{4.5}$ and $R_{2.3}$ and at 4 h for the slowest addition rate $R_{1.2}$.

Choosing when to stop the reaction depends on the operating temperature. The decision to operate a scaled-up reactor at 75 ^oC for 2.5 - 4 h or at 55-65 ^oC for 5.5 h will be based on comparing the cost of operating a reactor at higher temperature for shorter reaction time or lower temperature for longer reaction time. As T_b increases, ΔT increases will require more cooling energy to control this extra energy. At an initial batch during scale-up, slow addition rate $R_{1.2}$ (addition within 2 h) would be preferable at T_b 65 ^oC. If reactor temperature control is fine-tuned during scale-up, increasing addition rate at T_b between 55 – 65 ^oC could eventually speed up the initial rate of reaction and reduce the total reaction time and cost.

This study shows the need for more effective measures to control temperature during scale-up. The first 1 h of reaction was a very critical period of high T_r due to the high rate of epoxidation, a very exothermic reaction. Maintaining the optimal temperature throughout the

reaction time requires that heat transfer be improved during this first 1 h of reaction. This can be done by replacing the water bath with cooling water and using a reactor wall material with better thermal conductivity. In some studies on the effect of temperature on oxirane content, T_b was reduced by 5-10 ^oC during the H_2O_2 addition stage, then was subsequently raised to target temperature of 55 or 65 ^oC once H_2O_2 addition ended (Goud et al., 2006; Mungroo et al., 2008). This action was to reduce the extent to which temperature exceeded the target reactor temperature during H_2O_2 addition. However, in our study, it was observed that the reaction is still exothermic even after H_2O_2 addition ended; therefore, a gradual increase in T_b is required.

The gradual increase in T_b after H_2O_2 addition will help maintain a constant T_r throughout the reaction time, even at high H_2O_2 addition rate. When scaling up to a much greater batch size, this temperature gradient ($T_r - T_b$) must be greater than the 8-15 ^oC in the 300 g scale and might require a more gradual increase in T_b. Also, choosing a material like stainless steel with better thermal conductivity than glass is preferable for a scaled up design. Another way to improve temperature control is by minimizing the amount of heat produced by using variable H_2O_2 addition rate, as needed, to reduce ΔT. The variable H_2O_2 addition rate can be automated and synchronized with the T_b so that total reaction time would not increase. It was observed that the reaction was at least 83% complete at the end of H_2O_2 addition, therefore it is logical to add H_2O_2 during half of the total reaction time, thereby preventing any possible increase in the total reaction time during scale up.

Viscosity, hydroxyl values, and resin yield

The viscosity values at 40°C for the epoxidized samples were greater than 225 mPa·s and approximately five times greater than the viscosity of canola oil (Table 9). Samples epoxidized at

T_b = 75 °C were slightly more viscous than samples that were epoxidized at the same rate but lower T_b. These higher viscosities indicate that there was likely oxirane cleavage resulting in the formation of hydroxyl, carboxylic, and ketone groups that increased intermolecular bonding. The epoxy samples produced at T_b of 75 °C were subsequently confirmed to have higher hydroxyl values than samples produced at T_b of 55 °C and 65 °C for the same H_2O_2 addition rate (Table 9).

Table 9: Viscosity at 40 °C and hydroxyl values (mean ± SD) for canola epoxidized after 5.5 h reaction time at the different conditions of hydrogen peroxide addition rate (R) and bath temperature (T_b).

Sample	Apparent viscosity (mPa·s)	Hydroxyl value (mg KOH/g)
Canola Oil	54.5 ± 0.7	NA
$R_{4.6}$_T_b55	225.0 ± 1.1	5.8 ± 0.2
$R_{4.6}$_T_b65	234.5 ± 0.8	6.4 ± 0.4
$R_{4.6}$_T_b75	241.5 ± 0.7	7.1 ± 0.5
$R_{2.3}$_T_b55	226.5 ± 1.4	5.0 ± 0.9
$R_{2.3}$_T_b65	242.5 ± 1.5	6.0 ± 0.6
$R_{2.3}$_T_b75	250.0 ± 1.0	7.3 ± 0.4
$R_{1.2}$_T_b55	229.0 ± 0.5	4.5 ± 0.6
$R_{1.2}$_T_b65	250.0 ± 1.0	5.7 ± 0.7
$R_{1.2}$_T_b75	275.0 ± 0.5	9.1 ± 1.3

KOH = potassium hydroxide; NA = not applicable

Hydroxyl groups are major side products of epoxidation when the reaction continues at high temperature in the presence of excess water and H_2O_2 (Gamage et al., 2009). The viscosity values in Table 9 were positively correlated with the hydroxyl values (r = 0.85; p-value = 0.0038). Hydrogen bonding increased as the amount of hydroxyl groups increased, thereby, resulting in higher viscosity. Even though viscosity increased with oxirane content, the differences in viscosity for the final samples was not due to the differences in oxirane content because viscosity values were not significantly correlated with oxirane values (r = -0.46; p-value = 0.2209).

Resin yield obtained during the epoxidation process from the 9 treatments averaged 78.5±2.4%. This value was similar to the yield of 80.0% reported by Espinoza- Pérez (2009) for similar reaction and refining conditions. A resin yield of 90-95% was reported when solvent was used in the epoxidation process (Espinoza-Pérez et al., 2009; Pan et al., 2011b). Resin yield would have been higher if a solvent was used to recover resin which adhered to the wall of the flask, cheesecloth and catalyst; however, maximizing yield was not the main focus.

FT-IR analysis

The FTIR is a rapid, nondestructive analytical tool that is often used to show the presence of oxirane oxygen qualitatively or quantitatively. The FTIR spectra in Fig. 10 show the presence of epoxy groups at 822-833 cm^{-1} (Espinoza-Pérez et al., 2009; Vlček and Petrović, 2006). A canola oil spectrum, having no epoxy groups, served as a control and has no significant absorbance in this region. The absorbance observed at 823.3 cm^{-1} wavenumbers was linearly proportional to the oxirane values with an *r* value of 0.873 (*p*-values = 0.0021). This indicated that 87.3% variation of FTIR absorbance is accounted for by variation in oxirane content. The highest absorbance ($R_{4.6}$_T65) and the lowest absorbance ($R_{1.2}$_T75) in Fig. 10 corresponded to the highest and lowest oxirane values, respectively in Table 7. This indicates that there is a great potential for developing an FTIR calibration models to quantify oxirane content of epoxy resins that would eliminate time consuming, and potentially hazardous acid titrations. Parreira et al. (2002) developed a quantitative model in predicting epoxidized soybean oil using NIR spectroscopy, but nothing has been done in developing a more robust calibration model using advanced NIR (faster scan rate and better resolution) and statistical software. The predictive

model can be greatly improved by increasing the amount of samples, pretreatment of spectral data, and using more spectra or range of wavenumber.

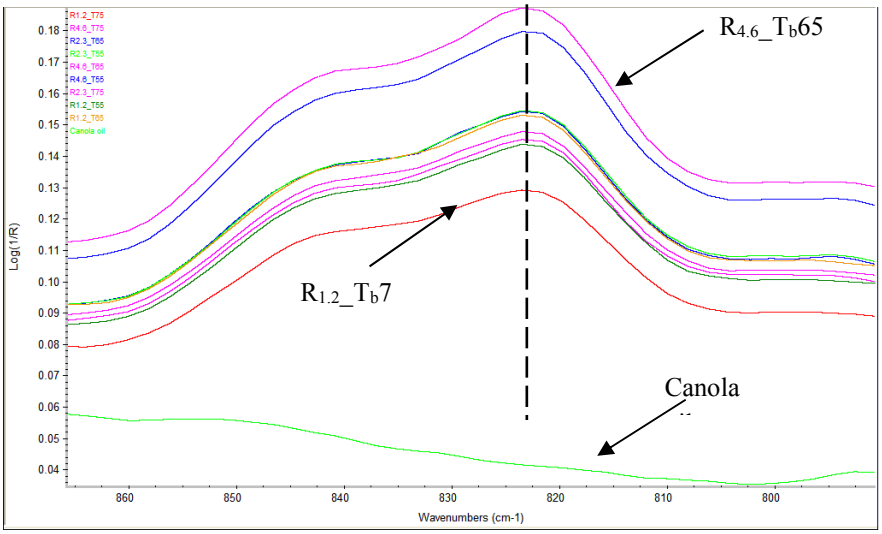

Fig. 10: FTIR spectra for epoxidized canola oil; the peak at 823.3 cm^{-1} shows the presence of epoxy groups. R – H_2O_2 addition rate and T_b – bath temperature.

Conclusion

The T_r markedly exceeded the T_b, and the deviation depended upon both the T_b and H_2O_2 addition rate. The T_r sharply increased at the early stage of the reaction due to high exothermic conditions and reaction rates, but then decreased as epoxidation became substantially complete, at which point heat transfer to the bath exceeded the heat generation rate from the reaction. This decrease in T_r occurred even as H_2O_2 addition was ongoing. The temperature rise likely contributed to undesirable oxirane ring cleavage, but the temperature-time profiles also provide helpful insight into the completion of epoxidation. The initial spike in the T_r would potentially be even greater at a larger scale, showing the need to develop strategies for improved temperature control. These strategies could be by: cooling with a water T_b that is at least 10-15 ^oC lower than

the T_r, using variable H_2O_2 addition rate with the lowest rate during high exothermic period, and using a reactor wall material with better thermal conductivity.

PAPER 2: PILOT SCALE (10 KG) PRODUCTION AND CHARACTERIZATION OF EPOXIDIZED SUCROSE SOYATE[2]

Abstract

The objective of this study was to develop and characterize the performance of a reactor and refining units that would produce 10 kg of epoxidized sucrose soyate (ESS) with a process timeframe and resin quality similar to the 300 g laboratory scale in order to meet the increasing demand for multiple applications in coatings and composite materials. Scale up challenges involve maintaining suitable reaction temperature and time, achieving high double-bond conversion, minimizing side reactions, and avoiding excessive refining time. To accomplish this, a 38 L stainless steel steam-jacketed GROEN kettle was modified for use as an epoxidation reactor. The modifications helped achieve adequate mixing, heat transfer and temperature control. Consequently, the reaction temperature was successfully controlled between 55-65 ^{o}C by varying the H_2O_2 addition rate and the fluid temperature in the reactor's jacket. Twenty 7-10 kg batches were produced which had similar resin quality as the lab scale, an overall 87.5% resin yield, and > 98% conversion of double bonds after batch three. The total production days were reduced from 8 to 4 after a 40 L refining funnel was fabricated for washing, gravity phase separation, and filtration, and an explosion-proof solvent extraction unit was adapted for devolatilizing hexane used during refining.

---

[2] This paper was published July 2015 as Monono, E.M., Webster, D.C., and Wiesenborn, D.P. Pilot Scale (10 kg) Production and Characterization of Epoxidized Sucrose Soyate. *Industrial Crops and Products 74 (2015) 987-997.* Ewumbua Monono had primary responsibility for collecting and analyzing laboratory data. Ewumbua Monono was the primary developer of the conclusions that are advanced here. Ewumbua Monono also drafted and revised all versions of this paper. Darrin Haagensen and Dennis Wiesenborn served as proofreader and checked the statistical analysis conducted by Ewumbua Monono.

Introduction

There has been increasing interest in using renewable and sustainable raw materials in the polymer and materials science communities because of environmental concerns and uncertainty in petroleum resources (Gandini, 2011; Meier et al., 2007). The renewable raw materials that are mostly used in polymer and materials science research include sugars and polysaccharides, vegetable oils and glycerol, lignin, and rosin (Gandini, 2011). All or just about all of these renewable materials are already well established for industrial use. However, many new products derived from such materials have not yet advanced beyond the initial trial stages. In the coatings and materials science industries, there is an interest in creating a better resin system derived from vegetable oil that will be competitive with petroleum-based resins. This led to the development of epoxidized sucrose ester of fatty acids which has been used in a variety of applications, including the preparation of thermoset coatings (Pan et al., 2011a; Pan and Webster, 2012).

Sucrose is a polyol having eight hydroxyl groups which can be fully substituted with fatty acids from vegetable oil to form sucrose ester of fatty acid (Fig. 5). Sucrose esters of unsaturated fatty acids were first reported in coatings in the early 1960s (Walsh et al., 1961), but achieving a high degree of substitution (DS) came much later. In the last decade, Procter and Gamble (P&G) developed a commercial process for sucrose esters with a high average DS of at least 7.7 [marketed under the trade name SEFOSE] (Corrigan, 2003). SEFOSE derived from soybean oil is usually referred to as sucrose soyate (SS). Epoxidation of SS has led to a novel and highly-functional class of resins. Epoxidized sucrose soyate (ESS) used in thermosets has demonstrated substantially improved hardness, storage modulus, and glass transition temperature compared to previous epoxidized vegetable oil-based resins (Pan et al., 2011a; Pan and Webster, 2011; Yan

and Webster, 2014). To meet the rising demand for ESS for application testing and commercialization, production of ESS beyond the lab bench scale was needed and there is a lack of literature on the epoxidation process at such scales.

The epoxidation process is highly exothermic; therefore, controlling the heat and mass transfer is critical for maximizing oxirane conversion and reducing reaction time and cost. Epoxidation occurs through well-known reaction mechanisms shown in Fig. 1. These mechanisms include *in-situ* peracetic acid formation and then double bond epoxidation. The peracetic acid formation is usually controlled by the dropwise addition of hydrogen peroxide (H_2O_2) into the reaction mixture, which aids in controlling the reaction temperature within the optimum range of 55-65 ^oC (Saurabh et al., 2011) by allowing time to dissipate reaction energy. There is always a concern with ring opening or side reaction at temperatures higher than the optimum range (Tan and Chow, 2010).

Vegetable oil epoxidation studies were generally done at a lab-bench scale of 25 – 300 g (Espinoza-Pérez et al., 2009; Goud et al., 2010; Sinadinović-Fišer et al., 2012; Vlček and Petrović, 2006), a scale at which the reaction energy is readily dissipated. Gamage et al. (2009) scaled up the epoxidation of rubber oil, neem, and mee fruit oil from 40 g to 1 kg batches for 5.5 h between 50 – 60 ^oC; they found it necessary to increase H_2O_2 addition time from 1 h to 2.5 h. Due to the difficulty in dissipating reaction energy during scale up, Gerlach and Geller (2004) showed that the overall reaction time doubled and tripled as 0.5 g, 5.0 g, 25 g, 50 g batches were scaled to a 100 g batch during epoxidation of poly-L-leucine between 22-35 ^oC. They also showed that the reaction time could be reduced from 20 h to 12 h by providing efficient mixing. During scale-up, the surface area to volume ratio of a sphere ($\frac{3}{radius}$) decreases as the radius of

the reactor increases. Therefore, it is easier to maintain the reactor temperature within the optimum range at a scale ≤ 300 g; but as the scale increases, the heat flux maybe insufficient to dissipate the reaction energy to avoid excessive temperature (Donati and Paludetto, 1997). Mixing should also be at a level to ensure sufficient mass and heat transfer.

Refining the product represents a significant portion of the total production time and cost. The production time could significantly increase during scale up if adequate refining units are not available to handle the larger volume of synthesized resin. The refining process involves steps to eliminate unreacted H_2O_2, catalyst, acetic acid, water, and solvent from the crude resin. The refining steps and equipment used to produce epoxidized vegetable oil is frequently not fully described in most epoxidation studies. In studies in which the refining process is described, there are some differences in the refining steps and the quantity of purifying reagents used (Espinoza-Pérez et al., 2009; Pan et al., 2011b).

Therefore, the objective of this study was to develop and characterize the performance of equipment to scale up the synthesis and refining of ESS to 10 kg batches. The reactor should achieve high double bond conversion similar to the lab scale while maintaining the same reaction time and temperature. The refining units and procedures should be sufficient to handle the larger volume of crude resin within a timeframe similar to the small scale.

Experimental Section

Overview of epoxidation process and equipment

The process steps for producing and refining of epoxidized sucrose soyate are shown in Fig. 11. The production step required a reactor in which intimate mixing can be achieved in a

three-phase system, and the reaction temperature can be maintained within an optimal range. The refining steps included all other steps after resin production in the reactor (Fig. 11).

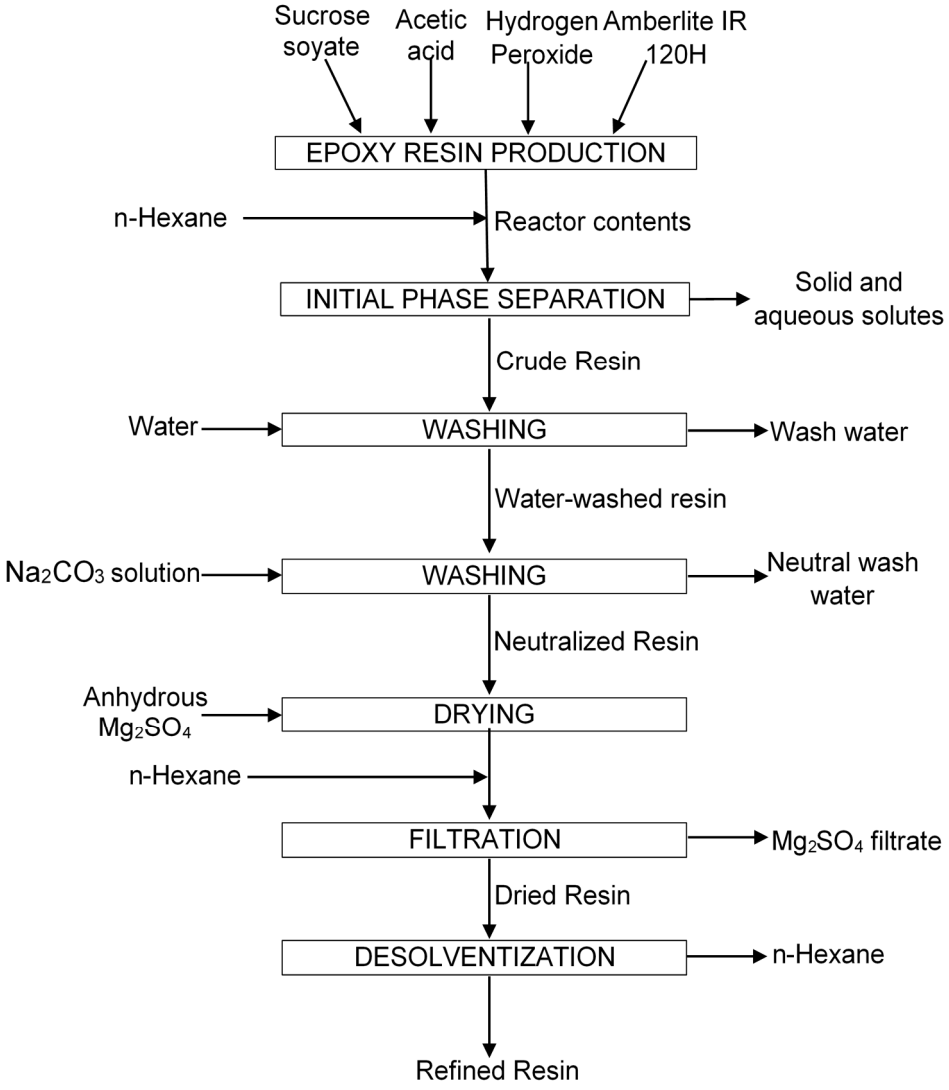

Fig. 11: Schematic diagram for the production and refining of epoxidized sucrose soyate.

A single process unit (funnel) was used as a gravity separatory funnel during the initial phase separation and washing steps and also as a filtration unit. A solvent recovery unit was required to easily remove n-hexane added during the refining steps. Hexane reduced the density

and viscosity of the resin (organic) phase, which improved phase separation between the organic and aqueous phases during washing, and increased filtration rate.

Apparatus design, fabrication, and safety considerations

Epoxidation Reactor

An existing 38 L stainless steel, steam-jacketed kettle (GROEN model TD/2-40; Jackson, MS) designed for food processing was modified for use as a reactor for epoxidation. The interior of the kettle is type 316 stainless steel while the jacket and exterior part is type 304 stainless steel. The dimensions of the kettle are shown in Fig. 12; the jacket area is 649 cm^2. The kettle has two agitators, and both are driven by a single 373 W variable speed electric motor. The primary, centered agitator has an anchor shape designed to sweep the kettle at a maximum of 300 rpm. The secondary agitator is a high speed counter-rotating bar-type mixer (maximum 900 rpm). Both agitators are of 316 stainless steel. The clearance between the primary agitator and the wall of the kettle is 1 cm. This clearance is small enough to ensure suspension of the catalyst beads during mixing without damaging the beads. Modifying the primary agitator should improve mixing to ensure sufficient mass and heat transfer. The unmodified kettle had no lid or insulation. The jacket had a port with one valve on both sides that allowed only one fluid to enter the jacket. The kettle is supported by two trunnions and chrome-plated arms. The arms hold the pipes and valves for the jacket fluid. A crank-operated gear mechanism (not shown in Fig. 12) is used to tip the kettle which aids in transferring products and cleaning.

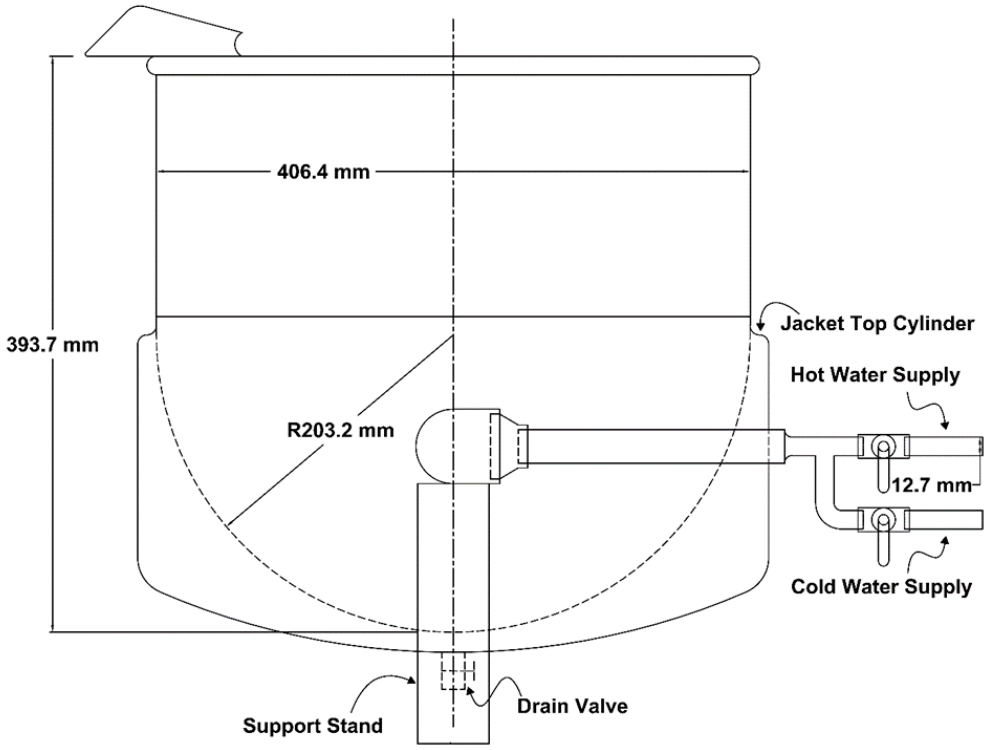

Fig. 12: A 38 L jacketed kettle for use as a reactor for epoxidation modified to allow rapid switching between jacket fluids at two different temperatures.

There were four major modifications made to the kettle that helped contain reactor contents and improve temperature control and mixing. In the first major modification, a 41 cm diameter lid of two symmetrical sections was fabricated with ports for an agitator, a thermocouple probe, and H_2O_2 addition. The three ports are of different sizes: a central 4 cm diameter port for an agitator shaft, a 2.2 cm diameter port for a glass connector (H_2O_2 addition) that is 10 cm from the central port, and a 0.9 cm diameter port for the thermocouple probe that is 10 cm from the central port and opposite to the H_2O_2 addition port. The two symmetrical sections were held together by two 0.635 cm bolts that were 15 cm apart and the two edges of the lid were clamped together. In the second modification, the outside wall of the kettle was

insulated with a flexible 2.54 cm thick polyolefin thermoplastic type insulation material (NOMACO Insulation; Tarboro, NC) with an R-value of 0.7 $\frac{m^2.K}{W}$ and a peel-and-stick backing. The pipes into and out of the jacket were insulated with a 1.27 cm thick polyethylene thermoset tubular material. Heating was needed during most of the reaction to prevent the reaction temperature from falling below the optimal range; therefore, the third modification was the addition of a 1.27 cm diameter valve on both the entrance and exit of the jacket to allow rapid manual cooling when the reactor temperature goes above the optimal range. The primary anchor-shaped agitator was modified to ensure suspension of the solid catalyst and improve mixing of the heterogeneous mixture (solid catalyst, aqueous phase, and organic phase). This fourth modification on the agitator was made by adding a stainless steel plate on both sides of the anchor as shown in Fig. 13. The secondary agitator was not needed and was removed to reduce splashing. Type 304 stainless steel sheets of 0.635 mm thickness with 2B coating/finish were used for additions to the agitator and to fabricate the lid and refining unit. The bolts and caps were also type 304 stainless steel materials.

Refining funnel

A refining funnel was fabricated to serve three purposes: mixing with wash liquids, gravity phase separation, and filtration. The main feature is a four-sided inverted pyramidal funnel with an open square top of 60 cm and a height of 40 cm. Attached to the bottom of the funnel was an 8 cm long pipe, followed by an 8 cm long T-pipe (with a 5 cm diameter viewing port to make visible the separation layer between the organic and aqueous phases), then an 8 cm long ball valve, and a 6 cm flexible hose pipe nipple. All these attachments at the bottom of the funnel have an ID of 5 cm. A 66 x 66 cm lid was also fabricated with two 1.27 cm opening at the

center. The openings were used to transfer reactor contents from the reactor into the refining funnel. One of the ports has a vacuum hose connector and the other a hose connector to the reactor.

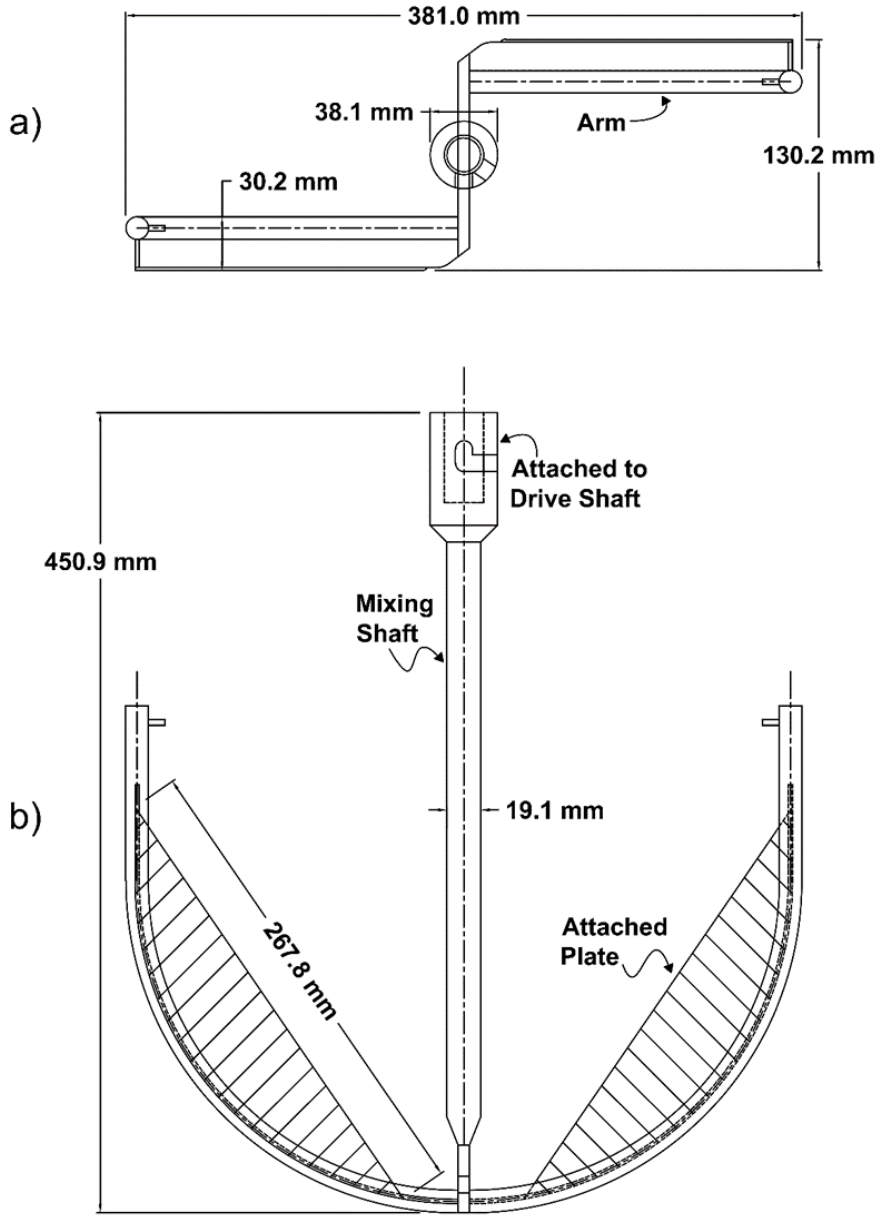

Fig. 13: The primary anchor-shaped agitator modified with a stainless steel plate for use in a reactor for epoxidation (a) top view (b) side view.

To use the refining funnel as a filtration unit, an alternate 66 x 66 cm lid was fabricated with an in-built reservoir of 43 cm length, 31 cm width, and 18 cm height. A 57 x 46 cm sieve plate, with 4.65 mm laser-cut holes spaced triangularly 4.65 mm apart, was attached with bolts to the base of the reservoir. A 57 x 46 cm Whatman #3 filter paper (Cole-Parmer; Vernon Hills, IL) was placed in between the sieve plate and the reservoir and was changed before each batch. A 2.54 cm threaded hole was added 4 cm from the top and 6 cm to the right edge of the funnel. A 1.27 cm vacuum hose nipple was attached to the threaded hole when the funnel was used as a filtration unit; however, this hole was otherwise closed with a 2.54 cm cap during washing of crude resin. A support stand was made with 4 polyurethane wheel casters with an aluminum core to support and move the funnel. The stand was 92.7 cm tall with a top funnel support area of 40.6 cm^2. At 30.5 cm from the ground, the support rods were bent outwards at 30^o to improve stability and prevent spilling the funnel's contents. The wheel casters have a wheel diameter of 10.2 cm and width of 5.1 cm.

Devolatilizing unit

An explosive-proof solvent extraction unit (Armfield model FT29; Ringwood Hampshire, England) was adapted for use as a batch devolatilizing unit. An 8 L Thermalloy stainless steel (type 304) pot was used to contain the resin and placed at the bottom of the devolatilizing chamber. Nitrogen was sparged through a solvent feed port into the resin to promote solvent removal. The sparge tube was a copper tube of 0.65 cm diameter that was spiral-wound three times in the section that rested at the bottom of the resin container. The sparge tube had 50 holes of 1 mm diameter spaced 4 cm apart, and the holes directed nitrogen gas upward.

Experimental procedure

Materials

Sucrose ester of soybean oil, SEFOSE 1618UC (sucrose soyate) was obtained from Procter and Gamble Chemicals (Cincinnati, OH). The ion exchange resin catalyst, Amberlite IR120, was purchased from Acros Organics (Morris Plains, NJ). Potassium hydroxide (KOH), 50% aqueous H_2O_2, pyridine, methanol, toluene, and 33% hydrogen bromide in acetic acid were purchased from Sigma Aldrich (St. Louis, MO). Glacial acetic acid, acetic anhydride, butyl alcohol, anhydrous Na_2CO_3, isopropyl alcohol (IPA), and hydrogen potassium phthalate were purchased from EDM Chemicals (Gibbstown, NJ). Anhydrous $MgSO_4$ was acquired from JT Baker (Center Valley, PA). Hexane was obtained from Macron Fine Chemicals (Center Valley, PA). Vacuum sealants were purchased from Airtech International (Chino, CA). Phenolphthalien (1%) in methanol and lab grade flexible clear tubing of 1.27 cm ID and 3.6 mm wall thickness were purchased from VWR (Chicago, IL).

Operational procedure

Epoxidation was carried out in the modified 38 L reactor with the modified mechanical agitator. The quantities of sucrose soyate, acetic acid, Amberlite IR 120H, and H_2O_2 were calculated for a 1 kg batch and then scaled to 7-10 kg batches of sucrose soyate. The amount of reactant for a 1 kg batch was calculated using a molar ratio of fatty acid unsaturation: acetic acid: H_2O_2 of 1:0.5:2. The reaction mixture (sucrose soyate, acetic acid, and Amberlite) was first heated to 40 – 45 ^oC while being mixed at 300 rpm. H_2O_2 addition was started once the reaction temperature reached 40 – 45 ^oC, which marked the beginning of the reaction time. H_2O_2 was added using a pump (FMI lab pump-model QV; Syosset, NY). The addition rate was varied

between 10 – 40 mL min^{-1} to maintain the reaction temperature between 55 – 65 ^{o}C. The addition rate profile was as follows: 40 mL min^{-1} at the beginning of H_2O_2 addition, 20 mL min^{-1} once the reaction temperature reached 50 ^{o}C, and 10 mL min^{-1} when the reaction temperature reached 60 ^{o}C. Once the reaction temperature started to fall after 1 - 1.5 h of H_2O_2 addition, the addition rate was increased to 20 mL min^{-1} when the reaction temperature reached 65 ^{o}C, 30 mL min^{-1} when it reached 62 ^{o}C, and 40 mL min^{-1} when less than 62 ^{o}C.

The reactor jacket was connected via tee fittings to two water baths at a circulating rate of 15 L min^{-1}: primary, hot water at 40-60 ^{o}C (VWR scientific, model 1187P; Frederick, MD) and secondary, cold water at 4 ^{o}C (Cole-Parmer, model R13L; Vernon Hills, IL). The temperature of the bath water circulating in the jacket was 40-45 ^{o}C during the first 2.0 – 2.5 h of reaction time. The temperature gradient between the reactor mixture and the jacket water served as a cooling mechanism when the reaction temperature increased. However, the reactor was rapidly cooled for 5-10 min whenever the reaction temperature reached 65 ^{o}C. To do this, the jacket fluid was switched from the primary water bath to the secondary water bath while the hot water in the jacket (8 L) was drained from the jacket to prevent entering the secondary water bath. Once the reaction temperature dropped to 60 – 61 ^{o}C, the jacket fluid was switched back to the primary water bath. This cooling cycle was repeated three to four times per batch over a period of 3-4 h.

Reaction and jacket temperatures were sensed every 15 s using two type T thermocouples (Omega; Stamford, CT) and the average was logged once per min using a CR10 datalogger (Campbell Scientific; North Logan, Utah). The thermocouple probe for the reaction mixture was housed in a stainless steel sheath of 350 mm length and 5 mm diameter, and it has a 300 mm retractable cable that can expand to 1.2 m. The probe tip was placed approximately 2 cm above

the stirring blade adjacent to the stirrer shaft. The jacket temperatures for three batches were measured by passing a thermocouple through the drain outlet of the jacket (Fig. 12). The water bath temperatures were monitored by resistance temperature detectors (RTDs) within the water baths.

The reaction was stopped at 5.5 h, then cooled to 45 ºC with the secondary water bath fluid; 0.3 L of hexane was then added for every 1 kg batch of resin. The hexane reduced the viscosity of the resin phase and facilitated quick separation of the aqueous and organic phases during washing. The reactor contents were transferred from the reactor to the refining funnel with the aid of a Duo-seal vacuum pump (The Welch Scientific Co., model 1400; Skokie, IL) at 510-640 mm Hg vacuum pressure. The reactor contents were allowed to separate by gravity in the refining funnel for 30 min. The lower aqueous layer that had residual H_2O_2, peracetic acid, acetic acid, and catalyst was drained out through the ball valve into a container. The catalyst was then removed by filtration in a hood and washed with Na_2CO_3 solution before being discarded.

The crude resin was washed twice with 1.5 L water (40 °C) per kg of resin. During each wash, the resin and water were first mixed for 30 s at 1,200 rpm using a 304 stainless steel 3-bladed propeller agitator of 60 cm shaft length and 2.54 cm blade length pitched at 45º, powered by a cordless driver (Bosch, model DDB 140; Peoria, IL). The organic and aqueous phases were then allowed to separate by gravity for 30 min. Next, the resin was washed twice with Na_2CO_3 solution at 40 °C (12.5 g of Na_2CO_3 per kg of resin per L of water) to neutralize and remove dissolved acetic acid. The funnel contents were mixed and allowed to stand for 1 h and 2 h during the first and second Na_2CO_3 washes, respectively. The resin was deemed completely neutralized when effervescence from the reaction between acetic acid and Na_2CO_3 stopped and

resin pH was above 7 as determined by a pH indicator strip. The last wash was sometimes left overnight to maximize the separation of the organic and aqueous phase. The neutralized resin (Fig. 11) was dried overnight with anhydrous $MgSO_4$ (approximately 20 percent of the weight of the undried resin). Additional hexane (0.1 L per 1 kg resin) was added during this drying process in order to increase the filtration rate of the resin. The hydrated $MgSO_4$ was removed by filtration under vacuum using a Whatman No. 3 filter paper. With the added hexane, the filtration process usually takes 24 h to complete. Hexane was removed from the filtered resin using the solvent extraction unit adapted for devolatilization described earlier. The pot with resin (3 – 3.5 kg portions) was placed in the bottom of the extraction unit. The bottom of the unit was heated to 60 ^{o}C with steam and under 750 mmHg vacuum pressure. Nitrogen gas was bubbled through the resin at 375 mmHg pressure at a rate of 9 m^3 h^{-1}. Nitrogen was supplied from a Parker-Balston nitrogen gas generator model AGS400OC (Haverhill, MA). The nitrogen bubbles caused the vacuum pressure to drop to 400 mmHg. Hexane removal usually takes 3 h to complete a 7-10 kg batch and the solid content for the refined resins were then analyzed.

Safety

The resin was produced in an explosion proof lab. A hood of 1.6 m length, 1.4 m width, and 0.5 m height was mounted 0.3 m above the reactor to remove organic vapors from acetic acid and hexane in the lab. The reactor's hood has a vent of 19 cm diameter that pulls air at a flow rate of 2,470 m^3 h^{-1} using an explosion-proof blower. Personnel also wore half-face respirators (3M model 5300; St. Paul, MN) and safety tight goggles while controlling reactor temperature and also while transferring and washing of crude resin. H_2O_2 is a strong oxidizer and bleach; therefore, butyl gloves (VWR; Chicago, IL) and the tight safety goggles were worn when

handling the reagent. Spill-containment pans of 71 cm x 76 cm and 5 cm depth were placed under the reactor and refining funnel as a routine precaution. Storing unreacted H_2O_2 in a waste container before disposal can be a safety hazard and neutralizing the H_2O_2 with ferrous sulphate is not cost effective. Therefore, the aqueous phase from the reactor was diluted 50% with water to reduce the concentration of unreacted H_2O_2. The waste containers were at most ¾ filled, and the caps were left loose during storage.

Evaluating the performance of the reactor and washing unit

Determining the overall heat transfer coefficient of the reactor

Estimation of the overall heat transfer coefficient (*U*) followed an approach similar to that used by Nassar and Mehrotra (2011) and Leveneur (2014). The system boundary for this analysis was the reactor contents and the portion of the agitator in contact with the reactor contents. The starting point of this analysis was the overall energy balance of the epoxidation process in the presence of all reactor contents, expressed in equation 1 as Stored energy = Reaction energy + Exchanged energy – Heat loss.

The assumptions used in conjunction with equation 1 were: the heat loss through the insulated wall and lid is negligible (q_{loss} =0), heat exchange is only through the jacket area, temperature is uniform within the jacket fluid, and temperature and composition of the reactor contents are uniform due to proper mixing.

To determine *U*, equation 1 was further simplified to equation 9 by performing an experiment without a reaction energy ($\Delta E_r \dot{M}_r V_r$) by not adding H_2O_2.

$$(m_r c_r + m_a c_a)\frac{dT_r}{dt} = UA(T_f - T_r) \qquad \text{(Eq. 9)}$$

By integrating equation 9, a new expression was obtained in equation 10

$$ln\frac{T_f - T_o}{T_f - T_r} = \frac{UA}{m_r c_r + m_a c_a} t \quad \text{(Eq. 10)}$$

In the experiment to collect temperature data over time, all reactants were added to the reactor at the beginning of the experiment and the contents were stirred at 300 rpm. However, water was added to equal the final volume of H_2O_2 solution needed. The temperature of the reactor contents was collected for 15 min as the jacket temperature was first set at 45 ºC and then later at 55 ºC. The temperatures (T_r = reaction at time *t*, T_o = *initial reaction,* T_f = *jacket fluid)* were obtained from type T thermocouples logged every 15 s intervals using a CR10 datalogger. The experimental values of $ln\frac{T_f - T_o}{T_f - T_r}$ were plotted against *t*. The average slope of the best-fit lines for both jacket temperatures 45 ºC and 55 ºC was equal to $\frac{UA}{m_r c_r + m_a c_a}$.

U was then calculated as *A,* $m_r c_r$ (equation 11), m_a, and c_a values could be estimated from reactor design, reactants, and agitator considering data in Table 10.

$$m_r c_r = m_{SS} c_{p_{SS}} + m_{H_2O_2} c_{p_{H_2O_2}} + m_{H_2O} c_{p_{H_2O}} + m_{Amberlite} c_{p_{Amberlite}} + m_{aceticS} c_{p_{acetic}} \quad \text{(Eq. 11)}$$

Evaluating the extent of epoxidation

Samples of resin were collected upon completion of all batches, for analysis as described under section 2.5. For three batches, the extent of the epoxidation reaction was also determined while reaction was still in progress at 2.5 and 4 h. Approximately 25 mL of the reactor contents were collected using a 25 mL pipette and while the contents were being stirred. The samples were refined and analyzed for oxirane content at those intermediate times. These values were compared to the final 5.5 h oxirane value.

Table 10: Mass and specific heat capacity for the reactants and agitator.

Reactants and Agitator	Mass (g)	Specific heat capacity (c_p) [J g^{-1} K^{-1}]	Reference for c_p
Sucrose soyate	10,000	2.1 (Soybean oil)	(Morad et al., 2000)
Hydrogen peroxide	3,410	2.62	(Gurvich et al., 1994)
Water	3,410	4.18	(Gurvich et al., 1994)
Amberlite IR 120	2,000	1.17	(DOW, No Date)
Acetic acid	1,575	2.04	(Gurvich et al., 1994)
Agitator	818	0.51	(Holman, 2002)

Evaluating the washing steps

Resin samples (0.5 – 0.6 g in duplicate) were collected before and after each wash for batches 6 and 7. The washing procedures are described in operational procedure in the operational procedure section and the samples collected were analyzed for acid number. A mole of acetic acid is 60.05 g and two moles of acetic acid are neutralized by one mole of Na_2CO_3.

Resin characteristics and yield

Oxirane oxygen (OO_e) content was determined in duplicate using the American Oil Chemist Society (AOCS) method Cd 9-57. The maximum theoretical oxirane oxygen content (OO_t) of 6.87% for sucrose soyate was calculated using equation 4 and an iodine value (IV_o) of 117 (Pan et al., 2011b). Therefore, the conversion of unsaturated to epoxy groups was calculated using equation 5.

The viscosity was measured in duplicate at 25 ºC using a HAAKE Viscotester model VT 550 (Paramus, NJ) with a cone-and-plate sensor PK 0.5º. The viscosity of the ESS resin was shown to be shear-thinning with a Flow Behavior Index of 0.83. For the purpose of routine viscosity measurements, data were collected at 200.1 rpm.

Acid number (AN) was determined by titration using the ASTM D974 standard method. Samples (0.5 g) in triplicate were dissolved in 3 mL 1:1 (v/v) isopropyl alcohol and toluene

mixture with 2 drops of phenolphthalein indicator. KOH (0.1 N) solution was titrated into the sample mixture until there was sharp color change. Acid number was then calculated using equation 12.

$$AN = \frac{56.1\ x\ volume\ x\ normality\ of\ KOH}{weight\ of\ sample} \quad \text{(Eq. 12)}$$

The resin yield was calculated using equation 13.

$$\text{Resin yield (\%)} = \frac{Weight(g) of\ refined\ epoxy\ resin}{Weight\ (g) of\ sucrose\ soyate}\ x\ 100 \quad \text{(Eq. 13)}$$

Nonvolatile content was determined by using ASTM standard method D1259 in which 0.9 – 1.1 g of resin samples were dried in an oven at 105 ^{o}C for 1 h and then allowed to cool in a desiccator before dry weight measurements.

Statistical analysis

SAS 9.3 (Cary, NC) was used to compare ($\alpha = 0.05$) the means of the oxirane content for the three batches in which samples were collected at 2.5, 4.0, and 5.5 h.

Results and Discussion

Resin production and characteristics

The overall goal was to develop process units to produce ESS in much greater quantity than previously attained. The final capability of the modified kettle (reactor) and refining unit was for a 10 kg batch of ESS, which is 33 times greater than the previous 300 g capability in the lab. The total working reactant volume for a 10 kg batch was 19 L, which is half of the reactor's volume. The batch size could not be increased above 10 kg because of splash concerns during vigorous mixing as the lid does not completely seal the top of the reactor. To better understand the epoxidation process steps at a larger scale, 7 kg and 9 kg batches were first made before the 10 kg batches. Production of the 7 kg and a few of the 9 kg batches was a learning process, and a

number of adjustments were made in subsequent batches to improve the resin quality and yield while reducing the total production time (epoxidation and refining) from 8 to 4 days. The evolution of this resin quality, yield, and production time can be seen in Table 11. A total of twenty batches of sucrose soyate were epoxidized and refined: two initial 7 kg batches, then five 9 kg batches, and thirteen 10 kg batches. It would have been cumbersome to put the data of all twenty batches in Table 11, therefore 8 representative batches were chosen that show the evolution of the ESS quality and yield of the first, middle, and last batches. The main difference between batches was the amount of SS being epoxidized, the timing of H_2O_2 addition, and some aspects of refining described below.

Table 11: Yield and properties of eight batches of epoxidized sucrose soyate from the twenty produced, showing consistency in oxirane content after the fourth batch event though the timing of H_2O_2 addition were different.

Batch #→ Parameters ↓	**1**	**2**	**4**	**6**	**7**	**9**	**14**	**20**
Sucrose Soyate (SS) in kg	7.0	7.0	9.0	9.0	10	10	10	10
Epoxidized SS (kg) [% yield]	4.1 [59]	5.05 [72]	8.9 [99]	9.1 [101]	10.2 [102]	10.0 [100]	9.2 [92]	9.9 [99]
Oxirane Content (%)	6.49±0.1	6.55±0.1	6.60±0.1	6.80±0.0	6.75±0.1	6.80±0.0	6.79±0.0	6.86±0.2
Conversion (%)	94.5	95.3	96.0	99.0	98.3	99.0	98.9	99.9
Nonvolatile Content (%)	99.5±0.0	99.1±0.2	99.3±0.1	99.6±0.1	99.2±0.0	99.8±0.0	99.6±0.0	99.8±0.0
Viscosity (mPa·s) at 22°C	2,236±6	2,380±5	2,369±8	2,555±4	2,465±3	2,411±8	2,489±7	2,601±10
Production Time (days)	8	8	4	4	4	4	4	4

A total of 165.5 kg of ESS was produced from the twenty batches, giving an 87.6% yield overall. The lowest yield recorded was 58.8% (batch 1) and the highest was 102% (batch 7). Theoretically, the maximum resin yield relative to the SS is expected to be 108% if all double bonds are epoxidized and every drop of resin is recovered. There are 0.495 moles of double

bonds in 100 g of SS (Pan et al., 2011b), and the oxygen added during epoxidation adds 7.92 g giving an ESS yield of approximately 108 g. Yield lower than 108% was mainly due to loss of resin which adhered to the filter paper, filter cake, catalyst, and containers during refining, but was also due to spillage in some batches. One of the first adjustments to improve the yield (beginning with batch 4) was to increase from 1 L to 2 L the amount of hexane added to the crude resin before refining. This additional hexane further reduced the viscosity and density of the crude resin, thereby resulting in a faster and more complete separation. The incorporation of the Armfield extraction unit for solvent removal was another adjustment that also helped reduce the epoxy resin production time per batch and improved yield. The solvent for the first two batches was removed using a Buchi 461 rotovap model RE 111 (Champaign, IL) in a 1 L glass beaker in which only 300 – 400 g of the resin could be devolatilized at a time for 4 – 5 h.

Even though the oxirane contents of the 7 kg batches were the lowest, they were still above 6.4% oxirane content (< 247 g of resin/equivalent oxirane bond), which is sufficient for use as biobased epoxy resin. An oxirane content of 6.45% in ESS has been shown to result in thermosets with better tensile and mechanical properties than epoxidized soybean oil with oxirane content of 6.90% (Pan et al., 2011a; Pan and Webster, 2011). This is due to the rigid sucrose core and higher epoxide functionality per molecule in ESS than in epoxidized soybean oil. However, higher oxirane content in ESS is desired in making composite materials, polymers, and coatings. The oxirane content steadily improved for the first three batches, then remained consistent thereafter. The oxirane content remained above 6.7% in all 10 kg batches, which represents greater than 97.6% conversion of double bonds. The improved consistency in oxirane content was due to better control of the reactor temperature that is discussed in the next sub

section. The conversion and viscosity of the ESS resin of the 10 kg batches were similar to ESS produced at a 170 g batch size by Pan et al. (2011b). The nonvolatile contents were greater than 99% and indicate the efficiency of the solvent extraction process.

Evaluating the performance of the reactor

Samples (25 mL) were collected at 2.5 h, 4 h, and 5.5 h (end time) for three 10 kg batches in which H_2O_2 addition ended before 2.5 h. These batches were not purposefully treated differently than the other 17 batches. The intention was to treat all batches the same way to determine reproducibility. However, as the reaction temperature was controlled manually using variable H_2O_2 addition rates and cooling fluid, the H_2O_2 addition time for the twenty batches varied between 2.3-3 h except the first 4 batches that were above 3 h (up to 3.5 h). As the cooling mechanism was better controlled, H_2O_2 addition rate was faster even as the batch size increased from 9 to 10 kg, thereby making the total addition time to be less than 3 h. There were thirteen batches in which H_2O_2 addition ended between 2.5-3 h, but there were three batches in which H_2O_2 addition ended before 2.5 h. Therefore, sampling at 2.5 h and 4 h was done for these three batches as a way to compare results with the previous 300 g study (Paper 1) which studied the epoxidation process conditions. These time intervals were also to evaluate the repeatability of double bond conversion and of reaction temperature over time. The values of the double bond conversion and the average reactor temperatures over time are shown in Table 12.

Continuing the reaction beyond 2.5 h was clearly necessary because conversion was quite low at this time interval. At 2.5 h, there was a significant difference (p-value=0.0002) in the conversion among the three batches, but there was no significant difference among batches as the reaction continued to 4 h and beyond. The differences in double bond conversion clearly

narrowed as the reaction reached 4 h and beyond even though differences were observed in the average reaction temperature (1-2 ^{o}C) and the H_2O_2 addition rate for these batches. In a previous 300 g batch experiment in which reaction temperature was not controlled within the optimum range, the conversion was at least 83% complete at 2.5 h and up to 99% by the end of 5.5 h (Monono et al., 2015b). In this study, there was a steady increase to 99% of double bonds converted to oxirane groups up to the 5.5 h reaction time. The reaction time of 5.5 h was within the most commonly reported reaction time of 5-7 h reported in epoxidation review papers (Saurabh et al., 2011; Tan and Chow, 2010). Continuing reaction time beyond 5.5 h in this study will likely not have improved the conversion percent but rather increase the processing cost and risk of oxirane degradation. High oxirane content is desired for a better-crosslinked network in composite materials, polymers, and coatings. This better network will in turn result in improved mechanical and thermal properties of the products.

Table 12: Double bond conversion, mean reaction temperature, and H_2O_2 total addition time for three ESS batches in which H_2O_2 addition ended before 2.5 h.

Parameters Measured	Batch 10			Batch 18			Batch 19		
	2.5 h	4 h	5.5 h	2.5 h	4 h	5.5 h	2.5 h	4 h	5.5 h
Conversion (%)	74.2	92.3	98.9	75.7	92.8	99.2	68.4	92.0	99.0
Mean Reactor Temperature (^{o}C)	58.6±6	59.1±5	59.6±5	59.0±6	59.9±5	60.1±5	58.1±6	59.3±5	59.7±4
H_2O_2 total addition time (min)		145			139			148	

The main goal during epoxidation was to maintain the reactor temperature within 55-65 ^{o}C. H_2O_2 addition was started when the reaction temperature climbed to 40 – 45 ^{o}C, and it took another 25 – 30 min for the reaction temperature to reach the lowest limit of 55 ^{o}C. This prolonged period of temperature rise caused most of the average reaction temperatures to be

below 60 ^{o}C (Table 12). The technique of starting H_2O_2 addition when the reaction temperature reached 40 - 45 ^{o}C has not been commonly used in most epoxidation studies. H_2O_2 addition started when the reaction temperature reached the optimal temperature range (Saurabh et al., 2011). In this study, the initial exothermic reaction was used to raise the reaction temperature from 40 - 45 ^{o}C to its optimal temperature range. This was an important strategy to maintain the primary water bath temperature below 45 ^{o}C and to easily control the reaction temperature at 60 ^{o}C during high exothermic reaction. The primary water bath set between 40 – 45 ^{o}C created a thermal gradient of 15 -20 ^{o}C between the primary water bath fluid and the reaction mixture. The thermal gradient served as a cooling mechanism but the heat transfer rate due to this thermal difference was lower than the reaction energy rate. Hence, very rapid cooling was sometimes needed when the reaction temperature increased above 65 ^{o}C. The was done by passing a cold water stream of 4 – 15 ^{o}C through the jacket, thereby increasing the thermal gradient and heat transfer rate.

The reaction temperature was maintained within 55 – 65 ^{o}C by varying the H_2O_2 addition rates (controlling reaction energy rate) and by varying the temperature of water bath fluid that circulated in the reactor jacket (controlling heat exchange rate). The water bath temperature and H_2O_2 addition rate profiles significantly evolved in the first five batches; thereafter, a common pattern was observed from batch 6 to 20. Since it would be too cumbersome to present all the 20 time-temperature-H_2O_2 addition rate profiles, the profiles for batches 2, 6, and 14 can be seen in Fig. 14, which shows the evolution of temperature. A sharp drop in the water bath temperature profiles represent periods when rapid cooling was done and the primary water bath was switched to the secondary water bath.

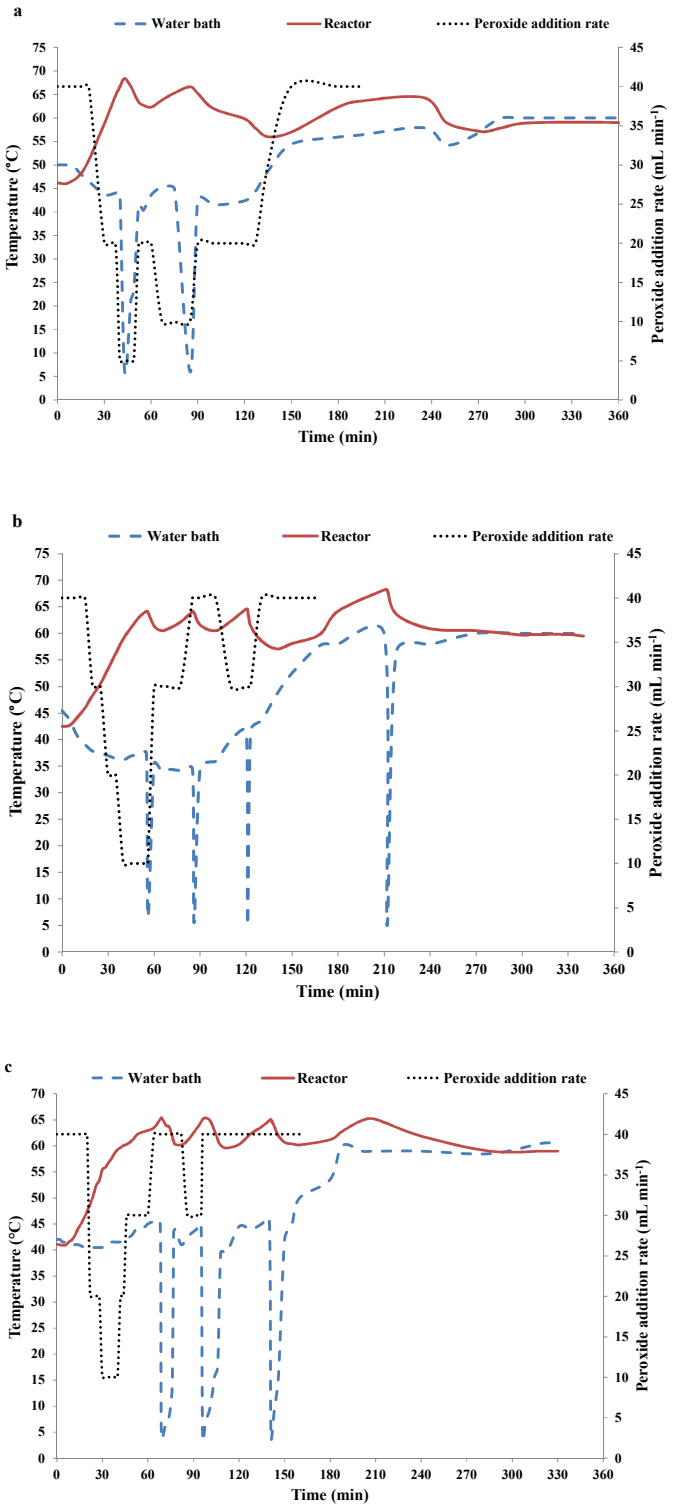

Fig. 14: Evolution of the time-temperature-H_2O_2 addition rate profiles for epoxidation batches (a) 2 (b) 6 (c) 14.

The water bath temperature for batch 2 (representative of the first 5 batches) started at 50 ºC as compared to 40 - 45 ºC for batches 6 and 14. Therefore, the overall average bath temperature for batch 2 was higher (45.5±13.7 ºC) than that for batches 6 (40.7±15.3 ºC) and 14 (39.5±14.8 ºC). As the reaction temperature was being maintained between 55-65 ºC, the water bath temperature for the reaction also influenced the rate at which H_2O_2 was added. Therefore, batch 2 had the lowest average addition rate (23.2±13.0 mL min^{-1}) which made the total addition time to be 3.25 h. Meanwhile, batches 6 and 14 had higher average addition rates of 30.0±9.9 mL min^{-1} and 28.7±10.3 mL min^{-1}, respectively. The higher addition rates made the total addition time to be approximately 2.8 h for both batches.

The double bond conversions at 5.5 h for batches 2, 6, and 14 were 95.8%, 99.0% and 98.9%, respectively (Table 11). Batch 2 may have needed more reaction time to complete the conversion of double bonds since its H_2O_2 addition was prolonged to 3.25 h compared to the 2.8 h for batches 6 and 14. The average reaction temperature during the 5.5 h period for batch 2 was 59.8±6.0 ºC compared to 59.0±6.3 ºC and 58.7±6.9 ºC for batches 6 and 14, respectively. Even with a lower overall average reaction temperature, the control of reaction temperature batches 6 and 14 was more stable after the first 25-30 min of temperature rise. The standard deviations were smaller for batches 6 (61.4±2.9 ºC) and 14 (61.2±2.6 ºC) than for batch 2 (61.1±3.5 ºC) once the reactor temperature reached 55 ºC after 25-30 min of reaction.

The water bath temperature was assumed to be the same as the jacket temperature during the production of ESS and when controlling the reaction temperature for the twenty batches. However, in a heat transfer analysis, it is important to obtain the actual jacket temperature because it is difficult to account for the changes in bath temperature when the water baths are

switched (Fig. 14). Therefore, a thermocouple was passed through the drain valve into the center of the jacket to measure the jacket temperature of the batch 20. The time-temperature profile for the reaction, jacket, and primary water bath are shown in Fig. 15. The most significant difference between the primary water bath and jacket temperature was during rapid cooling as the valve that supplied water to the jacket from the primary water bath was shut off. The jacket at that time received cooling fluid from the secondary water bath. The jacket temperature was 1.5 ºC higher than the primary water bath between the first rapid cooling and the second rapid cooling. In any other period, both temperatures were within a margin of 0.2 ºC.

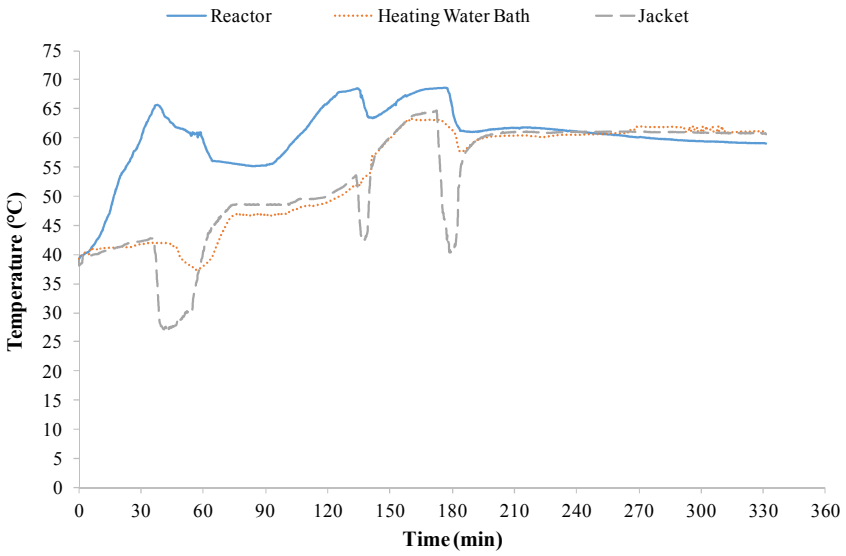

Fig. 15: The time-temperature profiles of the epoxidation batch 20 for the reactor, primary water bath, and jacket fluids.

The ability of the jacket to transfer heat into and out of the reaction mixture is partly determined by the overall heat transfer coefficient (*U*). The value of *U* is largely determined by the reactor design (material, heat transfer area, mixing, and insulation) and the amount and type of reactants. The *U* value was measured in the absence of chemical reaction, but with the required volume of H_2O_2 replaced by H_2O. Once the jacket fluid temperature was set first at 45

ºC and then later at 55 ºC, the temperature of the reactor contents rose from 35 to 40 ºC and from 44 to 50 ºC, respectively. The slopes of the best fit lines when $ln\frac{T_f-T_o}{T_f-T_r}$ data were plotted against *t* were 0.00126 s^{-1} and 0.00124 s^{-1} for jacket temperatures 45 ºC and 55 ºC, respectively; therefore, an average slope of 0.00125 s^{-1} was used to calculate the U value together with equation 14:

$$\frac{UA}{m_r c_r + m_a c_a} = 0.00125\ s^{-1} \qquad \text{(Eq. 14)}$$

The resulting *U* value for the reactor was approximately 1,069 W m^{-2} K^{-1}. This *U* value is within the typical range of 500 – 1,900 W m^{-2} K^{-1} for steam-jacketed vessels (Lienhard IV and Lienhard V, 2011). There was no epoxidation when these data were collected, but the value during epoxidation is likely very similar. The *U* value may be used to help estimate the heat transfer rate, and a higher *U* value is better for heat transfer. The *U* value is actually determined by the conductive heat transfer resistance of the reactor wall and the convective heat transfer resistances at the interfaces of this wall with jacket fluid and reactor contents. The *U* value is inversely proportional to the sum of these individual heat transfer resistances. The value of *U* is expected to fall slightly as the viscosity of the resin increases as a result of epoxidation.

In this paper, heat transfer rate was controlled by changing the thermal gradient between the reaction mixture and jacket fluid. At a much larger scale, increasing the thermal gradient might not be sufficient to control heat transfer except the heat transfer surface area is increased. This could be done by passing spiral tubes with cooling fluid through the reaction mixture.

Evaluating the performance of the washing unit

The main goal of the washing unit is to purify the crude resin by eliminating excess and dissolved acid to a level less than an acid number (AN) of 0.5. In the first six batches, the AN was not analyzed, because more emphasis was placed on the synthesis of the crude resin. Most

epoxidation studies do not have details of their washing process which should include washing steps, ratio of wash liquid and/or Na_2CO_3 solution to resin, temperature of wash liquid, method of mixing, and phase separation time. Pan et al. (2011b) and Espinoza et al. (2009) had six washing steps but the later elaborated on the other washing parameters mentioned earlier. Therefore, the washing process and steps were consolidated from the six washing steps reported (Table 13). The amount of Na_2CO_3 used for the first six batches was 45 – 50 g per kg of resin and was based on the amount used by Espinoza et al. (2009). However, it was necessary to analyze a new amount of Na_2CO_3 needed since the washing steps were slightly different from Espinoza et al. (2009). The first two water washes for batch 7 reduced AN almost 40% (Table 13). The AN of 19.7 after the second water wash was used to calculate the acid equivalent (E_a) for the 10 kg batch as seen in equation 15.

$$E_a = \frac{(19.7\ x\ 10{,}000)\ mg}{56100\ mg/eq} = 3.51\ moles \qquad \text{(Eq. 15)}$$

Table 13: Acid number (AN) after each washing step for batches 7 and 8.

Washing Steps	Batch 7	Batch 8
Crude	32.3±0.5	31.4±0.6
1st water wash	23.3±0.3	22.6±0.2
2nd water wash	19.7±0.2	19.2±0.3
1st Na_2CO_3 wash	9.0±0.1	9.1±0.1
2nd Na_2CO_3 wash	0.4±0.0	0.3±0.1
3rd water wash	0.4±0.0	/

The total amount of acetic acid in the 10 kg batch after the second water wash was 211 g considering 3.51 moles of acetic acid. Therefore, the amount of Na_2CO_3 needed to neutralize the 211 g of acetic acid was 187 g. The actual amount of Na_2CO_3 used was 250 g (an excess of 33% added to the calculated amount) so as to account for acetic acid in the aqueous portion at the bottom of the crude resin that was not completely drained and to ensure an acceptable AN value.

The 250 g of Na_2CO_3 for a 10 kg batch was half the amount used in the first six batches. The Na_2CO_3 wash was divided into two in order to reduce the amount of effervescence or possible spillage. The third water was not carried out from batch 8 to 20 because the analysis of batch 7 in Table 13 showed that there was no difference in the AN after the third water wash. The four washing steps were deemed adequate for this scale of process but methods to reduce carbonate should be developed for larger production scale especially by increasing the number of water washes, the amount of water used per wash, or by the use of countercurrent washing unit. In this study, the total amount of Na_2CO_3 can still be reduced by performing three water washing steps followed by one Na_2CO_3 washing step.

Conclusion

A reactor with capacity to produce 10 kg ESS was adapted from an existing jacketed kettle. The modifications improved the heat transfer capability that enabled the reaction temperature to be maintained within 55-65 ^oC and allowed H_2O_2 addition be completed in less than 3 h. The modification in the stirrer and the reactor's jacket temperature via two water baths eased the manual control of reaction temperature especially during peak exothermic activities. Meanwhile, the reaction energy rate was controlled by varying the H_2O_2 addition rate. The reaction was stopped at 5.5 h but the time-temperature profiles suggested that the reaction could be stopped at 5 h, because the reaction and jacket temperatures were the same which indicated negligible reaction beyond 5 h.

Refining units were designed and fabricated to safely and efficiently purify the ESS resin produced. These units helped reduce the total production time from 8 to 4 days. The total production time of 4 days could be further reduced by use of higher capacity separation and

filtration units. The resin quality and reaction time was similar to that achieved at the lab scale but as the ESS process is further scaled up, research is needed to minimize material cost and process time. Further research can be done to determine the best ratio of reactants, explore the recycling of Amberlite IR 120, and reduce the amount of Na_2CO_3 and $MgSO_4$ needed per kg of resin produced. Further work should also be done to minimize the amount of aqueous waste during refining which will in turn reduce costs of process and waste water. The H_2O_2 addition rate and jacket temperature were controlled manually, but could be automated in the future using the results of this study.

PAPER 3: OPTIMIZING THE REAGENT AMOUNTS AND PROCESS CONDITIONS OF EPOXIDIZED SUCROSE SOYATE FOR INDUSTRIAL SCALE PRODUCTION[3]

Abstract

There is a growing need to produce epoxidized sucrose soyate (ESS) at an industrial scale for large scale applications in coatings and material science. Industrial scale production of ESS requires optimization of the process conditions to minimize cost without compromising resin quality. Therefore, a robust model was developed that predicts the conversion of double bonds to oxirane under different process scenarios. Data for the model were obtained by epoxidizing 30 g of sucrose soyate at three reactor temperatures (55, 60, and 65 ^{o}C), three molar ratios of acetic acid to oil unsaturation (0.25:1, 0.375:1, and 0.5:1), three molar ratios of H_2O_2 to oil unsaturation (1:1, 1.5:1, and 2:1), three catalyst amounts (1.5, 3.75, and 6 g), and three reaction times (3.5, 4.5 and 5.5 h). The model was highly significant with an adjusted R^2 of 97.6% and predicted R^2 of 96.8%. The RMSE of 0.54 showed that the model was a good fit in predicting optimal epoxidation conditions at different process levels. ESS samples epoxidized at 60 – 65 ^{o}C for 4.5-5 h had conversion >98% even when reagent amounts were reduced by 18-20%. Similar resin quality was also observed when one of the optimal conditions was scaled-up 100 times to a 3 kg batch. Therefore, as long as mixing and temperature control are efficient, this model can be used to epoxidize vegetable oil-based compounds to any scale.

---

[3] This paper will be submitted for publication under the authorship of Ewumbua Monono, James Bahr, Scott Pryor, Dean Webster, and Dennis Wiesenborn. Ewumbua Monono had primary responsibility for collecting and analyzing laboratory data. Ewumbua Monono was the primary developer of the conclusions that are advanced here. Ewumbua Monono also drafted and revised all versions of this paper. The co-authors served as proofreader and checked the statistical analysis conducted by Ewumbua Monono.

Introduction

The interest in biobased resins that will be competitive with petroleum-based resins in polymers, coatings, and composite materials has propelled interest in epoxidized sucrose esters of fatty acids. Sucrose esters of unsaturated fatty acids (Fig. 5) were first reported in the early 1960s (Walsh et al., 1961), and the interest in using them as biobased resins arose in the last decade when a high degree of substitution (DS) of fatty acids for sucrose hydroxyl groups was achieved. An average DS of ≥ 7.7 was obtained by Procter and Gamble (P&G) and marketed under the trade name SEFOSE (Corrigan, 2003). SEFOSE derived from soybean oil is referred to as sucrose soyate (SS). Epoxidation of SS has led to the development of novel and highly-functional classes of resins used as thermosets in coatings (Kovash et al., 2014; Nelson et al., 2013; Yan and Webster, 2014), and composite materials (Hosseini et al., 2013). The thermosets and materials from epoxidized sucrose soyate (ESS) have been shown to substantially improve hardness, storage modulus, and glass transition temperature compared to previous epoxidized vegetable oil-based resins (Hosseini et al., 2013; Yan and Webster, 2014).

Epoxidation of SS was successfully scaled up to 10 kg batches (Monono et al., 2015a), but there is a growing interest to produce the resin at an industrial scale to meet the demand for new products in the coatings and material science industries. Synthesizing ESS at an industrial scale requires the optimization of the epoxidation process conditions and reagents used, which will in turn reduce the production cost and time. The epoxidation reaction is exothermic and occurs through well-known reaction mechanisms (Fig. 1). These mechanisms include *in-situ* peracetic acid formation and then double bond epoxidation. Peracetic acid formation, which usually uses Amberlite IR120H as the catalyst, is controlled by the dropwise addition of

hydrogen peroxide (H_2O_2) into the reactor contents. The peracetic acid reacts with the double bonds in fatty acids to form epoxy groups, and acetic acid is regenerated. The amounts of reagents (acetic acid, H_2O_2, and Amberlite) used during epoxidation is usually based either on molar ratios relative to double bonds, or weight percent of vegetable oil/SS being epoxidized. Varying the reagent amounts, temperature, and reaction time has been shown to be the main factors that directly influence the conversion of double bonds (Saurabh et al., 2011). However, mixing or stirring rate and H_2O_2 addition time or rate will influence these main factors if they are not adequate or well controlled.

The epoxidation mixture is in three phases (organic, aqueous, and solid) and proper mixing is very important to achieve acceptable results. Different optimum stirring rates (300 – 1,800 rpm) and mixing mechanisms have been reported; however, the differences in threshold speeds and mixing has been mainly due to the different quantity of oil epoxidized and/or stirrer used (Tan and Chow, 2010). The most important consideration is that mixing should assist heat transfer and be sufficient to ensure that the reactants mix properly; increasing stirring speed above this minimum does not influence epoxidation (Dinda et al., 2008; Espinoza-Pérez et al., 2009). Varying the H_2O_2 addition rate influences the conversion rate; however, this effect is minimal if all the required amounts of H_2O_2 is added at least 1.5 h before the end of the reaction (Monono et al., 2015b). The main factors that directly influence oxirane formation are molar ratio of H_2O_2 to unsaturation, molar ratio of acetic acid to unsaturation, amount of Amberlite catalyst, reaction temperature, and reaction time.

Many studies have tried to optimize the epoxidation process conditions, including reagent use, but these studies had some limitations. Some studies analyzed 2-3 factors at a time but not

the effects of all the main factors simultaneously (Gamage et al., 2009; Goud et al., 2007; Mungroo et al., 2008; Rangarajan et al., 1995; Vlček and Petrović, 2006). The design matrix of these studies were not well-defined and number of treatments were not adequate for a robust model. Other studies analyzed 4 of the main factors simultaneously with well-defined experimental design, but the studies either did not include the effect of varying catalyst amounts or the reaction time (Espinoza-Pérez et al., 2009; Milchert et al., 2010). All the main factors including stirring speed were studied by Mungroo et al. (2011), but the independent effect of the acetic acid and H_2O_2 were not studied and no model was proposed. In all of these optimization studies above, the reaction temperature was cooled manually or controlled by H_2O_2 addition, which likely added variability within the experimental units. Therefore, there is a need to develop a robust model that will include all the main factors while keeping other process conditions constant.

The molar ratio of 1:0.5:2 of oil unsaturation: acetic acid: H_2O_2 with Amberlite added at 20% of oil weight has been commonly used (Monono et al., 2015b; Pan et al., 2011b) or shown to be the optimal ratio with conversion of double bonds to oxirane > 95% (Espinoza-Pérez et al., 2009; Gamage et al., 2009; Vlček and Petrović, 2006). However, in some of the optimization studies, lower molar ratios of acetic acid and H_2O_2 to unsaturated bond and lower amounts of Amberlite at certain reaction temperatures and times have also yielded up to 90% conversion (Milchert et al., 2010; Mungroo et al., 2011; Mungroo et al., 2008). Therefore, a reduction in the amounts of acetic acid or H_2O_2 or Amberlite or all reagents may still yield a conversion > 95% if all other factors are at their optimal conditions. Many epoxidation studies have shown that the rate of epoxidation increases with temperature but at temperatures above 65 ^oC, the oxirane

bonds formed can be cleaved if reaction continues after an acceptable conversion is attained (Tan and Chow, 2010). To minimize the risk of oxirane cleavage and maximize oxirane formation, most epoxidation studies have used reaction temperatures and between 55-65 ^{o}C and 5-6 h (Saurabh et al., 2011).

At lab scale, time and money are not usually major considerations, but at an industrial scale they are always key to any production process. It is therefore necessary to develop a model that can predict conversion at different process scenarios using the five main factors that directly influence epoxidation. The hypothesis of this study was that conversion greater than 98% can be achieved even with reduction of at least 10% in inputs.

Materials and Methods

Materials

Sucrose ester of soybean oil, SEFOSE 1618UC (sucrose soyate) was purchased from Procter and Gamble Chemicals (Cincinnati, OH). The ion exchange resin catalyst, Amberlite IR120, was purchased from Acros Organics (Morris Plains, NJ). Potassium hydroxide (KOH), 50% aqueous H_2O_2, carbon tetrachloride, pyridine, methanol, toluene, hydrogen chloride, Wijs solution, and 33% hydrogen bromide in acetic acid were purchased from Sigma Aldrich (St. Louis, MO). Glacial acetic acid and potassium dichromate were purchased from Alfa-Aesar (Ward Hill, MA). Acetic anhydride, butyl alcohol, anhydrous Na_2CO_3, isopropyl alcohol (IPA), and hydrogen potassium phthalate were purchased from EDM Chemicals (Gibbstown, NJ). Anhydrous $MgSO_4$ was acquired from JT Baker (Center Valley, PA). Hexane was obtained from Macron Fine Chemicals (Center Valley, PA). Phenolphthalien (1%) in methanol and potassium

iodide were purchased from VWR (Chicago, IL). Sodium thiosulfate was obtained from Mallinckrodt (Paris, KY).

Reactors

Optimization of Epoxidation

The reactors used in the optimization study are part of a Chemspeed AutoPlant A100 (Chemspeed Technologies; Baselaugst, Switzerland) parallel reactor system configured with 10 fully automated miniplant units. Each miniplant unit has two reactors as seen in Fig. 16. The reactors are made of stainless steel 1.4571 and have a volume of 100 mL. The head and the vessel are connected with a quick coupling system for easy access to the reactants. Each reactor head has a slide valve, allowing for the direct dispensing of reagents into the reactor that does not require continuous addition with the onboard syringe pumps. Each reactor fits snugly into a double jacket for heating and cooling of the vessel. Heating is achieved through electrical cartridges located in the double jacket. Cooling of the double jacket is provided by circulating precooled silicone oil using a Huber Polystat cc 3 cooling and heating bath (Huber; Cary, NC). The internal reactor and jacket temperatures are measured using PT 100 temperature probes. The Chemspeed operational Autosuite^{TM} 1.1.1.1 and the miniplant firmware 1.8.1.1 software provide automatic control of the pump flowrate, stirring speed, and temperature (jacket and reaction).

The mechanical stirrer within each reactor vessel has an anchor shape which is designed for proper mixing of the vessel contents. The gap between the stirrer and the bottom and side wall of the reactor was originally 1 mm. However, the gap was increased to 2.5 mm to prevent the Amberlite IR 120H catalyst beads from getting damaged during epoxidation.

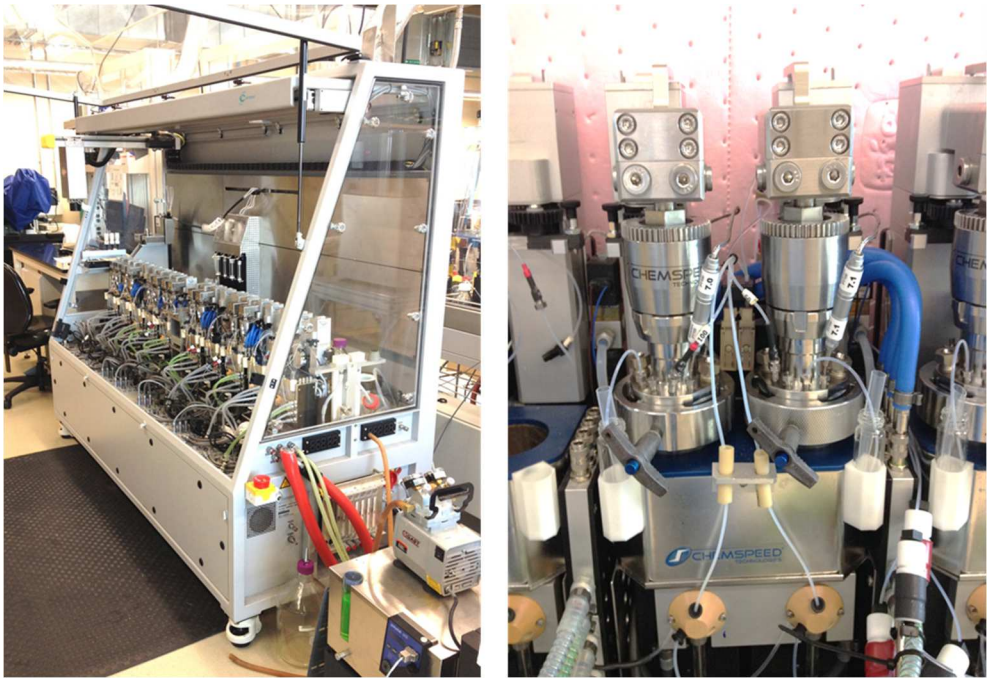

Fig. 16: Chemspeed Auto plant A100 parallel reactor system with 10 miniplants (left), and close up view of a Miniplant featuring two 100 mL mechanically stirred reaction vessels and dual syringe pumps for liquid addition (right).

Scale-up

A 10 L jacketed glass reactor (Fig. 17) was used to scale up one of the optimal sets of process conditions from the 100 mL Chemspeed experiment to a 3 kg batch. The Chemglass reactor has an automated temperature control system, Huber Cryostat 430 (Cary, NC), that heats and cools the reactor as needed to maintain a constant reaction temperature. The reactor system has a chemical metering pump (Prominent beta/4, Pittsburgh, PA) for the controlled addition of H_2O_2. Stirring is provided by an Optichem stirring motor with a controller (Chemglass model CG-2033-11; Vineland, NJ) and glass shaft fitted with 2 top and bottom impellers. The impellers can be seen in the top left photo in Fig. 17.

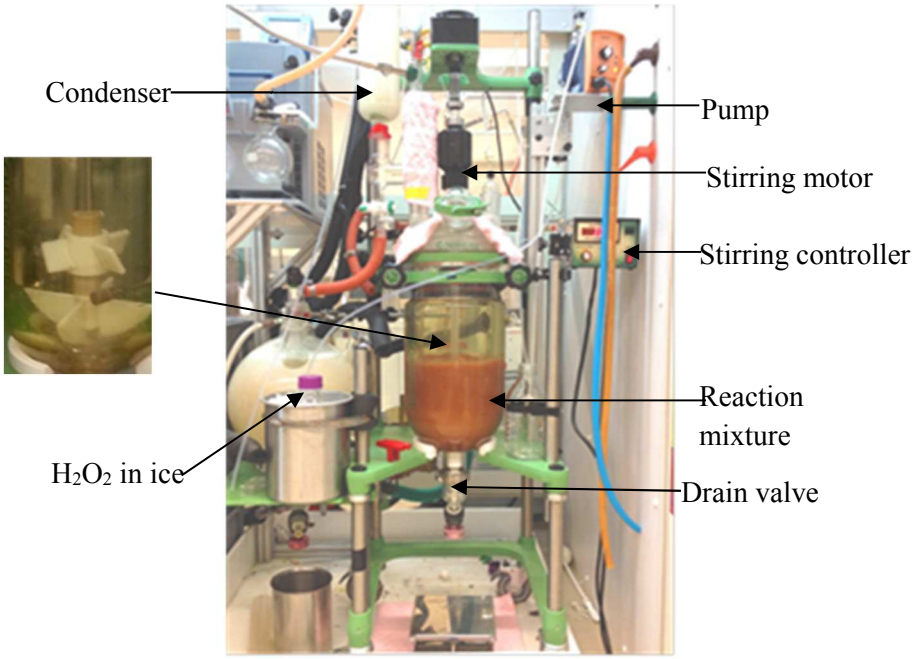

Fig. 17: Chemglass jacketed reactor (10 L) for control reaction synthesis and refining.

The bottom impeller, positioned 1 cm from the bottom of the vessel, has 4 upright quarter shaped Teflon blades 10 cm long. The top impeller, positioned 4.5 cm from the bottom impeller has 4 square-shaped '4 cm' Teflon blades pitched at 45°. The reactor has a drain opening at its bottom, allowing the washing steps to be done in the reactor. The reactor head has a reflux condenser.

Epoxidation process

Epoxidation reactions for the optimization study were carried out in seven Chemspeed reactors in which the stirrers were modified as described above. Sucrose soyate (30 g) with 0.1485 moles of molar unsaturation (calculated based on fatty acid composition) was epoxidized at three reactor temperatures (55, 60, and 65 °C), three molar ratios of acetic acid to oil unsaturation (0.25:1, 0.375:1, and 0.5:1), three molar ratios of H_2O_2 to oil unsaturation (1:1, 1.5:1, and 2:1), three catalyst amounts (1.5, 3.75, and 6 g), and three reaction times (3.5, 4.5 and 5.5 h). All reagents except H_2O_2 were loaded into the reactors and the reactor contents were

heated to the set point reaction temperatures. Once the reaction temperatures were attained, H_2O_2 was added dropwise over 2.5 h. The H_2O_2 addition rates were 0.91, 0.68, or 0.46 g min^{-1} mol^{-1} unsaturation, based on the molar ratio of H_2O_2 to oil unsaturation. The reaction timer started when H_2O_2 addition started. The reaction temperature was maintained at the set point temperature throughout the reaction time period while the contents were stirred at 400 rpm. Mixing at 400 rpm was deemed sufficient as solid brownish Amberlite could be seen throughout reaction mixture (Fig. 17).

At the end of the reaction time, the reaction contents were cooled to 40 ºC and then 15 mL of n-hexane was added to each reactor. Amberlite IR120 was filtered off using cheesecloth as each reactor's content was transferred to a 250 mL separatory funnel. The filtrates were allowed to stand in the separatory funnels for 15 min and the lower aqueous layer was then discarded. The organic layer (crude resin) was first washed twice with 30 mL of water and then twice with 30 mL saturated Na_2CO_3 solution. The resin was deemed completely neutralized when effervescence stopped and resin pH was above 7, as determined by a pH indicator strip. The saturated Na_2CO_3 solution was prepared by mixing 40 g of anhydrous sodium carbonate in 100 mL of water. The crude resin was dried overnight with anhydrous magnesium sulfate. The amount of magnesium sulfate used was approximately 20% of the weight of the undried resin. The hydrated magnesium sulfate was removed by filtration under vacuum with Whatman No. 4 filter paper. During the filtration phase additional 10 mL of n-hexane was added to ease filtration and recover resin on the wall of the beaker. Hexane was removed using a nitrogen evaporator water bath (Organomation; Berlin, MA). The water bath set at 60 ºC and nitrogen gas was

bubbled through the resin at 0.5 -0.7 L min^{-1} for approximately 30 min. The resin was then put in a vacuum oven (VWR; Chicago, IL) at 40 ^{o}C and 15 kPa for 4 h.

The data collected from the optimization study was used to develop a model to predict the extent of epoxidation at various process conditions. The model was validated with 7 combinations of factors having predicted conversion of >98.0%. The epoxidation process for validation was similar to that of the optimization experiment described above.

One of the optimal conditions was then scaled-up to a 3 kg batch. The epoxidation was performed in the 10 L jacketed glass reactor (Fig. 17) at 60 ^{o}C and 5 h. The reagent amounts were based on the molar ratio of H_2O_2 to oil unsaturation of 1.73:1 (1,750 g H_2O_2), molar ratio of acetic acid to oil unsaturation of 0.44:1 (400 g acetic acid), and 520 g of Amberlite (17.3% of SS weight). All reactants except H_2O_2 were preheated to 60 ^{o}C while being stirred at 300 rpm. The 1,750 g of H_2O_2 was then added dropwise over 2.5 h at a rate of 0.79 g min^{-1} mol^{-1} unsaturation. A syringe was used to collect approximately 25 mL of samples at 2.5, 3.0, 3.5, 4.0, and 4.5 h while the reactor contents were stirred. Reactor and jacket temperature data were sensed every 5 s using two type *T* thermocouples (Omega; Stamford, CT) and logged using *Spycontrol* computer software (Huber; Cary, NC). Data from each thermocouple were then averaged every 1 min. At the end of the reaction, the reactor contents were cooled to 40 ^{o}C and approximately 1 L of n-hexane was added to the mixture. The aqueous portion with Amberlite was drained. The crude resin was first washed twice with 3 L of water and then twice with 3 L saturated Na_2CO_3 solution. The crude resin was dried overnight with anhydrous magnesium sulfate. The hydrated magnesium sulfate and hexane were removed using equipment and the procedure described in Monono et al. (2015a).

Resin characterization

Iodine value (IV_o) for sucrose soyate was determined analytically through the ASTM method D5554. The value of 119.5±0.3 was used to calculate the maximum theoretical oxirane oxygen content (OO_t), which was 7.0%, using equation 4.

Actual oxirane oxygen (OO_e) content was determined in duplicate using the American Oil Chemist Society (AOCS) method Cd 9-57. Therefore, the conversion of double bonds to oxirane was calculated using equation 5.

Hydroxyl value was determined for samples that were epoxidized for 5.5 h at 60 ^oC and 65 ^oC using the standard method AOCS Tx 1a-66 as one measure of degradation of oxirane groups. The results are reported in mg KOH per equivalent of the hydroxyl group in 1 g of sample.

The viscosity was measured in duplicate at 25 ^oC using a HAAKE Viscotester model VT 550 (Paramus, NJ) with a cone-and-plate sensor PK 0.5^o. The viscosity of the ESS resin was shown to be shear-thinning with a Flow Behavior Index of 0.83. For the purpose of routine viscosity measurements, data were collected at 200.1 rpm.

Moisture contents were determined using a Karl Fischer titrator (Mettler-Toledo, Columbus, OH). Nonvolatile contents were determined using ASTM D1259-06 in which 0.9-1.0 g samples were dried in an air oven for 2 h at 105 ^oC.

Experimental design

The Box-Behnken design was used to optimize the epoxidation process. The design had 5 independent factors: molar ratio of H_2O_2 to unsaturated double bonds (x_1), molar ratio of acetic acid to unsaturated double bonds (x_2), Amberlite amount (x_3), reaction temperature (x_4), and

reaction time (x_5). Each factor had three levels (low, medium, and high). Table 14 shows the levels of each factor and the amount of reagent used based on 30 g of SS with a molar unsaturation of 0.1485.

Table 14: Experimental design levels for each factor and the reagent amounts based on 30 g of sucrose soyate (0.1485 molar unsaturation) epoxidized during the optimization study.

Level	Factors [x_i]					Reagent Amounts (g)		
	AA:U [x_1]	**H_2O_2:U [x_2]**	**Amb (weight% of SS) [x_3]**	**Time (h) [x_4]**	**Temp (^oC) [x_5]**	**AA**	**H_2O_2**	**Amb**
Low	0.25:1	1:1	5.0	3.5	55	2.25	10.15	1.5
medium	0.375:1	1.5:1	12.5	4.5	60	3.375	15.23	3.75
High	0.5:1	2:1	20.0	5.5	65	4.5	20.25	6

AA:U - molar ratio of acetic acid to unsaturated double bonds; H_2O_2:U – molar ratio of hydrogen peroxide to unsaturated double bonds ; Amb –Amberlite IR 120H; SS - sucrose soyate; Temp – reaction temperature.

The Box-Behnken design for 5 factors at three levels each resulted in 46 experimental treatments (Table 15). The 46 experimental treatments include 41 treatments in which 3 factors are always at the medium level and 2 factors are at either low or high levels, and 5 replicates in which all the factors are at the medium level. Each treatment consisted of a Chemspeed reactor with SS being epoxidized at a given reagent ratio, temperature, and time. Seven experimental treatments were run simultaneously, and the response variable was the conversion (%) of double bonds to oxirane.

Table 15: Box-Behnken design matrix with five uncoded independent factors showing the conversion of double bonds to oxirane and viscosity at 25 °C for each run.

Std Order	Factors					Reagent Amounts (g)			Conversion (%)	Viscosity mPa·s
	AA:U	H_2O_2:U	Amb (Wt % of SS)	Time (h)	Temp (°C)	AA	H_2O_2	Amb		
1	0.5:1	1.5:1	20	4.5	60	4.5	15.2	6	90.5±1.2	1,700±10
2	0.25:1	1:1	12.5	4.5	60	2.25	10.14	3.75	54.3±0.1	806±6
3	0.375:1	2:1	12.5	3.5	60	3.375	20.25	3.75	79.8±0.2	1,252±3
4	0.375:1	1.5:1	5	5.5	60	3.375	15.2	1.5	65.5±0.3	989±4
5	0.375:1	2:1	20	4.5	60	3.375	20.25	6	95.9±0.5	1,875±4
6	0.25:1	1.5:1	5	4.5	60	2.25	15.2	1.5	52.7±0.4	805±3
7	0.375:1	1.5:1	5	4.5	55	3.375	15.2	1.5	51.3±0.8	731±4
8	0.5:1	1.5:1	12.5	5.5	60	4.5	15.2	3.75	89.9±0.0	1,536±11
9	0.375:1	1:1	5	4.5	60	3.375	10.14	1.5	45.1±0.5	723±4
10	0.375:1	1.5:1	5	3.5	60	3.375	15.2	1.5	56.0±0.3	823±10
11	0.375:1	1.5:1	20	4.5	55	3.375	15.2	6	79.7±0.7	1,219±2
12	0.375:1	2:1	12.5	4.5	65	3.375	20.25	3.75	93.8±0.9	1,824±11
13	0.25:1	1.5:1	12.5	5.5	60	2.25	15.2	3.75	75.8±0.2	1,123±8
14	0.25:1	2:1	12.5	4.5	60	2.25	20.25	3.75	81.6±0.6	1,301±4
15	0.5:1	1:1	12.5	4.5	60	4.5	10.14	3.75	65.1±0.2	1,005±6
16	0.375:1	1.5:1	20	5.5	60	3.375	15.2	6	87.9±0.6	1,424±7
17	0.375:1	1.5:1	12.5	3.5	55	3.375	15.2	3.75	66.5±0.2	1,095±3
18	0.25:1	1.5:1	12.5	4.5	65	2.25	15.2	3.75	80.2±1.0	1,320±9
19	0.25:1	1.5:1	12.5	4.5	55	2.25	15.2	3.75	62.4±0.0	859±2
20*	0.375:1	1.5:1	12.5	4.5	60	3.375	15.2	3.75	86.6±0.5	1,316±5
21*	0.375:1	1.5:1	12.5	4.5	60	3.375	15.2	3.75	80.8±0.9	1,295±5
22	0.375:1	1.5:1	5	5.5	65	3.375	15.2	3.75	90.7±0.3	1,695±7
23	0.375:1	1:1	12.5	4.5	65	3.375	10.14	3.75	73.9±0.1	1,051±4
24*	0.375:1	1.5:1	12.5	4.5	60	3.375	15.2	3.75	84.1±0.2	1,321±3
25	0.375:1	1.5:1	5	4.5	65	3.375	15.2	1.5	65.4±0.4	935±3
26	0.5:1	1.5:1	12.5	4.5	65	4.5	15.2	3.75	91.2±0.0	1,788±9
27*	0.375:1	1.5:1	12.5	4.5	60	3.375	15.2	3.75	84.6±0.1	1,355±8
28	0.375:1	1:1	20	4.5	60	3.375	10.14	6	74.2±0.1	1,098±3
29	0.375:1	1.5:1	12.5	3.5	65	3.375	15.2	3.75	78.9±0.5	1,263±12
30	0.375:1	1.5:1	20	3.5	60	3.375	15.2	6	81.1±1.2	1,255±7
31	0.375:1	2:1	12.5	5.5	60	3.375	20.25	3.75	89.9±0.5	1,730±10
32	0.5:1	1.5:1	12.5	3.5	60	4.5	15.2	3.75	78.5±0.2	1,149±3
33	0.375:1	1.5:1	20	4.5	65	3.375	15.2	6	91.6±0.1	1,796±5
34	0.375:1	1:1	12.5	5.5	60	3.375	10.14	3.75	66.2±0.2	915±3
35	0.375:1	2:1	5	4.5	60	3.375	20.25	1.5	68.9±0.3	965±11
36	0.375:1	1:1	12.5	4.5	55	3.375	10.14	3.75	58.5±0.1	851±5
37	0.375:1	2:1	12.5	4.5	55	3.375	20.25	3.75	78.8±0.0	1,154±10
38	0.25:1	1.5:1	20	4.5	60	2.25	15.2	6	82.1±0.2	1,317±6
39	0.25:1	1.5:1	12.5	3.5	60	2.25	15.2	3.75	70.0±0.1	1,133±4
40*	0.375:1	1.5:1	12.5	4.5	60	3.375	15.2	3.75	83.1±0.1	1,316±5
41	0.375:1	1.5:1	12.5	5.5	55	3.375	15.2	3.75	76.2±0.1	1,243±3
42	0.5:1	2:1	12.5	4.5	60	4.5	20.25	3.75	93.5±0.2	1,775±5
43	0.5:1	1.5:1	12.5	4.5	60	4.5	15.2	1.5	62.6±0.2	937±8
44	0.375:1	1.5:1	12.5	4.5	60	3.375	15.2	3.75	83.3±0.2	1,318±4
45	0.5:1	1.5:1	12.5	4.5	55	4.5	15.2	3.75	74.0±0.5	996±4
46	0.375:1	1:1	12.5	3.5	60	3.375	10.14	3.75	55.1±0.2	843±7

AA:U - molar ratio of acetic acid to unsaturated double bonds; H_2O_2:U – molar ratio of hydrogen peroxide to unsaturated double bonds ; Amb –Amberlite IR 120H; SS - sucrose soyate; Temp – reaction temperature. * denote replicates with coefficient of variation of 2.5%

Statistical analysis

Statistical analysis was performed using Minitab 17 (State College, PA) at 0.05 significance level. Minitab was also used to create analysis of variance (ANOVA) tables for the model, calculate coefficients of determination (R^2), plot response surfaces for a subset of optimal conditions, and determine the correlation coefficients between the conversion, viscosity, and the temperature difference between the reaction mixture and jacket fluid (ΔT).

The root mean square errors (RMSE) for the predicted and actual conversion were calculated using equation 16.

$$\text{RMSE} = \sqrt{\frac{1}{n}\sum_{i=1}^{n}(y_i - x_i)^2} \qquad \text{(Eq. 16)}$$

n is the total number of samples, y_i is the predicted value, and x_i is the observed value.
The program developed a non-linear regression model by using a second order polynomial (equation 17).

$$Y = \beta_o + \sum \beta_i x_i + \sum \beta_{ii} x_{ii}^2 + \sum \beta_{ij} x_{ij} \qquad \text{(Eq. 17)}$$

Y is the conversion, β_o is the offset term, β_i is the linear effect factor x_i, β_{ii} is the quadratic effect of factor x_i, β_{ij} is the interaction effect between the input factors x_i and x_j, and $[1 \leq i, j \leq 5]$

Results and Discussion

Analysis of resin quality

The direct measure of epoxidation is the content of oxirane oxygen. The oxirane values for each sample were obtained from oxirane titration, and the values were used in equation 5 to determine the conversion in Table 15. Before oxirane titration was carried out, the moisture and nonvolatile contents were measured to adjust oxirane values if needed. The moisture and nonvolatile contents were less than 150 ppm and greater than 99.8%, respectively, for all the

samples. This indicates that the refining process was effective in removing water and hexane from the resin.

Conversion varied from 45.1 – 95.9% for the samples in Table 15, and is discussed in detail in sections 3.2 and 3.3. Values <100% may signify, not only that a portion of double bonds were not epoxidized, but also that some oxirane groups were degraded. Hydroxyl groups are a common product of oxirane cleavage when the epoxidation reaction is carried out at high temperatures, especially above 65 ^{o}C, in the presence of excessive water and H_2O_2 (Gamage et al., 2009). Even though the reactions were carried out between 55 - 65 ^{o}C, the hydroxyl values for the samples were determined to check for oxirane cleavage. The hydroxyl values were less than 2.8 mg KOH/g of resin, indicating minimal oxirane cleavage.

The viscosity values varied from 723 – 1,875 mPa·s (Table 15) and were positively correlated with oxirane values (r=0.94; *p-value* <0.0001). The regression relationship of viscosity (V) and conversion (c) can be expressed in the expression, $V = 271e^{0.0195*C}$ ($R^2 = 0.94$). Viscosity values were not significantly correlated to hydroxyl values (r=-0.303; *p-value* =0.052) and no trend between the values were observed ($R^2 = 0.09$). In an earlier study, viscosity significantly correlated with hydroxyl; however, high hydroxyl values were observed at temperatures greater than 65 ^{o}C used in that study (Monono et al., 2015b).

Model development and optimization

The response surface method (RSM) is a useful tool to better understand and optimize reaction processes after important factors and levels have been identified. The central composite design (CCD) and the Box-Behnken are the two main types of RSM design. The CCD has two main levels and three additional levels generated at the central and axial points. The Box-

Behnken is limited to two main levels and the central points. In this study, the axial points were deemed not of interest, for example, a molar ratio of H_2O_2 to unsaturation less than 1:1 or above 2:1. The Box-Behnken was then useful to avoid the selection of axial points and limit the experimental design to the defined levels for those factors. The Box-Behnken design for 5 factors gives 46 experimental units instead of 52-54 units for a full CCD.

The model to predict the conversion was first developed by considering all the linear, square, and interaction terms in equation 17. None of the interaction terms in the model were statistically significant (*p-value* >0.05). The lack of interaction signifies that the effect of each factor in the conversion is independent of the other factors. Therefore, a reduced model was developed without interaction terms for the five factors as seen in equation 18.

$$Y = -672 + 23.42x_1 + 9.46x_2 + 17.82x_3 + 33.51x_4 + 14.77x_5 - 2.76x_1^2 - 0.24x_2^2 - 1.58x_3^2 - 3.20x_4^2 - 0.11x_5^2 \quad \text{(Eq. 18)}$$

Where Y is conversion in %, x_1 is acetic acid in g; x_2 is H_2O_2 in g; x_3 is Amberlite IR120H in g; x_4 is time in h; and x_5 is temperature in ^oC. The model is based on epoxidation of 30 g of SS. The model is highly significant and excellent with a R^2, adjusted R^2, and predicted R^2 of 98.2%, 97.6%, and 96.8%, respectively. The lack-of-fit for the model was not significant (*p-value* = 0.498), which indicates that the error due to the model was minimal compared to pure errors from the replicates. The linear effect of all the factors is positive while the quadratic effect of all the factors is negative.

The corresponding ANOVA from the model can be seen in Table 16. The model shows that all retained factors significantly (*p-value* <0.0001) influenced the conversion. Even though some factors had a greater source of variation (SOV) than others, the *p*-values indicate that all the factors were important in modeling the conversion. The ANOVA shows that more than 98%

of the variation in the conversion was due to variation in the levels of the 5 factors, and less than 2% of the variation was due to error.

Table 16: Analyses of variance of the reduced regression model for the optimization of epoxidized sucrose soyate. Values in parenthesis represent percent variation attributable to source of variation.

Source of Variation	DF	Adjusted SS	Adjusted MS	F-Value	P-Value
Model	10	7,552.36	755.24	186.22	<0.0001
Linear	5	6,856.0	1,371.2	338.11	<0.0001
Acetic Acid (x_1)	1	464.4 (6.0%)	464.4	114.51	<0.0001
H_2O_2 (x_2)	1	2,251.5 (29.3%)	2,251.5	555.17	<0.0001
Amberlite (x_3)	1	2,902.52 (37.7%)	2,902.52	715.69	<0.0001
Time (x_4)	1	362.9 (4.7%)	362.9	89.48	<0.0001
Temperature (x_5)	1	874.68 (11.4%)	874.68	215.68	<0.0001
Square	5	696.35 (9.1%)	139.27	34.34	<0.0001
x_1^2	1	106.53	106.53	26.27	<0.0001
x_2^2	1	311.79	311.79	76.88	<0.0001
x_3^2	1	556.51	556.51	137.22	<0.0001
x_4^2	1	89.02	89.02	21.95	<0.0001
x_5^2	1	66.90	66.90	16.50	<0.0001
Error	35	141.94 (1.8%)	4.06		
Lack-of-Fit	30	123.65	4.12	1.13	0.498
Pure Error	5	18.30	3.66		
Total	45	7,694.30			

The greatest SOV in conversion was due to the range of Amberlite amounts (>37%) and H_2O_2 ratios (>29%) while reaction time and the amount of acetic acid were the least SOV (<6%). The SOV for each factor can clearly be seen in Fig 18 which shows the main effect of each factor as the other factors were held at their optimal levels (acetic acid at 1:0.44 molar ratio (4.0 g), H_2O_2 at 1:1.93 molar ratio (19.5 g), Amberlite at 18.3% of oil weight (5.3 g), reaction time at 5.0 h, and temperature at 65 ^oC). These optimal levels were determined at the peaks of each optimization plots in Minitab. The shapes of the plots were similar to those in Fig 18.

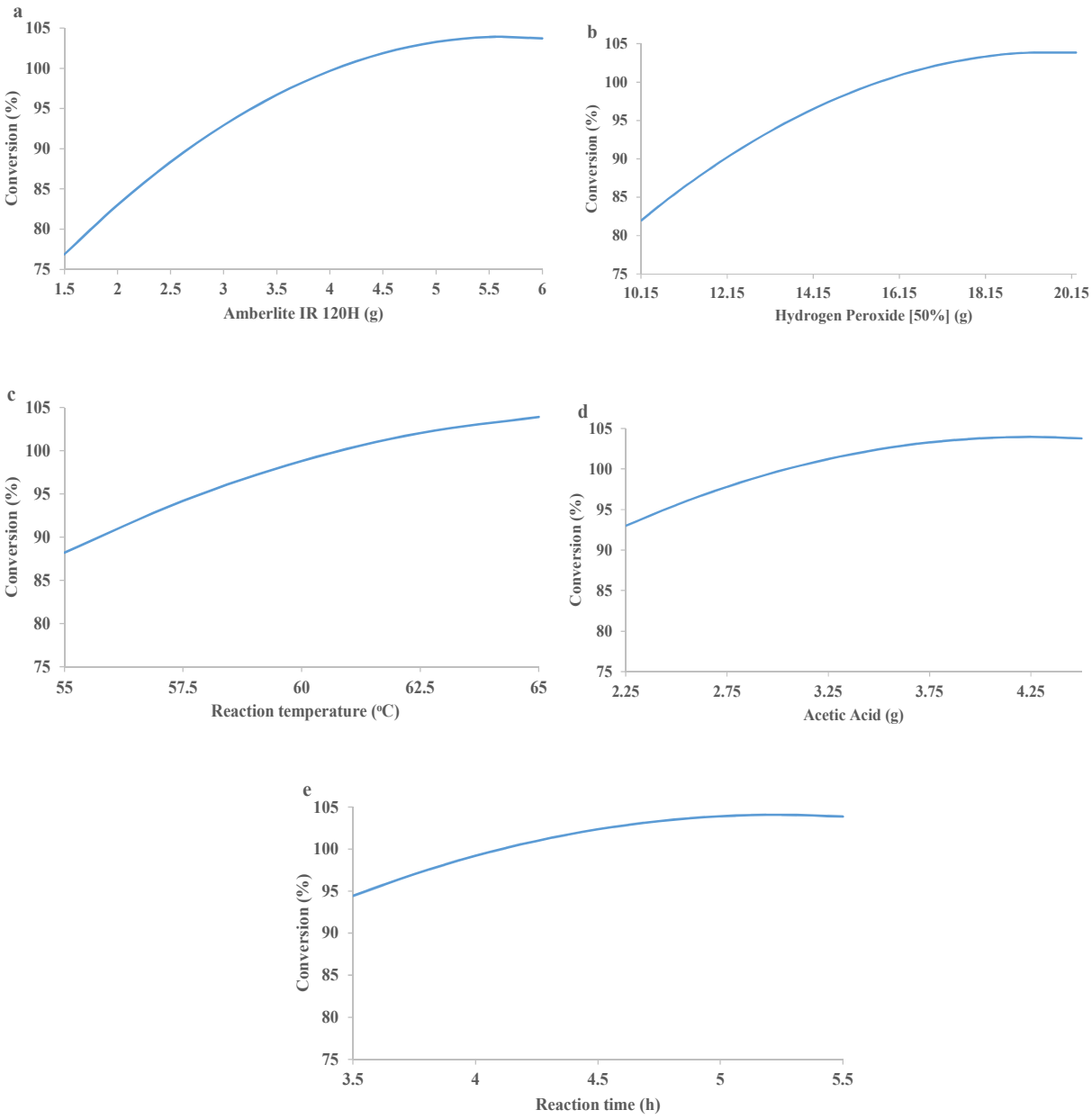

Fig. 18: Main effects plot of conversion of double bonds to oxirane of each factor (a) Amberlite IR (b) H_2O_2 (c) temperature (d) acetic acid (e) reaction time when the other factors are at their optimal level (acetic acid at 1:0.44 molar ratio (4.0 g), H_2O_2 at 1:1.93 molar ratio (19.5 g), Amberlite at 18.3% of oil weight (5.3 g), reaction time at 5.0 h, and temperature at 65 ^oC).

The factors are arranged from Fig 18 a-e based on their degree of variation observed from the model. The optimal predicted conversion of 103.5% was observed when all factors were at

the optimal levels. A conversion of 103.1 % is predicted when all factors are at the highest levels. This is an empirical model, however, and the actual conversion will never exceed 100%. Therefore, the region >100% in the main effects plot in Fig. 18 is best viewed as approaching 100% conversion.

The high variation observed from Amberlite may have been due to the wide range of values being tested (5 to 20% of SS weight). In the other reagents, their low levels were half their high levels. The lowest reported level of Amberlite before this study was 6%, and was associated with up to 66% conversion (canola oil epoxidized for 5 h at 65 ^{o}C with 0.5:1 molar ratio of acetic acid to double bonds and 1.5:1 molar ratio of H_2O_2 to double bonds) (Mungroo et al., 2008). The model developed in this study shows that at least 77% conversion can be achieved with 5% of Amberlite (1.5 g) when other factors at their optimal levels (Fig 18 a). The graph (Fig 18a) also shows that the lowest level of Amberlite needed to achieve 100% conversion was at 13.5% of oil weight (4.05 g). The high variation in conversion observed when varying H_2O_2 ratios was expected because H_2O_2 is the oxidizer and it is consumed during the process. Fig 18b shows that a H_2O_2 molar ratio of 1:1 (10.15 g) can accomplish only 82% conversion and H_2O_2 is needed in excess (1.6:1 molar ratio, 16 g) to achieve a 100% conversion. H_2O_2 is the most expensive reagent as seen in Table 5 and it is not recyclable; therefore, the model can be used to determine the minimum possible level of H_2O_2 that can yield acceptable conversion.

The reaction temperature was a relatively important source of variation with approximately 12%. Temperature influences the rate of a chemical reaction, as shown by the Arrhenius equation and increasing temperature increases the rate of epoxidation. Fig 18c clearly shows how conversion increases with increase in reaction temperature and the absence of a

plateau indicates minimal oxirane cleavage at 65 ^{o}C. The effect of oxirane cleavage would have been significant as the reaction temperature increased above 65 ^{o}C. The model shows that at 55 ^{o}C, conversion cannot attain 90% and up to 99% conversion can be achieved at 60 ^{o}C. The SOV due to acetic acid was only 6% and approximately 93% conversion can be achieved at the lowest level of acetic acid (0.25:1, 2.25 g) as seen in Fig 18d. This may be due to the fact acetic acid is being regenerated after an oxirane bond is formed; therefore, the amount remains approximately constant throughout the process. Conversion of 100% can be achieved when acetic acid is at a molar ratio of 0.34:1 (3.1 g). The variation of 4.7% due to reaction time indicates that increasing reaction time from 3.5 to 5.5 h resulted in a minor increase in conversion compared to the increase observed in the other factors (Fig 18e). The model shows that up to 95% conversion can be achieved in just 3.5 h when other factors are at the optimal level. Others studies have shown a conversion of 75-80% under similar epoxidation conditions (Gamage et al., 2009; Vlček and Petrović, 2006).

Validation of the model

The goal of this study is to optimize the epoxidation process, that is, to achieve an acceptable conversion and minimize the process cost. The plots in Fig 18 show the variation of one factor at time but the contour plots in Fig 19 show regions with different factor combinations that will yield the same conversion. The contour plots in Fig 19 were developed for H_2O_2 against Amberlite at different temperatures while acetic acid and reaction time values were held constant at their optimal levels at 0.44:1 molar ratio (4 g) and 5 h, respectively. Acetic acid and reaction time were held constant because the SOV from these factors was < 6% each. Temperature below 60 ^{o}C were not considered in contour plots because the maximum possible conversion at these

temperatures was <98%. The main goal of the contour plots was to determine experimental runs that can be used to validate the model developed.

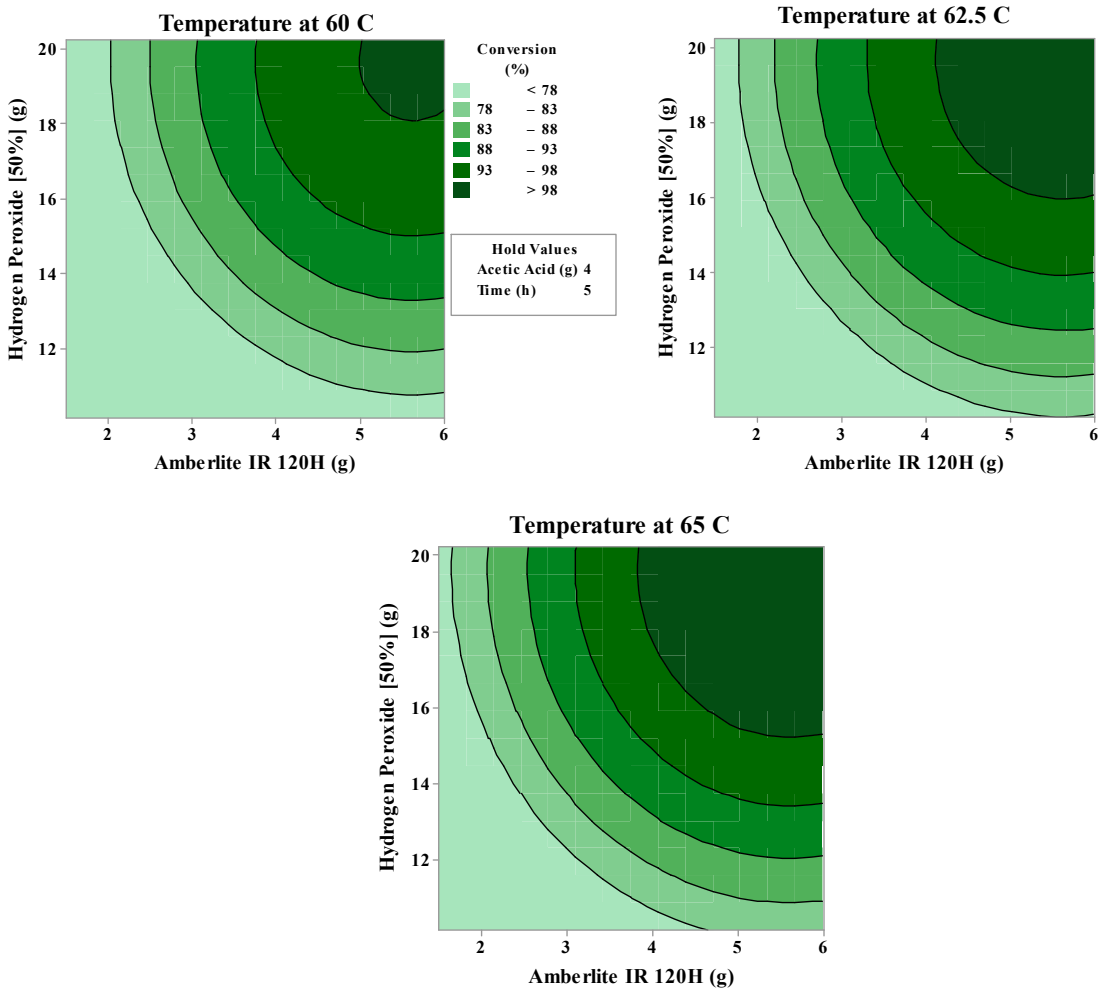

Fig. 19: Contour plots of conversion (epoxidation of sucrose soyate) as a function of hydrogen peroxide and Amberlite at 60, 62.5, 65 °C. Conversion was predicted using acetic acid and reaction time at 4 g and 5 h, respectively.

High oxirane content is desired for a better crosslinked network in composite materials, polymers, and coatings. Achieving high conversion >98% means the oxirane contents are <0.15% of the theoretical maximum oxirane content for a particular vegetable oil. A conversion of 98% in ESS can easily be achieved if the process conditions are well controlled (Monono et al., 2015a; Pan et al., 2011b). The contour plots show that there are many scenarios of Amberlite

and H_2O_2 that will yield a conversion >98% at reaction temperatures ≥ 60 ^oC. Therefore, six combinations (V1-V6 in Table 17) were selected from the contours plots when the reaction temperature was set at 60, 62.5, and 65 ^oC. Two combinations were selected from each plot and the points were randomly selected from the > 98% region. One additional scenario was added to Table 17 in which the acetic acid and reaction time were reduced to 3.7 g and 4.5 h, respectively. The latter scenario (V7, Table 17) was selected using the model in Minitab. This was to also to validate the model outside the optimal range for acetic acid and reaction time.

Table 17: Seven experimental runs at the optimal conditions to validate the model developed

Run #	Factors					Reagent Amounts (g)			Predicted Conversion (%)	Observed Conversion (%)
	AA:U	H_2O_2:U	Amb (Wt % of SS)	Time (h)	Temp (^oC)	AA	H_2O_2	Amb		
V1	0.44:1	1.78:1	17.3	5.0	60.0	4.0	18.0	5.2	98.0	98.0±0.2
V2	0.44:1	1.88:1	18.3	5.0	60.0	4.0	19.0	5.5	98.9	98.2±0.1
V3	0.44:1	1.70:1	17.3	5.0	62.5	4.0	17.2	5.2	99.5	98.5±0.3
V4	0.44:1	1.78:1	16.0	5.0	62.5	4.0	18.0	4.8	99.6	99.3±0.2
V5	0.44:1	1.73:1	16.7	5.0	65.0	4.0	17.5	5	102.0	99.9±0.5
V6	0.44:1	1.60:1	17.0	5.0	65.0	4.0	16.2	5.1	99.8	99.5±0.5
V7	0.41:1	1.83:1	17.3	4.5	65.0	3.7	18.5	5.2	99.8	99.2±0.1

AA:U - molar ratio of acetic acid to unsaturated double bonds; H_2O_2:U – molar ratio of hydrogen peroxide to unsaturated double bonds ; Amb –Amberlite IR 120H; SS - sucrose soyate; Temp – reaction temperature.

The differences between the predicted and observed values for the conversions in Table 17 were within ±1, except V5 in which the predicted value was above 100%. An RMSE of 0.54 was calculated for the predicted versus observed values. The predicted value of V5 was set at 100% instead of 102% when the RMSE was calculated. The acceptable RMSE for a model will vary based on the expectation of a model's precision. Generally, a RMSE ≤ 1 is considered to indicate a good fit for a model (Seaman et al., 1999).

The results in Table 17 indicate that a conversion of > 98% can still be achieved even with a significant reduction of up to 18-20% in the amount of reagents and reaction time compared to other studies (Espinoza-Pérez et al., 2009; Monono et al., 2015a; Pan et al., 2011b). The conversion >98% also indicates that side reactions were negligible at 60 – 65 ^{o}C and 4.5 - 5 h of reaction.

Scaled up production

Scaling up an optimal scenario is also an important step to validate the model. Therefore, scenario V1 in Table 17 was randomly selected and scaled up 100 folds from 30 g to 3 kg, using the 10 L reactor described in Fig. 17. Samples of approximately 25 mL were collected at 2.5 (when H_2O_2 addition ended), 3.0, 3.5, and 4.5 h to evaluate the extent of epoxidation at these time intervals, as well as at 5 h. A conversion of 98.1% was obtained at 5 h and was similar to the conversion of 98% observed in scenario V1 (Table 17). Thus, there was excellent agreement between the model prediction, the 30 g validation, and the 3 kg scale-up

The temperatures for the reaction mixture and jacket fluid were collected every 1 min and used to calculate their difference, ΔT (Fig. 20). The reactor temperature remained constant at 60 ^{o}C throughout the reaction process, except for a slight increase to 61.9 ^{o}C observed in the first 15 min of H_2O_2 addition. The increase was due to the exothermic reaction. But the controller adjusted the jacket temperature to bring the reaction back down to the set point temperature. The exothermic nature of the reaction can clearly be seen from the ΔT profile, and the profile was similar to the profile in Monono et al. (2015b) in which the reaction temperature varied while the jacket or water bath temperature was mostly constant.

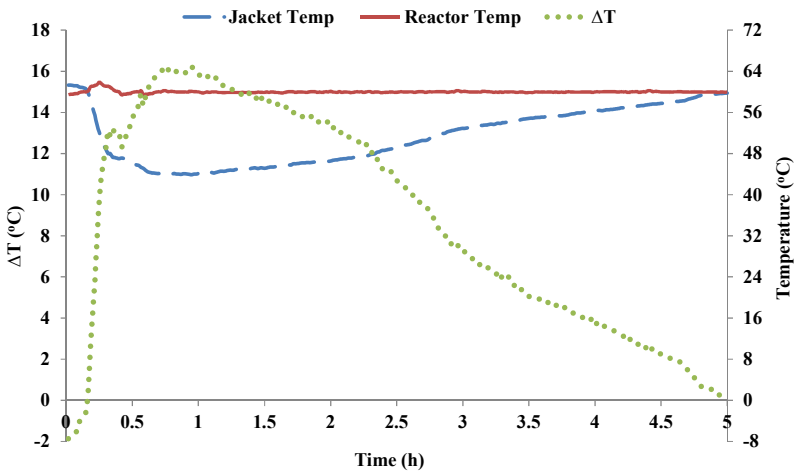

Fig. 20: Temperature-time profile for the jacket fluid, reaction mixture, and the difference between reaction and jacket temperatures, ΔT in the epoxidation of 3 kg of sucrose soyate at 60 °C for 5 h.

The steep upward ΔT slope observed within the first 15 min indicates the very high initial rate of epoxidation. Due to this high rate of epoxidation, the jacket fluid temperature was dropped sharply by the controller to counteract the heat generated. The rate of reaction was expected to slowly fall as the epoxidation progressed towards completion. The maximum ΔT of 16.3 °C was attained at 45 min of reaction and thereafter ΔT gradually fell even as H_2O_2 addition continued to 2.5 h. The maximum ΔT represents the point at which the heat generation rate was maximum; however, the reaction temperature was constant because the heat generation rate equaled the heat removal rate.

Table 18 shows the conversion, percentage of the total ΔT peak area, and the viscosity of samples obtained at each time interval. Conversion increased as the reaction time increased, however, the rate of conversion reduced over time. At 2.5 h (half the total reaction time), up to 78% of conversion was observed and only a 20% increment was achieved in the last 2.5 h of reaction. Even with lower amounts of reagents, the conversion at 2.5 h for this 3 kg batch was 3% higher than the 75% conversion observed in a previous study (Monono et al., 2015b). The

viscosity values in Table 18 show a strong relationship with conversion value (r=0.97) as was also observed among Table 15.

Table 18: Analysis of samples showing the extent of epoxidation at different time intervals

Time (h)	Oxirane oxygen (%)	Conversion (%)	Percentage of the total ΔT	Viscosity mPa·s at 25 °C
2.5	5.48±0.03	78.3±0.5	73.0	1,227±2
3.0	5.89±0.02	84.3±0.3	83.2	1,306±5
3.5	6.37±0.03	90.9±0.4	90.2	1,580±3
4.0	6.58±0.06	94.0±0.4	95.3	1,663±6
4.5	6.72±0.00	96.0±0.1	98.7	1,831±9
5.0 (Final)	6.87±0.01	98.1±0.1	100	1,898±4

The values of conversion and percentage of the total ΔT at each time interval in Table 18 were close to each other. ΔT is indicative of the heat energy released during epoxidation, and the energy will correspond to percentage of oxirane bonds formed at each time interval if oxirane cleavage is minimal (Monono et al., 2015b). Therefore, the cumulative ΔT can be used as an indicator of the extent of epoxidation if process conditions are kept constant.

Conclusion

A regression model was developed with linear and quadratic terms and validated at higher scale (100 times). The effect of interaction between the factors was not significant, which may be due to the levels used for each factor in this study. The model showed a wide range of combinations that can yield high conversion >98%, even when the reagent amounts were reduced by up to 20% of what was used in other studies. This shows that a significant reduction in reagent cost can be achieved especially w H_2O_2 which is the most significant cost and is not recyclable. The parameters from the model can be scaled up to any size as long as mixing and temperature control are adequate.

GENERAL CONCLUSIONS

The main objectives of this dissertation were to scale-up the production of ESS to 10 kg batches (paper 2) and to provide process information for an industrial scale production of ESS by developing a model that predicts the conversion of double bonds to oxirane under different process scenarios (Paper 3). Before the scale-up, it was necessary to study the behavior and effect of reaction temperature at different process conditions (Paper 1). Based on the information in this dissertation, the 10 kg process could be a model for other researchers developing new biobased resins

The experiment in paper 1 was done with canola oil and the findings on the behavior of the reaction temperature at different H_2O_2 addition rates, water bath temperatures, and reaction times were important to plan the temperature control systems in a 38 L reactor to epoxidize 10 kg of sucrose soyate. Canola oil and sucrose soyate are both vegetable oil-based compounds for which the epoxidation process conditions will be similar. A protocol was developed to manually control the reaction temperature between 55-65 ^oC after the initial rise to 55 ^oC within the first 20-30 min during scale-up for the 20 batches of ESS produced.

A total of 165.5 kg of ESS was produced with similar and acceptable resin quality from batch to batch. The resin quality and total reaction time of the 10 kg batches were similar to that of the 300 g batches. This indicated that mixing of the three phases of the reaction mixture was adequate and temperature was controlled within the optimal range. The total production time (synthesis and refining) was reduced from 8 days to 4 days when adequate refining units were fabricated and modified. One of the refining units, a 40 L separatory funnel, was designed to both wash the resin and later remove hydrated $MgSO_4$ by filtration.

The success observed in producing twenty batches of ESS called for the optimization of the process conditions for industrial scale production. The model developed from the optimization study showed that the amounts of reagents can be reduced significantly by 18-20% without compromising the conversion efficiency. The model prediction at a 30 g scale was validated at a 3 kg scale, which again indicates that mixing was adequate and reaction temperature was well controlled.

The resin produced was used by other researchers at NDSU to develop other biobased resins like polyol, polyurethane, and epoxy-anhydride, and samples were given to many companies that requested the resin for their own applications testing. One of the other biobased resins, methacrylated ESS (MAESS), was produced in the 38 L reactor designed for ESS production. The MAESS was used to develop pultruded composite materials by a local company, Tecton Products. Some of the ESS resin was also used as adhesives in wood composite research.

RECOMMENDATIONS FOR FUTURE WORK

Amberlite IR 120 H^+ form is an acidic ion exchange resin (AIER) that has commonly been used as a catalyst in the epoxidation of vegetable oil. Being solid and insoluble, it easily separates from the resin, and studies show that the catalyst can be reused at least 4-5 times (Mungroo et al., 2008; Vlček and Petrović, 2006). The catalyst was washed with solvent and then dried in those studies before recycling. Future study can be done to explore simpler purification options or if the catalyst can be reused without this solvent washing step. Also, there are other cationic forms of AIER that have not been used in the epoxidation of vegetable oils. These are Amberlite IR 120 Na^+ form and Marathon C. Even though Amberlite IR 120 H^+ form is cheaper than the other AIER, it will be valuable to compare their performances and determine the optimal quantity needed.

Further research can be done to standardize the refining steps of the crude resin and quickly remove acetic acid, excess H_2O_2, water, and solvent. The standard refining process, as conducted in this study, usually takes three days to complete; but, the process time can be further reduced if other equipment and process techniques are tested. Reduction of the amount of Na_2CO_3 and $MgSO_4$ needed per kg of resin produced should also be explored. This could result in an important material cost saving at an industrial scale.

Cost reduction of ESS will facilitate the future production of this resin at an industrial scale. The most significant reagent cost in Table 5 is sucrose soyate. The sucrose soyate was food grade and price was not for a commercial scale production; therefore, it is vital to explore cheaper options to produce sucrose soyate for resin production.

LITERATURE CITED

Abdullah, B.M., Salimon, J., 2010. Epoxidation of Vegetable Oils and Fatty Acids: Catalysts, Methods and Advantages. *J. Appl. Sci*. 10(15), 1545-1553.

Adhvaryu, A., Erhan, S.Z., 2002. Epoxidized soybean oil as a potential source of high-temperature lubricants. *Ind. Crop. Prod.* 15(3), 247-254.

Aldrich., 2013. Amberlite and Amberlyst Resins. Technical Information Bulletin.

AOCS., 1998. Calculated iodine value. in: *Official and recommended methods of the American Oil Chemist's Society*, AOCS press. Chamgaign.

AOCS., 2003. Iodine value of fats and oils. Wijs methods. in: *Method Tg 1a-64. Official and recommended methods of the American Oil Chemist's Society*, AOCS Press. Champaign.

Benaniba, M.T., Belhaneche-Bensemra, N., Gelbard, G., 2001. Stabilizing effect of epoxidized sunflower oil on the thermal degradation of poly(vinyl chloride). *Polym. Degrad. Stabil*. 74(3), 501-505.

Bisio, A., 1985. Introduction to scaleup. in: Scaleup of chemical process, (Eds.) A. Bisio, R.L. Kabel, John Wiley & Sons. New York, pp. 1-33.

Bouchareb, B., Benaniba, M.T., 2008. Effects of epoxidized sunflower oil on the mechanical and dynamical analysis of the plasticized poly(vinyl chloride). *J. Appl. Polym. Sci.* 107(6), 3442-3450.

Caccavale, F., Iamarino, M., Pierri, F., Tufano, V., 2011. Control and Monitoring of Chemical Batch Reactors. Springer, London. pp 184.

Cahoon, E. B., 2003. Genetic Enhancement of Soybean Oil for Industrial Uses: Prospects and Challenges. *AgBioForum* 6(1&2):11-13

Cai, C., Dai, H., Chen, R., Su, C., Xu, X., Zhang, S., and Yang, L., 2008. Studies on the kinetics of in situ epoxidation of vegetable oils. *Eur. J. Lipid Sci. Tech.* 110 (4), 341-346.

Cai, S.-F., Wang, L.-S., and Fan, C.-L., 2009. Catalytic Epoxidation of a Technical Mixture of Methyl Oleate and Methyl Linoleate in Ionic Liquids Using MoO(O2)2•2QOH (QOH = 8-quinilinol) as Catalyst and NaHCO3 as co-Catalyst. *Molecules* 14, 2935-2946.

Corrigan, P.J., (2003). Synthesis of polyol fatty acid polyesters. Google Patents.

Crum, C.W., Prescott, J.M., Christensen, P.J., 1992. Genetic approach to increased nutritional value in oilseed meal. World Conference on Oilseed Technology and Utilization, Budapest, Hungary. AOCS Press. pp. 334-338.

Dinda, S., Patwardhan, A.V., Goud, V.V., and Pradhan, N.C., 2008. Epoxidation of cottonseed oil by aqueous hydrogen peroxide catalysed by liquid inorganic acids. *Bioresource Technol.* 99 (9), 3737-3744.

Donati, G., Paludetto, R., 1997. Scale up of chemical reactors. *Catal. Today* 34, 483-533.

DOW., No Date. Ion Exchange Resins: Product Information. *DOWEX Company*, Accessed Nov 14, 2014 http://msdssearch.dow.com/PublishedLiteratureDOWCOM/dh_0060/0901b803800609a0.pdf?filepath=liquidseps/pdfs/noreg/177-01722.pdf&fromPage=GetDoc,%205.

Dul'neva, L.V., and Moskvin, A.V., 2005. Kinetics of Formation of Peroxyacetic Acid. *Russ. J. Gen. Chem.* 75 (7), 1125-1130.

Eissen, M., Metzger, J.O., 2002. Environmental performance metrics for daily use in synthetic chemistry. *Chem-Eur. J.* 8(16), 3580-3585.

Espinoza-Perez, J.D., 2009. Production, characterization, and raw material cost analysis of a canola oil-epoxy resin applied to composites. PhD Dissertation, North Dakota State University. Fargo, pp. 151.

Espinoza-Pérez, J.D., Haagenson, D.M., Pryor, S.W., Ulven, C.A., Wiesenborn, D.P., 2009. Production and characterization of epoxidized canola oil. *T. ASABE* 52 (4), 1289-1297.

Espinoza-Pérez, J.D., Nerenz, B.A., Haagenson, D.M., Chen, Z., Ulven, C.A., Wiesenborn, D.P., 2011. Comparison of curing agents for epoxidized vegetable oils applied to composites. *Polym. Composites*, 32(11), 1806-1816.

Fenollar, O., García, D., Sánchez, L., López, J., Balart, R., 2009. Optimization of the curing conditions of PVC plastisols based on the use of an epoxidized fatty acid ester plasticizer. *Eur. Polym. J.* 45(9), 2674-2684.

Gall, R.J., Greenspan, F.P., 1955. A Modified Peracid Process for Making Epoxy Compounds from Unsaturated Fatty Acid Esters. *Ind. Eng. Chem.* 47(1), 147-148.

Gamage, P.K., O'Brien, M., and Karunanayake, L., 2009. Epoxidation of some vegetable oils and their hydrolysed products with peroxyformic acid - optimised to industrial scale. *J. Natl. Sci. Found. Sri.* 37 (4), 229-240.

Gandini, A., 2011. The irruption of polymers from renewable resources on the scene of macromolecular science and technology. *Green Chem.* 13 (5), 1061-1083.

Gerbase, A.E., Gregorio, J.R., Martinelli, M., Brasil, M.C., and Mendes, A.N.F., 2002. Epoxidation of soybean oil by the methyltrioxorhenium-CH2Cl2/H2O2 catalytic biphasic system. *J. Am. Oil Chem. Soc.* 79 (2), 179-181.

Gerlach, A., Geller, T., 2004. Scale-Up Studies for the Asymmetric Juliá–Colonna Epoxidation Reaction. *Adv. Synth. Catal.* 346 (9-10), 1247-1249.Goud, V.V., Dinda, S., Patwardhan, A.V., Pradhan, N.C. 2010. Epoxidation of Jatropha (Jatropha curcas) oil by peroxyacids. *Asia-Pac. J. Chem. Eng.* 5(2), 346-354.

Goud, V. V., S. Dinda, A. V. Patwardhan, and N. C. Pradhan. 2010. Epoxidation of Jatropha (Jatropha curcas) oil by peroxyacids. *Asia-Pac. J. Chem. Eng.* 5(2):346-354.

Goud, V.V., Patwardhan, A.V., Dinda, S., and Pradhan, N.C., 2007. Epoxidation of karanja (Pongamia glabra) oil catalysed by acidic ion exchange resin. *Eur. J. Lipid Sci. Tech.* 109 (6), 575-584.

Goud, V.V., Patwardhan, A.V., and Pradhan, N.C., 2006. Studies on the epoxidation of mahua oil (Madhumica indica) by hydrogen peroxide. *Bioresource Technol.* 97 (12), 1365-1371.

Grompone, M.A., 2011. Sunflower oil. Second ed. in: Vegetable oils in food technology: composition, properites and uses, (Ed.) F.D. Gunstone, John Wiley & Sons Ltd. West Sussex, UK, pp. 137-168.

Guenter, S., Reith, R., Rowbottom, K.T. 2003. Ullmann's encyclopedia of industrial chemistry. 6th ed. John Wiley & Sons.

Gunstone, F.D. 2004. Rapeseed and canola oil: production, processing, properties and uses. Blackwell Publishing Ltd, Oxford.

Gunstone, F.D. 2011. Production and trade of vegetable oils. Second ed. in: Vegetable oils in food technology: composition, properties and uses, (Ed.) F.D. Gunstone, John Wiley and Sons. West Sussex, UK, pp. 1-24.

Guo, A., Javni, I., and Petrovic, Z., 2000. Rigid polyurethane foams based on soybean oil. *J. Appl. Polym. Sci.* 77 (2), 467-473.

Guo, A., Petrovic, Z.S., 2005. Vegetable oils-based polyols. in: Industrial Uses of Vegetable oils, (Ed.) S.Z. Erhan, AOCS Press. Champaign, IL, pp. 110-130.

Guo, A., Zhang, W., Petrovic, Z., 2006. Structure–property relationships in polyurethanes derived from soybean oil. *J. Mater. Sci.* 41(15), 4914-4920.

Gurbanov, M.S., Mamedov, B.A., 2009. Epoxidation of flax oil with hydrogen peroxide in a conjugate system in the presence of acetic acid and chlorinated cation exchanger KU-2×8 as catalyst. *Russ. J. Gen. Chem.* 82(8), 1483-1487.

Gurvich, L.V., Veyts, I.V., Alcock, C.B., 1994. Thermodynamic Properties of Individual Substances,. Fourth ed. CRC Press, Boca Raton, FL

Hilker, I., Bothe, D., Prüss, J., Warnecke, H.J., 2001. Chemo-enzymatic epoxidation of unsaturated plant oils. *Chem. Eng. Sci.* 56(2), 427-432.

Holman, J.P., 2002. Heat Transfer. ninth ed. McGraw-Hill.

Hosseini, N., Ulven, C., Webster, D., Nelson, T.J., 2013. Utilization of flax fibers and glass fibers in a bio-based resin. in: *The 19th International Conference on Composite Materials*, July 28-August 2. Montreal, Canada.

ICIS Chemicals., 2006-2008. Indicative Chemical Prices A-Z. Accessed June15th, 2015 http://www.icis.com/chemicals/channel-info-chemicals-a-z/.

Korver, O., Katan, M.B., 2006. The Elimination of Trans Fats from Spreads: How Science Helped to Turn an Industry Arounda. *Nutr. Rev.* 64(6), 275-279.

Kovash, C.S., Pavlacky, E., Selvakumar, S., Sibi, M.P., Webster, D.C., 2014. Thermoset Coatings from Epoxidized Sucrose Soyate and Blocked, Bio-Based Dicarboxylic Acids. *ChemSusChem* 7(8), 2289-2294.

La Scala, J., Wool, R.P., 2005. Rheology of chemically modified triglycerides. *J. Appl. Polym. Sci.* 95(3), 774-783.

Lathi, P.S., Mattiasson, B., 2007. Green approach for the preparation of biodegradable lubricant base stock from epoxidized vegetable oil. *Appl. Catal B-Environ*. 69(3–4), 207-212.

Leveneur, S., Zheng, J., Taouk, B., Burel, F., Wärnå, J., Salmi, T., 2014. Interaction of thermal and kinetic parameters for a liquid–liquid reaction system: Application to vegetable oils epoxidation by peroxycarboxylic acid. *J. Taiwan Inst. Chem. E.* 45 (4), 1449-1458.

Lichtenthaler, F.W., Peters, S., 2004. Carbohydrates as green raw materials for the chemical industry. *Comptes Rendus Chimie*. 7(2), 65-90.

Lienhard IV, J.H., Lienhard V, J.H., 2011. A Heat Transfer Textbook, fourth ed. Phlogiston Press, Cambridge, Massachussetts.

Luong, T.M., Schriftman, H., Swern, D., 1967. Direct hydroxylation of fats and derivatives with a hydrogen peroxide tungstic acid system. *J. Am. Oil Chem. Soc.* 44(5), 316-320.

Mahajan, S., Konar, S., Boocock, D.B., 2006. Determining the acid number of biodiesel. *J. Am. Oil Chem. Soc.* 83(6), 567-570.

Meier, M.A.R., Metzger, J.O., Schubert, U.S., 2007. Plant oil renewable resources as green alternatives in polymer science. *Chem. Soc. Rev.* 36 (11), 1788-1802.

Meyer, P.P., Techaphattana, N., Manundawee, S., Sangkeaw, S., Junlakan, W., and Tongurai, C., 2008. Epoxidation of soybean oil and jotropha oil. *Thammasat Int. J. Sci.* 13, 1-5.

Milchert, E., A. Smagowicz, and G. Lewandowski. 2010. Optimization of the Epoxidation of Rapeseed Oil with Peracetic Acid. *Org. Progress Res. Dev.* 14(5):1094-1101.

Monono, E., D. Webster, and D. Wiesenborn. 2015a. Pilot scale (10 kg) production and characterization of epoxidzed sucrose soyate. *Ind. Crop. Prod. 74 (2015) 987-997*.

Monono, E.M., Haagensoon, D.M., Wiesenborn, D.P., 2015b. Characterizing the Epoxidation Process Conditions of Canola Oil for Reactor Scale-up. *Ind. Crop. Prod. 67 (2015) 364-372*.

Morad, N.A., Kamal, A.A.M., Panau, F., Yew, T.W., 2000. Liquid specific heat capacity estimation for fatty acids, triacylglycerols, and vegetable oils based on their fatty acid composition. *J. Am. Oil Chem. Soc*, 77(9), 1001-1005.

Mungroo, R., Goud, V.V., Naik, S.N., and Dalai, A.K., 2011. Utilization of green seed canola oil for in situ epoxidation. *Eur. J. Lipid Sci. Tech.* 113 (6), 768-774.

Mungroo, R., Pradhan, N., Goud, V., and Dalai, A., 2008. Epoxidation of Canola Oil with Hydrogen Peroxide Catalyzed by Acidic Ion Exchange Resin. *J. Am. Oil Chem. Soc.* 85 (9), 887-896.

Nassar, N.N., Mehrotra, A.K., 2011. Design of a laboratory experiment on heat transfer in an agitated vessel. *Educ. Chem. Eng.* 6 (3), 83-89.

Nelson, T., Masaki, B., Morseth, Z., Webster, D., 2013. Highly functional biobased polyols and their use in melamine–formaldehyde coatings. *J. Coating Tech. Res.* 10(6), 757-767.

Okieimen, F.E., Bakare, O.I., Okieimen, C.O., 2002. Studies on the epoxidation of rubber seed oil. *Ind. Crop. Prod.* 15(2), 139-144.

Orellana-Coca, C., Camocho, S., Adlercreutz, D., Mattiasson, B., Hatti-Kaul, R., 2005. Chemo-enzymatic epoxidation of linoleic acid: Parameters influencing the reaction. *Eur. J. Lipid Sci. Tech.* 107(12), 864-870.

P&G., 2009. Chempol® MPS Wins the 2009 Presidential Green Chemistry Challenge Award.

P&G., 2014. Price quote for a drum of sucrose soyate (SEFOSE 1618U). Personal communication.

Pan, X., Nelson, T.J., Webster, D.C. 2012. Novel biobased dual-cure coating system. *Prog. Org. Coat.* 73(4), 344-354.

Pan, X., Sengupta, P., Webster, D.C., 2011a. High Biobased Content Epoxy–Anhydride Thermosets from Epoxidized Sucrose Esters of Fatty Acids. *Biomacromolecules* 12 (6), 2416-2428

Pan, X., Sengupta, P., and Webster, D.C., 2011b. Novel biobased epoxy compounds: epoxidized sucrose esters of fatty acids. *Green Chem.* 13 (4), 965-975.

Pan, X., Webster, D.C., 2011. Impact of Structure and Functionality of Core Polyol in Highly Functional Biobased Epoxy Resins. *Macromol. Rapid Comm.* 32 (17), 1324-1330.

Pan, X., and Webster, D.C., 2012. New Biobased High Functionality Polyols and Their Use in Polyurethane Coatings. *ChemSusChem* 5 (2), 419-429.

Parreira, T.F., Ferreira, M. M.C., Sales, H.J.S., and de Almeida, W.B., 2002. Quantitative Determination of Epoxidized Soybean Oil Using Near-Infrared Spectroscopy and Multivariate Calibration. *Appl. Spectrosc.* 56 (12), 1607-1614.

Patil, H., Waghmare, J., 2013. Catalyst for epoxidation of oils: a review. *Discovery* 3(7), 10-14.

Petrović, Z.S., Zlatanić, A., Lava, C.C., and Sinadinović-Fišer, S., 2002. Epoxidation of soybean oil in toluene with peroxoacetic and peroxoformic acids — kinetics and side reactions. *Eur. J. Lipid Sci. Tech.* 104 (5), 293-299..

Przybylski, R. 2011. Canola/rapeseed oil. Second ed. in: Vegetable oils in food technology: composition, properties and uses, (Ed.) F.D. Gunstone, John Wiley & Sons Ltd. West Sussex, UK, pp. 107-136.

Rangarajan, B., A. Havey, E. Grulke, and P. Culnan. 1995. Kinetic parameters of a two-phase model for in situ epoxidation of soybean oil. *J. Am. Oil Chem. Soc.* 72(10):1161-1169.

Rushton, A., Ward, A.S., Holdich, R.G. 2000. Solid-liquid filtration and separation technology. Second ed. Wiley-VCH, Weinheim, Germany.

Rüsch gen. Klaas, M., and Warwel, S., 1999. Complete and partial epoxidation of plant oils by lipase-catalyzed perhydrolysis. *Ind. Crop. Prod.* 9 (2), 125-132.

Salzano, E., Agredaa, A.G., Russob, V., Seriob, M.D., and Santacesaria, E., 2012. Safety criteria for the epoxydation of soybean oil in fedbatch reactor. *Chem. Eng. T.* 26, 39-44.

Santacesaria, E., Tesser, R., Di Serio, M., Turco, R., Russo, V., and Verde, D., 2011. A biphasic model describing soybean oil epoxidation with H_2O_2 in a fed-batch reactor. *Chem. Eng. J.* 173 (1), 198-209.

Saurabh, T., Patnaik, M., Bhagt, S.L., and Renge, V.C., 2011. Epoxidation of vegetable oils: a review. *Int. J. Adv. Eng. Techn.* 2 (4), 491-501.

Seaman, D. E., J. J. Millspaugh, B. J. Kernohan, G. C. Brundige, K. J. Raedeke, and R. A. Gitzen. 1999. Effects of Sample Size on Kernel Home Range Estimates. *J. Wildlife Manage.* 63(2):739-747.

Sheldon, R.A., 1991. Heterogeneous Catalytic Oxidation and Fine Chemicals. in: Studies in Surface Science and Catalysis, (Eds.) J.B.C.B.D.D.G.P.R.M. M. Guisnet, C. Montassier, Vol. Volume 59, Elsevier, pp. 33-54.

Sinadinovic-Fiser, S., Jankovic, M., and Petrovic, Z.S., 2001. Kinetics of in situ epoxidation of soybean oil in bulk catalyzed by ion exchange resin. *J. Am. Oil Chem. Soc.* 78 (7), 725-731.

Sinadinović-Fišer, S., Janković, M., Borota, O., 2012. Epoxidation of castor oil with peracetic acid formed in situ in the presence of an ion exchange resin. *Chem. Eng. Process.* 62, 106-113

Swern, D., Billen, G.N., Findley, T.W., Scanlan, J.T., 1945. Hydroxylation of Monounsaturated Fatty Materials with Hydrogen Peroxide. *J. Am Chem. Soc.* 67(10), 1786-1789.

Tan, S.G., and Chow, W.S., 2010. Biobased Epoxidized Vegetable Oils and Its Greener Epoxy Blends: A Review. *Polymer-Plastics Techn. Eng.* 49 (15), 1581-1590.

USDA., 2015. Oilseeds: World market and trade. January 2015 ed. in: United States Department of Agriculture: Foreign Agricultural Service, USDA.

USDA-ERS., 2012. Soybeans & Oil Crops. Oct 10th 2012 ed, USDA; Economic Research Service.

USDA-ERS., 2013. Projections for U.S. Soybean Supply and Use: USDA Soybean Baseline, 2010-19. May 27, 2012 ed. in: Market Outlook, USDA

USDA-ERS., 2015. Projections for U.S. Soybean Supply and Use: USDA Soybean Baseline, 2010-19. Dec 24th, 2015 ed. in: Market Outlook, USDA.

USDA-NASS., 2013. Statistics by Subject, USDA-NASS.

Vlček, T., and Petrović, Z., 2006. Optimization of the chemoenzymatic epoxidation of soybean oil. *J. Am. Oil Chem. Soc.* 83 (3), 247-252.

Wakeman, R.J., 2011. Liquid-solid separation. *A to Z Guide to Thermodynamics, Heat & Mass Transfer, and Fluids Engineering*.

Walsh, T., Bobalek, E., Hall, D., 1961. Preparation and characterization of unsaturated sucrose esters. *Div. Org. Coatings Plastic Chem.* 21, 125-148.

Wang, H., Tang, H., Wilson, J., Salley, S., Ng, K.Y.S., 2008. Total Acid Number Determination of Biodiesel and Biodiesel Blends. *J. Am. Oil Chem. Soc.* 85(11), 1083-1086.

Wang, T. 2011. Soybean oil. Second ed. in: Vegetable oils in food technology: composition, properties and uses, (Ed.) F.D. Gunstone, John Wiley & Sons Ltd. West Sussex, UK, pp. 59-106.

Yan, J., Webster, D., 2014. Thermosets from highly functional methacrylated epoxidized sucrose soyate. *Green Material* 2 (3), 132 –143.

APPENDIX A: SAS CODES ANALYSIS (PAPER 1)

```
Oxirane analysis;
data spspplot;
input Tb R t rep Conversion;
datalines;
55 4.55 2.5 1 89.09
55 4.55 2.5 2 89.68
55 4.55 2.5 3 91.75
55 4.55 2.5 4 88.45
65 4.55 2.5 1 93.43
65 4.55 2.5 2 92.48
65 4.55 2.5 3 93.00
65 4.55 2.5 4 93.30
75 4.55 2.5 1 96.00
75 4.55 2.5 2 95.36
75 4.55 2.5 3 96.00
75 4.55 2.5 4 95.36
55 2.27 2.5 1 86.65
55 2.27 2.5 2 89.33
55 2.27 2.5 3 87.05
55 2.27 2.5 4 86.22
65 2.27 2.5 1 94.57
65 2.27 2.5 2 93.04
65 2.27 2.5 3 93.92
65 2.27 2.5 4 93.25
75 2.27 2.5 1 94.55
75 2.27 2.5 2 96.09
75 2.27 2.5 3 93.54
75 2.27 2.5 4 92.64
55 1.14 2.5 1 83.33
55 1.14 2.5 2 83.24
55 1.14 2.5 3 83.77
55 1.14 2.5 4 83.87
65 1.14 2.5 1 91.14
65 1.14 2.5 2 91.47
65 1.14 2.5 3 88.33
65 1.14 2.5 4 89.86
75 1.14 2.5 1 92.55
75 1.14 2.5 2 93.29
75 1.14 2.5 3 94.86
75 1.14 2.5 4 92.47
55 4.55 4.0 1 91.6
55 4.55 4.0 2 91.66
55 4.55 4.0 3 91.06
55 4.55 4.0 4 91.97
65 4.55 4.0 1 92.27
65 4.55 4.0 2 92.27
65 4.55 4.0 3 92.27
65 4.55 4.0 4 93.94
75 4.55 4.0 1 95.00
75 4.55 4.0 2 93.03
75 4.55 4.0 3 92.42
```

75 4.55 4.0 4 93.48
55 2.27 4.0 1 91.42
55 2.27 4.0 2 92.61
55 2.27 4.0 3 94.26
55 2.27 4.0 4 93.44
65 2.27 4.0 1 94.45
65 2.27 4.0 2 94.17
65 2.27 4.0 3 93.67
65 2.27 4.0 4 92.75
75 2.27 4.0 1 91.35
75 2.27 4.0 2 93.00
75 2.27 4.0 3 93.78
75 2.27 4.0 4 93.4
55 1.14 4.0 1 88.23
55 1.14 4.0 2 89.39
55 1.14 4.0 3 91.02
55 1.14 4.0 4 87.59
65 1.14 4.0 1 92.03
65 1.14 4.0 2 96.37
65 1.14 4.0 3 91.92
65 1.14 4.0 4 91.69
75 1.14 4.0 1 98.3
75 1.14 4.0 2 97.02
75 1.14 4.0 3 94.27
75 1.14 4.0 4 97.31
55 4.55 5.5 1 96.97
55 4.55 5.5 2 96.21
55 4.55 5.5 3 98.49
55 4.55 5.5 4 94.39
65 4.55 5.5 1 95.76
65 4.55 5.5 2 94.39
65 4.55 5.5 3 96.52
65 4.55 5.5 4 97.0
75 4.55 5.5 1 92.88
75 4.55 5.5 2 93.18
75 4.55 5.5 3 92.88
75 4.55 5.5 4 92.98
55 2.27 5.5 1 97.47
55 2.27 5.5 2 92.83
55 2.27 5.5 3 91.24
55 2.27 5.5 4 91.65
65 2.27 5.5 1 95.18
65 2.27 5.5 2 93.63
65 2.27 5.5 3 94.51
65 2.27 5.5 4 94.69
75 2.27 5.5 1 91.74
75 2.27 5.5 2 93.49
75 2.27 5.5 3 94.06
75 2.27 5.5 4 94.03
55 1.14 5.5 1 94.72
55 1.14 5.5 2 93.34
55 1.14 5.5 3 93.39
55 1.14 5.5 4 93.28

```
65 1.14 5.5 1 95.7
65 1.14 5.5 2 95.41
65 1.14 5.5 3 97.07
65 1.14 5.5 4 95.15
75 1.14 5.5 1 93.63
75 1.14 5.5 2 92.15
75 1.14 5.5 3 92.20
75 1.14 5.5 4 93.31
;;
ods graphics off;
ods rtf file='split_split_plot.rtf';
proc anova;
class rep Tb R t;
model Conversion=rep Tb R Tb*R t Tb*t R*t Tb*R*t;
test h=Tb e=rep*Tb;
test h=Tb Tb*R e=rep*Tb*R;
means Tb/lsd e=rep*Tb;
means R/lsd e=rep*Tb*R;
means t/lsd;
means Tb*R Tb*t b*t Tb*R*t;
title 'ANOVA for the RCBD with a Split-split Plot Analysis';
run;
ods rtf close;
```

SAS code for correlation and regression analysis between oxirane and FT-IR absorbance for sample at 5.5 h

```
data spspplot;
input Oxi Abs;
datalines;
6.37 0.180
6.33 0.185
6.14 0.145
6.19 0.153
6.27 0.154
6.16 0.147
6.18 0.144
6.32 0.155
6.12 0.128

Proc Corr;
Var Oxi Abs;
run;

Proc reg;
model Oxi = abs;
run;
```

APPENDIX B: TEST ON THE EFFECT OF STIRRING SPEED DURING EPOXIDATION (PAPER 1)

300 g of canola oil was epoxidized in dupucate at a bath temperature of 60 ºC for 5.5 h using molar ratio of oil unsaturation: acetic acid: H_2O_2 of 1:0.5:2. The oxirane content was not significantly different (*p-value* =0.12) at stirring speeds between 400 – 600 rpm.

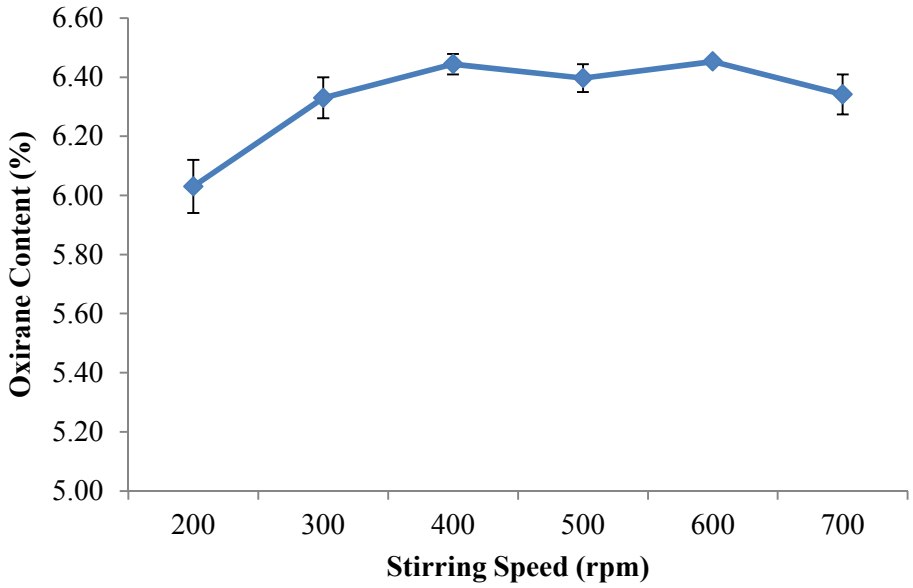

Fig. B1: Oxirane content at various speed of 300 g canola oil epoxidized 60 ºC for 5.5 h

APPENDIX C: PHOTOS OF SEPARATORY FUNNEL AND SOLVENT EXTRACTION UNIT (PAPER 2)

Fig. C1: Pictures of the separatory funnel used as a washing and a filtration unit

Fig. C2: Pictures of the solvent extraction unit adapted to remove solvent from the refined resin

APPENDIX D: YIELD AND PROPERTIES OF ALL TWENTY (7-10 KG) BATCHES OF ESS (PAPER 2)

Table D1: Yield and properties of 20 batches of epoxidized sucrose soyate produced in the 38 L reactor.

Parameters	1st Batch (07-02-12)	2nd Batch (07-24-12)	3rd Batch (08-14-12)	4th Batch (09-05-12)	5th Batch (09-19-12)	6th Batch (10-03-12)	7th Batch (01-07-13)
Sucrose Soyate (SS) in kg	7.0	7.0	9.0	9.0	9.0	9.0	10
Epoxidized SS (kg) [% yield]	4.1 [58.8]	5.05 [72.1]	8.3 [92.2]	8.9 [99.0]	6.6 [73.3]	9.1 [101]	10.2 [102]
Oxirane Content (%) [EEW g/eq]	6.49±0.11 [246.5±4.2]	6.55±0.06 [244.2±2.2]	6.68±0.07 [239.7±2.3]	6.6±0.05 [242.0±1.9]	6.74±0.06 [237.2±2.3]	6.89±0.01 [232.2±0.4]	6.71±0.04 [238.3±1.4]
Nonvolatile Content (%)	99.5±0.04	96.7±0.25	98.7±0.05	97.7±0.04	98.4±0.02	98.6±0.09	99.2±0.03
Viscosity (mPa·s) at 22°C	2,236±6	2,380±5	2,335±10	2,369±8	2,402±11	2,555±4	2,465±3
Production Time (days)	8	8	8	4	4	4	4

Parameters	8h Batch (02-20-13)	9th Batch (07-03-13)	10th Batch (08-12-13)	11th Batch (02-13-14)	12th Batch (04-17-14)	13th Batch (05-01-14)	14th Batch (05-27-14)
Sucrose Soyate (SS) in kg	10	10	10	10	10	8.0	10
Epoxidized SS (kg) [% yield]	10.0 [100]	9.8 [98]	10.1 [101]	8.7 [87]	5.5 [55]	7.1 [90]	9.2 [92]
Oxirane Content (%) [EEW g/eq]	6.80±0.03 [235.3±1.0]	6.75±0.05 [236.3±1.4]	6.73±0.06 [237.9±1.6]	6.49±0.11 [246.5±4.2]	6.74±0.10 [237.4±3.9]	6.61±0.05 [242.1±2.0]	6.79±0.0 [235.6±0.4]
Nonvolatile Content (%)	99.8±0.02	99.6±0.01	99.7±0.03	99.5±0.01	99.7±0.4	99.5±0.01	99.3±0.04
Viscosity (mPa·s) at 22 °C	2,397±4	2,411±8	2,345±5	2,198±9	2,351±11	2,286±3	2,489±7
Production Time (days)	4	4	4	4	4	4	4

Table D1: Yield and properties of 20 batches of epoxidized sucrose soyate produced in the 38 L reactor (continued).

Parameters	**15th Batch (05-29-14)**	**16th Batch (06-02-14)**	**17th Batch (06-05-14)**	**18th Batch (06-10-14)**	**19th Batch (06-12-14)**	**20th Batch (06-24-14)**
Sucrose Soyate (SS) in kg	10	10	10	10	10	10
Epoxidized SS (kg) [% yield]	9.0 [90]	9.2 [92]	8.9 [89]	9.1 [91]	8.4 [84.0]	9.9 [99]
Oxirane Content (%) [EEW g/eq]	6.60±0.01 [242.4±0.5]	6.76±0.20 [236.7±7.0]	6.81±0.07 [235.0±2.3]	6.89±0.18 [232.2±6.6]	6.77±0.20 [236.3±7.0]	6.86±0.2
Nonvolatile Content (%)	98.9±0.02	99.6±0.01	99.0±0.03	99.8±0.02	99.3±0.04	99.8±0.0
Viscosity (mPa·s) at 22 °C	2,279±6	2,325±9	2,402±8	2,424±3	2,342±6	2,601±10
Production Time (days)	4	4	4	4	4	4